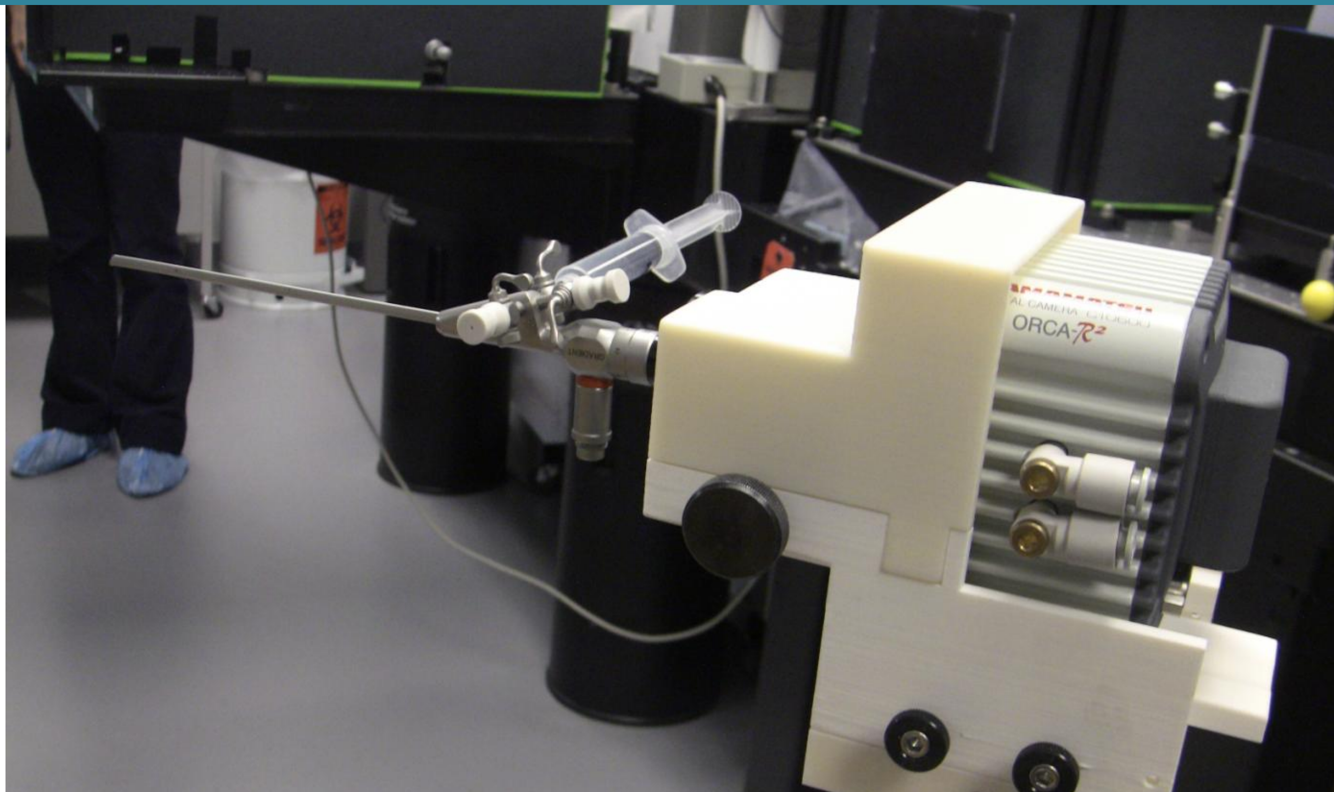

Quantitative Molecular Endoscope for Real-Time Optical Imaging of Colorectal Cancer

EXECUTIVE SUMMARY

Dr. Thomas Wang and the Michigan Network for Translation Research (NTR) center have assigned us the task of developing a quantitative molecular endoscope for *in vivo* real-time optical imaging of colonic dysplasia in animal models for immediate use by cancer researchers. We aim to improve the current technique by making the endoscope system capable of simultaneous reflectance and fluorescence imagery capture. We need to design a robust optical housing that attaches to a Karl Storz small animal urethrocystoscope (Model 27030BA), houses two specified cameras, and an optical system including a dichroic mirror, a fluorescence filter, and a convex lens. The researchers at the NTR center expressed a need for a compact, handheld system with well-aligned optics. Additionally, we aim to manufacture a tripod adapter so that the researchers have the option of securing the device on a tripod.

We have translated the requirements of a compact and handheld system to engineering specifications that minimize focal length, total mass and total storage volume. We intend to use a lens with focal length between 20mm and 50mm. The total mass of the system including the cameras will be between 1150 and 2000 grams. The mass of the fluorescence camera and the reflectance camera are 1100 grams and 37 grams respectively. Finally the total storage volume of the system will be a maximum of $6.3x10^{-3}$ m^3. We additionally intend to keep deflection less than 2mm in the optical channel between the end of the housing and the larger camera that sits across it. As for ergonomic specifications, the design will include modifications for handling the devices and features for small focus adjustments.

Our final design is a combination of ideas from various design concepts that we felt would make the best possible final product. It is made up of 6 separate pieces including the base platform, dovetail slide mechanism, mirror holder, detachable handle, tripod adaptor and a cover. All of these pieces were manufactured at the University of Michigan's 3D printing lab in the Duderstadt Center using their Dimension Elite FRM machine. The base platform holds all of the optical components including the mirror holder that secures the dichroic mirror. The platform also holds the dovetail slide mechanism that the fluorescence camera sits on to allow for positional adjustments. The contoured handle can be attached to and removed from the base platform. The tripod adapter gives the user the option to attach the device to a tripod that provides a stable environment. We manufactured a cover that fits into grooves in the housing to aid in preventing light scattering during the procedure.

Of the 6 pieces manufactured, only 4 are vital to the operation and function of the device. The tripod adapter and cover were judged as accessories and were paid for by the NTR center. The total cost of the 4 vital parts that were manufactured and the fasteners that were purchased was $390.37. Our validation process confirmed that our device met all the engineering specifications we had proposed including the ergonomic specifications. The total mass was 1772 grams, maximum storage volume was 0.004675 m^3, maximum deflection was 0.013 mm, and the focal length was 50 mm.

We were able to achieve our goal of creating a housing with a low mass. Nevertheless, the weight of the Hamamatsu camera makes it difficult for the researcher to hold the system steady causing difficulty when trying to capture images. The tripod adapter does provide stability, but lacks the necessary movement to move the scope in and out of the colon. Overall, the device does succeed in its ability to capture focused images of the cancer polyps for the fluorescence and reflectance cameras. However, the design could be even more effective if a track, providing motion in the X-Y plane, was to be implemented into the tripod adapter and a better adjustment system for the Point Grey Research camera was to be installed.

Team Photo: Right to Left Daniel Fuchs, Elizabeth Eisenstein, Radhika Gurumurthy.

Final Design Photo: (Cover shown on the cover page photo).

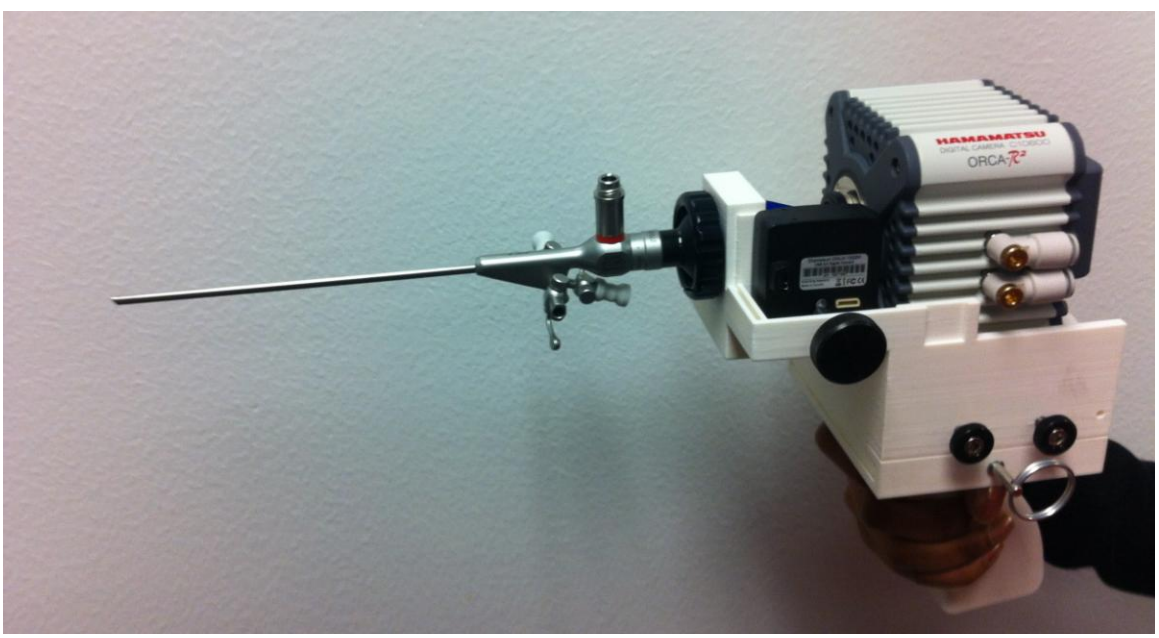

ABSTRACT

The aim of this project is to develop a robust optical housing for a molecular endoscope to capture real-time imaging of colorectal cancer cells used for research in mice. The two image channels hold separate cameras, and by using a dichroic mirror the light is split and reflected at 45° and the fluorescent light is transmitted through the mirror. The light splitting allows the cameras to simultaneously collect the reflectance and near-infrared fluorescence. The fluorescence images mark the positions of the fluorescent dyes linked to tumor cells while the reflectance intensity calibrates the geometry of the colon from the distal end of the scope to the tissues. Current colorectal research methods in mice require scoping the mouse twice with different filters and one camera. After the procedure the images are overlaid, however these images do not correctly match due to the different movement of the researcher while scoping the mice. The overlapping of non-congruent images leads to inaccurate geometry of the colon and therefore locations of cancerous polyps. The simultaneous image capture will correct the colon geometry and accurately specify the location of the cancerous cells. If successful, these research methods can help reduce the amount of missed colorectal cancer diagnoses.

INTRODUCTION

We will be working with Dr. Thomas Wang and the Michigan Network for Translational Research center (NTR) to develop a quantitative molecular endoscope for real time optical imaging of colorectal cancer. The endoscope housing and optical system is intended for immediate use by researchers in the molecular probes team of the NTR center who conduct experiments to validate fluorescence microendoscopy for imaging colonic dysplasia *in vivo* in mice.

Background

Colorectal cancer is the third most diagnosed form of cancer in the United States, and the third leading cause of cancer related deaths in the country. Most cases of colorectal cancer develop gradually from a growth or tumor in the epithelium of the colon. A polyp is a benign tumor that can potentially develop into cancer. Adenomatous polyps, or adenomas, are pre-cancerous polyps, and dysplasia is another pre-cancerous condition where the abnormal maturation of cells occurs in the colon or rectum lining [1].

Currently, white light endoscopy is used for cancer detection by detecting substantial changes in shape, color, or texture of the colon epithelial tissue [2]. However white light endoscopy is insensitive to changes on the molecular level that can develop as normal epithelium in the colon and then transform into dysplasia. Additionally, white light endoscopy does not have the capability to distinguish between dysplasia and hyperplasia. Hyperplasia is a normal response to a stimulus that usually results in benign tumors or organ enlargement instead of malignant conditions [3]. Average polyp miss rates with standard white light endoscopy have been reported as high as 22%, with flat and depressed lesions reported as being most challenging to identity [4].

Figure 1: Common adenomas; flat and depressed variations that are hardest to identify [5].

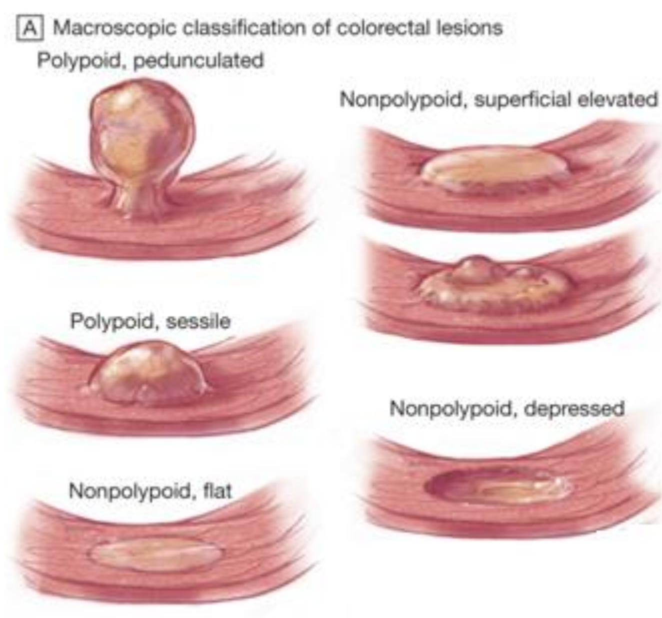

As the use of white light endoscopy alone fails to identify changes on the molecular level, the *in vivo* use of targeting agents with fluorescence dyes allows for more accurate and early detection of cancerous cells [2,4]. The capability of *in vivo* targeting agents and detection clearly surpasses standard white light endoscopy methods.

The Network for Translational Research (NTR) team at The University of Michigan has isolated a Near Infrared (NIR) labeled peptide with the amino acid sequence QPIHPNNM that is highly specific to colonic adenomas in mice models [2]. The mice subjects used are genetically engineered such that adenomas spontaneously developed in their distal colons and can be repeatedly used for cancer research.

Dr. Thomas Wang an M.D/Ph.D in internal medicine oversees the NTR research, and Supang Khondee and Bishnu Joshi conduct the experiments with the current research methods. Chien-hung Tseng and the other contacts were interviewed to understand project outcomes and requirements. Our main sponsor and team contacts are Dr. Thomas Wang and Chien-Hung Tseng at NTR center.

Current Procedures

For current experiments, the mouse is anesthetized and the colon is rinsed. A rigid Karl Storz small animal urethrocystoscope (Model 27030BA) is inserted, typically up to 5cm, into the distal colon of the mouse. The endoscope is mounted on an imaging system consisting of a grip and housing that holds a telescoping lens and CCD camera. The current research set-up is shown below in Fig. 2.

Figure 2: Demonstration of current single camera system with the endoscope attached.

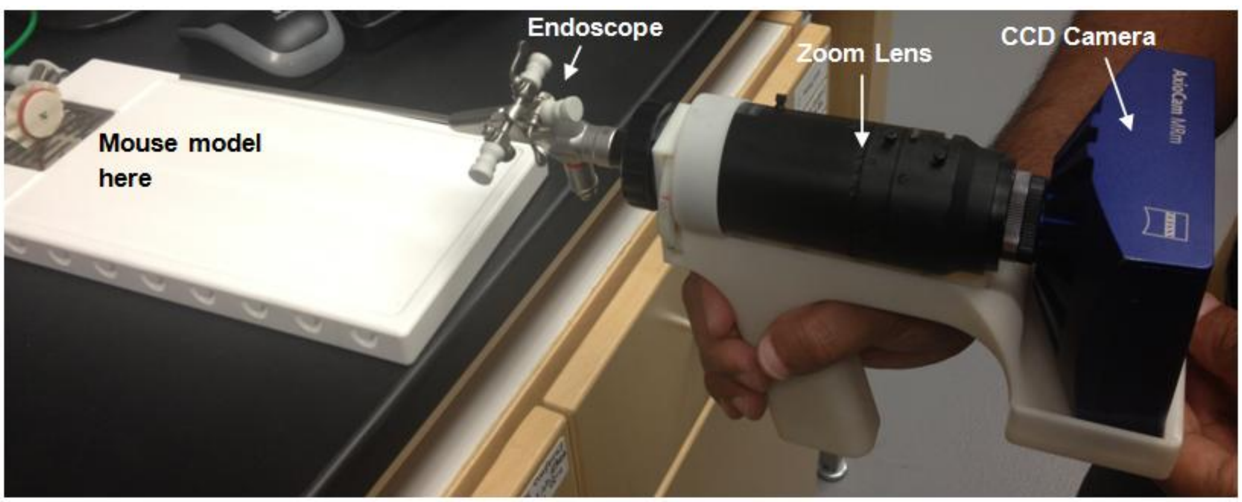

The endoscope has laser sources (wavelength of 671nm) for collecting imaging of the geometry of the colon and the location of the fluorescent polyps. Between the lens and the endoscope, there is a filter such that the camera can collect imagery for the white light and the fluorescence separately. First white light is used to locate lesions and regions of interest (ROIs). The fluorescent peptides are then delivered to the mouse colon and allowed to incubate for 5 minutes, and the model is rinsed again. White light reflectance and fluorescence images are captured consecutively for each adenoma [2]. The collected white light images with areas of ROIs are superimposed onto respective fluorescence images, and finally the images are analyzed using a Matlab program developed by NTR center researcher Duan Xiyu.

Project Motivation

The current research method used at the NTR center requires scoping the mouse twice so that white light and fluorescence images are captured separately [6, 7]. During the scopes, the colon and the path of the handheld scope do not remain static; therefore capturing images for the exact same region with the identical orientation has proved to be very difficult [7]. Additionally, overlapping these different images results in incorrect geometries of the mouse colon.

The raw NIR fluorescence intensities are greatly dependent on angle and distance from the closest tissue. Simultaneous and continuous collection of the light reflected from the laser and fluorescence can be used to correct the raw NIR signal which reduces the over or underestimation of fluorescence concentration significantly shown in Fig. 3 below [8].

In a clinical setting, real-time NIR endoscopy with corrected intensities and accurate superimposition of images will allow for effective identification of diseased regions in the colon epithelium [6]. The use of simultaneous image capture is especially pertinent for regions, which can only be identified with the help of fluorescence.

Figure 3: Corrected NIR intensity shows constant concentration for both cancerous foci at various distances [8].

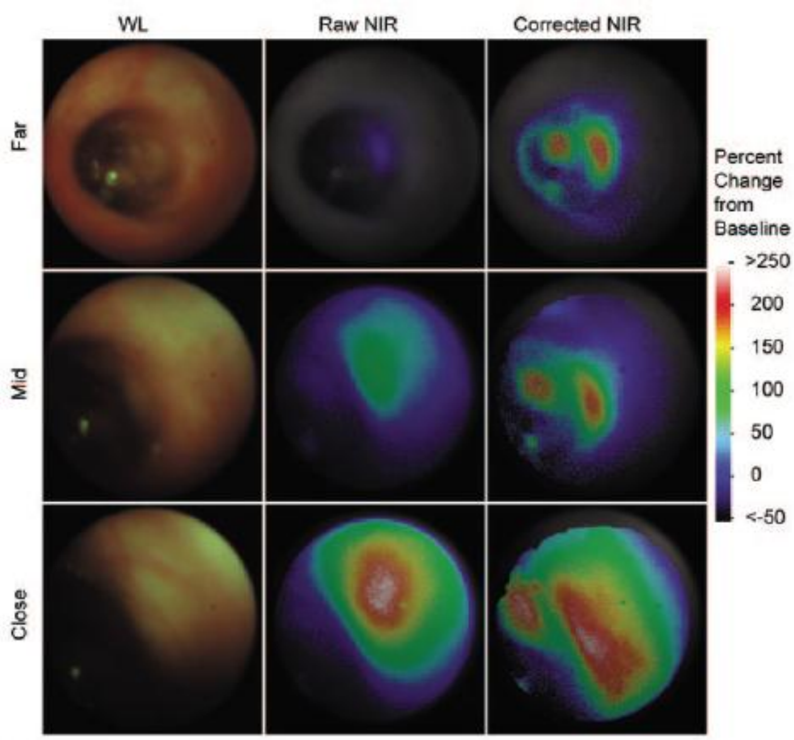

PROJECT DESCRIPTION

The aim of the quantitative molecular endoscope project is to improve the current NIR fluorescence imaging technique by developing an integrated system that will allow for simultaneous video capture of laser reflected light and fluorescence imagery. The project requirements are to design a robust optical housing that attaches to the molecular endoscope, and houses two cameras, a dichroic mirror, a convex lens, and a single bandpass filter for the fluorescent camera. Secondly, we aim to synchronize the real-time image capturing of the two cameras and update the existing Matlab code to standardize and superimpose the two types of images.

Technical Benchmarks

Along with the current single-camera system, a housing prototype implementing the double-camera system was built by a previous Mechanical Engineering 450 team. The single camera system, and the previous dual camera system shown below serve as technical benchmarks for our design. We gathered feedback on both designs from users Bishnu, who had also attempted some experiments with the housing prototype, Supang, and Dr. Thomas Wang.

The sponsor and researcher continue to use the single camera device, which has one large telescoping lens and a handle designed for ease of use. However, this design does not allow for the capture of reflection and fluorescence light images simultaneously. The researcher can only switch filters to see the reflection or fluorescence coming from the endoscope. The analysis program they use can overlap captured images but cannot correct for changes in position that occur because external movement of the researcher while scoping the mouse. A figure of the full demonstration with the one lens is seen in Fig. 2 on Pg. 8**.**

The 'box' prototype created by a previous Mechanical Engineering 450 team at The University of Michigan failed to meet many parameters established by the researchers and sponsors using the device. The design was too small to hold the new cameras, the casing for the dichroic glass was not sturdy, and the focal point of the lens was not calculated accurately and therefore the cameras had large slots to correct for focus. The shape of the prototype did not allow for enough clearance for filter connections to the endoscope at taps close to the box housing. Additionally, the team did not consider how the device would be handled during research. The design had no method for supporting or holding the housing, and therefore the design is unusable [9,10]. This feedback we received was used to develop our project requirements and engineering specifications described in the following sections.

Figure 4: Top (left) and front (right) view of previous ME450 design. The front view shows the attachment point for the endoscope, and the top view features slots for adjusting the cameras.

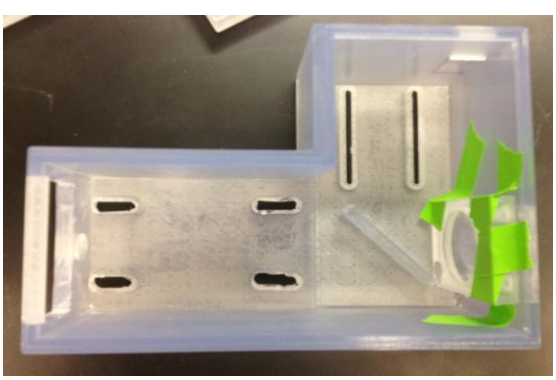

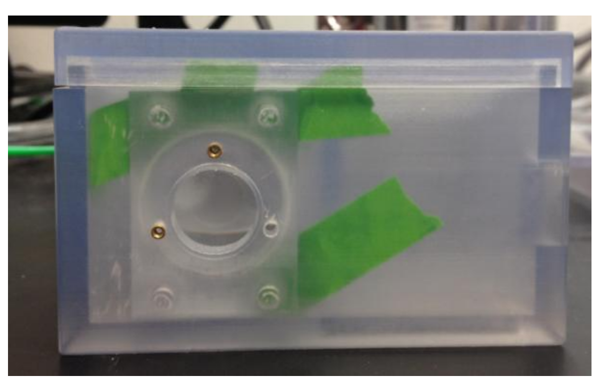

PROJECT REQUIREMENTS

The requirements for the endoscope imaging system include both dimensional specifications of the design and ergonomic factors that contribute to the ease of use for the researcher. The system needs to include two cameras specified by our sponsors, a dichroic mirror, a convex lens, and a single band pass filter for the fluorescent light. All of the optical components have strict dimensions that need to be accounted for in the design. The imaging system attaches to the endoscope that the researcher handles while inspecting the colon of the mice for cancerous cells.

A Point Grey Research (Chamelon CMLN-132SM) camera is to be used for reflected light capture, and requires a USB connection to the computer. Secondly, A Hamamatsu (ORCA-R^2 C10600) camera is used for fluorescence capture and has a Firewire connection to a Hamamatsu controller, which is then connected to the computer. The cameras are presented with their main dimensions in Fig. 5 below.

Figure 5: (Left) Image of the small Point Grey Chameleon CCD Camera 2.0 with specifications LXHXW 44mm X 41mm X 25.5mm. (Right) Image of the large ORCA-R^2 Digital CCD Camera with LXHXW specification measured as 95.45mm X 95.51mm X 66.53mm, and back extrusion with dimensions 58.93mm X 45.14mm X 23.69mm.

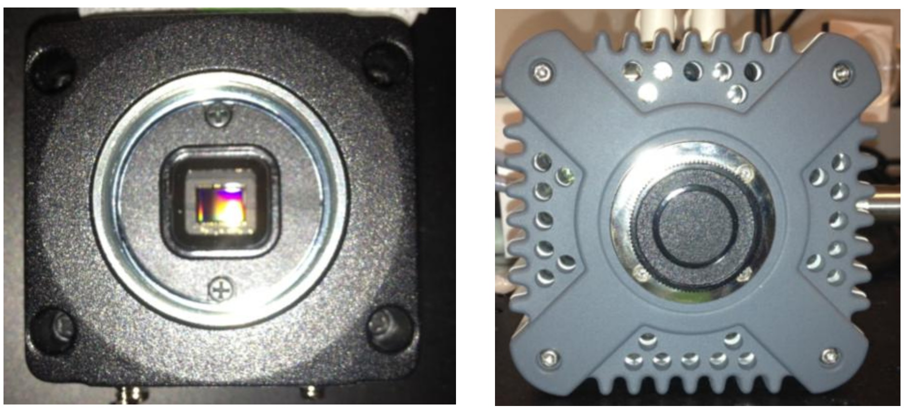

Our interviewees expressed a need for a robust, compact system with well-aligned optics. They prefer a handheld device to a system that rests on the table as the endoscope is usually moved around the distal end to locate lesions. The sponsors expressed a preference for the stable grip with the optics and camera resting above the housing as shown in Fig. 2 on Pg. 8 [7,9]. Each scope of the mouse colon can last up to 5 minutes for each procedure, therefore the device needs to be comfortable to hold and stable such that the weight of the device will not cause the research unnecessary movement.

Secondly, the cameras need to be synchronized so that the image capturing start and stops simultaneously. The Point Grey Research camera comes with the software FlyCap2, while the Hamamatsu camera comes with HCImage Live, therefore the existing Matlab program that processes the captured images needs to be updated to use the different software and superimpose the images accurately [6, 7]. We intend to explore trigger settings in the two image capture programs to synchronize the images and the time frames. Differences in image sizes and pixels as well as phase changes (rotation) due to optics will have to be accounted for while updating the Matlab code before the images can be properly superimposed.

Engineering Specifications

The engineering specifications were determined based on the needs of the researcher using the device, the dimensional parameters of the cameras, dichroic mirror, and lens needed for the design, and the method in which the endoscope and imaging system is used during experimental studies/procedures.

Minimize Focal Length

The focal length and diameter of the convex lens are both important engineering specifications for the design, as these parameters affect the final volume and total mass of the housing. The focal length of the lens determines the distance between the beginning of the housing where the endoscope is attached and the position of the cameras. A lens with a shorter focal length will have a shorter distance between the endoscope and the cameras, and therefore a smaller volume of the housing. The focal length of the lens used in the previous design is 50mm, and we aim to use a lens with a focal length between 20 and 50mm. The lower bound for the focal length was established from the low availability of 1 inch diameter convex lenses from ThorLabs.

The image in Fig. 6 demonstrates the reflecting and transmission of light, which will be used in the optical system of the quantitative molecular endoscope. Additionally, the sponsor advised us to purchase a lens with 25.4 mm diameter. This lens needs to be the same size of the lens of the endoscope such that the diverging light coming from the endoscope is converged immediately. Any lens smaller than 25.4mm would allow light to diverge and scatter outside of the optical system.

Figure 6: Beam splitting off of a dichroic mirror. Focal length is the distance between the first and second lenses. For the light reflected off the mirror, focal distance is the addition of the light before and after the mirror.

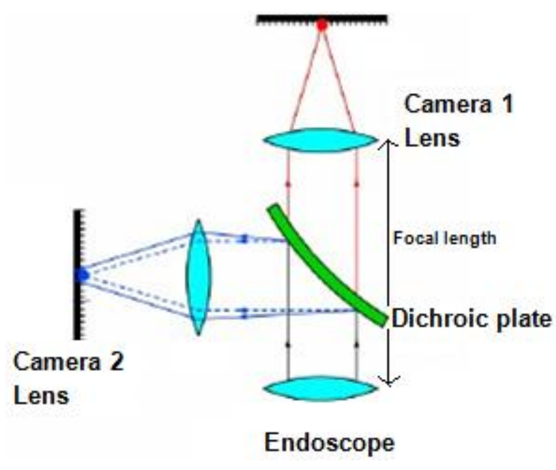

Minimize Total Mass

The main project requirements are for the optical housing to be lightweight, maneuverable, and handheld. Interpolating these requirements into engineering specifications, we need to design a system and choose a material with the least possible total mass. However, we have two main constraints for total mass. The mass of the ORCA-R^2 Hamamatsu Digital CCD camera is 1100 grams, and the mass of the Chameleon CCD Camera is 37 grams. Therefore our final housing will have a mass greater than 1150 grams. We aim to design and fabricate a system with a total mass slightly greater than the mass of the two cameras.

To develop an upper mass constraint, we measured the mass of the previous ME450 team's 'box' prototype. The prototype has a mass of 170 grams. Since the cameras used for the 'box' prototype are both smaller than the cameras intended for the new design, the new housing model will be a larger design and therefore have a greater mass. Additionally, to allow for a handle and enclosed tunnels to prevent light scattering, the upper constraint for the mass is 2000 grams. Therefore, there is 850 grams to allow for variation in the design of our system, the materials we decide to use, and the complexity of the adjustment platforms we have considered.

Minimize Total Volume

The project requirement for the housing to be lightweight, maneuverable, and handheld motivates us to minimize the total volume of the housing as well as the total mass. We intend to design and fabricate a housing that is compact and small enough to comfortably use and maneuver during the research procedures. The existing 'box' prototype has a volume of $3.28x10^{-4}$ m^3, but this volume accounts for two much smaller cameras. For the new design, the volume of the Hamamatsu camera is $6.7x10^{-4}$ m^3 and the volume of the Chameleon camera is $3.4x10^{-5}$ m^3 in Fig. 5 on Pg. 11. Therefore, the new housing model must have a volume greater than $7.035x10^{-4}$ m^3, which is already a larger volume than the existing model.

Figure 7: Dimensioned drawing to qualify how we calculated the maximum storage volume.

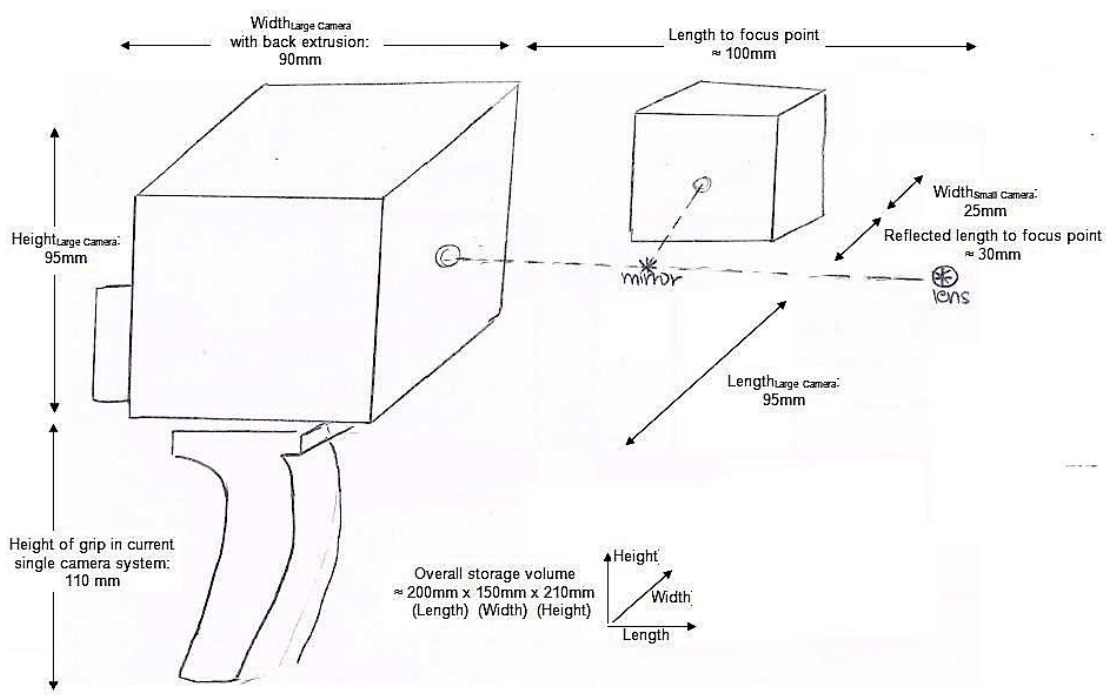

For our design to meet other project requirements we need to have a handling system and other grips to hold the optical housing. Additionally we discovered that the light channels would be longer than the focal lengths of the lens, because the focus points of the cameras is at a farther distance from the first lens than the focal length. Furthermore, we decided to define the volume as the total maximum storage volume that could contain the entire optical system.

The diagram in Figure 7, illustrates how we calculated the new volume specification. The height was calculated by measuring the height of the handle used in the one camera system, shown on Fig. 2 on Pg. 8, and added the height of the larger camera. To measure the width, we measured the width of the larger camera and added the width of the smaller camera. Additionally for the width measurement, we added the approximate focus length for the smaller camera. Then to find the length, we measured the length of the larger camera, the larger camera's extrusion and added the approximate maximum distance for the focus point of the camera based on the focal length of the larger lens and input from our sponsor. Finally, we calculated the dimensions of the maximum storage volume to be 200mm (L) by 150mm (W) by 210 mm (H). The final maximum storage volume is $6.3x10^{-3}m^3$.

The benchmark designs have a smaller total mass and total volume, however, the new design incorporates larger cameras. The differences in these measurements are also accounted for in the QFD diagram below on Pg. 15.

Maximum Material Deflection

As we started to build the mock up for our optical housing we identified additional engineering specifications that were crucial for the success of our design. The focus measurements for the two cameras and the optical alignments of the first lens, the dichroic mirror, the band pass filter, and the camera lenses are crucial aspects needed to produce a usable image of the mouse colon. As shown above in Fig. 7 on Pg. 13, the handle for the system is approximately 210mm away from the end of the base plate. This distance does not account for the length of the endoscope, which is approximately 250mm**.** Depending on the choice of the material and the mass of the endoscope, it is probable that the material could experience a deflection near the end of the housing, a distance approximately 210mm from the handle. However, a deflection of the material would interfere with the optical alignment of the front lens, the filter, and the camera lens. The platform connecting the front face of the Hamamatsu camera and the main lens is where the deflection of the material might occur. Therefore, we aim to choose a material and a design that will limit or negate the possibility of deflection. In order to give a realistic parameter, we determined that the housing material had to have a deflection of less than 2mm at the lens housing, for the image quality and the optical alignment to be successful.

Optical and Ergonomic Specifications

Our aim is to design and build a system such that the cameras will be able to move precise increments for easy focus adjustments. Additionally, the design must rigidly enclose all optical components such that exterior movement of the researcher will not cause the cameras to move out of focus. Any movement of the lens, cameras, or dichroic mirror would result in bad image quality and require reexamining the mouse. Furthermore, we have to encase the optical components without damaging the lens, dichroic mirror, or the filter. Secondly, we want to develop a handle/grip system that will allow the researcher to hold and balance the endoscope and cameras in the correct position without the hassle of holding a large and heavy object during the experiments.

QFD

The following diagram presents our design requirements and the engineering specification compared to our design and the previous designs used by the NTR researchers. The numerical weights of the requirements evaluate how the engineering specifications meet those requirements. Additionally, the rating system for the design comparison shows how the current models relate to our design. As stated above, the two existing methods have a smaller mass and volume because they do not require the larger camera. A rating of 10 indicates higher priority. For the engineering specifications, the importance rating is 1-3 where 1 is the most important.

	Weight	Total Mass	Total Volume	Focal Length	Maximum Material Deflection	**Design Comparison**	Future Optical Housing	Previous ME450	Single Camera
Project Requirements	**Rated 1-10**					**Rated 0-5**			
Lightweight	**9**	10	8	5	3		3	4	4
Hand Held	**9**	6	9	6	3		4	0	5
Ease of Use/ Maneuverable	**9**	10	9	7	3		4	2	5
Accurate Optical Alignment	**8**	6	4	10	10		5	1	4
Reduces Scatter	**6**	3	5	9	7		4	2	5
Imports images simultaneously and overlays the images correctly	**10**	-	-	7	10		4	0	0
Total	51	35	35	44	36				
Normalized	1	.69	.69	.77	.71				
Importance Rating	**1-4**	2	3	4	1				
Measurement Unit	-	g	m^3	mm	mm				
Future Optical Housing		1150-1450	$8.7x10^{-4}$ $1.3x10^{-3}$	20-50	0-2				
Previous ME450 Prototype		170	$3.3x10^{-4}$	50	-				
Single Camera &Telescoping Lens System		-	-	-	-				

Final Engineering Specifications

The final engineering specifications are cited below. The deflection is measured at a point 60mm away from the Hamamatsu camera along the main base platform.

Table 1: Summary of project requirements and specifications

Engineering Specification	Proposed
Total Mass	1150g ≤ m ≤ 2000g
Maximum Storage Volume	.006375 m^3
Maximum deflection from Hamamatsu camera to endoscope attachment	≤ 2mm
Focal Length	30mm ≤ f ≤ 50mm

CONCEPT GENERATION

Functional Decomposition

The function decomposition in Fig. 8 on Pg. 17 demonstrates the flow of inputs and outputs of our system and the flow of information, materials, and power. The main input for the quantitative endoscope for real-time fluorescent and reflectance imaging is the laser and the power inputs for the two cameras. After the laser enters the endoscope and travels into the mouse, the laser hits the targeted areas in the mouse colon and reflects light back through the endoscope. After light exits the endoscope, the diverging light is immediately converged through the first lens. The light is then transmitted and reflected off of the dichroic mirror. The reflected light is captured by the Point Grey Research camera and transmitted to the computer software for visualizing. Simultaneously, the transmitted light wavelength is filtered through the single band pass filter and then captured by the Hamamatsu camera and electrically transmitted to the computer software for viewing. The viewer/researcher observes the image for the focus and image quality. If the focus needs adjusting, the user will mechanically adjust the cameras position by moving the camera through the manufactured slots. After the cameras are repositioned the light will be captured by the two cameras and again electrically transmitted to the camera software for screening.

Concept Selection Process

During the brainstorming process, we discussed different sections of the functional decomposition diagram and how we could satisfy each requirement. For example, we discussed multiple possibilities concerning how the lens would fit into our system. We talked about putting the lens into a separate piece that would allow the lens to snap in and be secure, but we also considered building the lens holder into the platform design that would have a slot that the lens could be placed into. Using this process allowed us to generate a multitude of ideas for each section of the flow chart. We then generated design concepts individually piecing together different combinations of ideas we had produced to satisfy the system requirements. The following pictures are sketches of what we considered to be our top 5 design concepts. For other design concepts see Appendix E on Pg.'s 71-74.

Figure 8: Functional decomposition of system

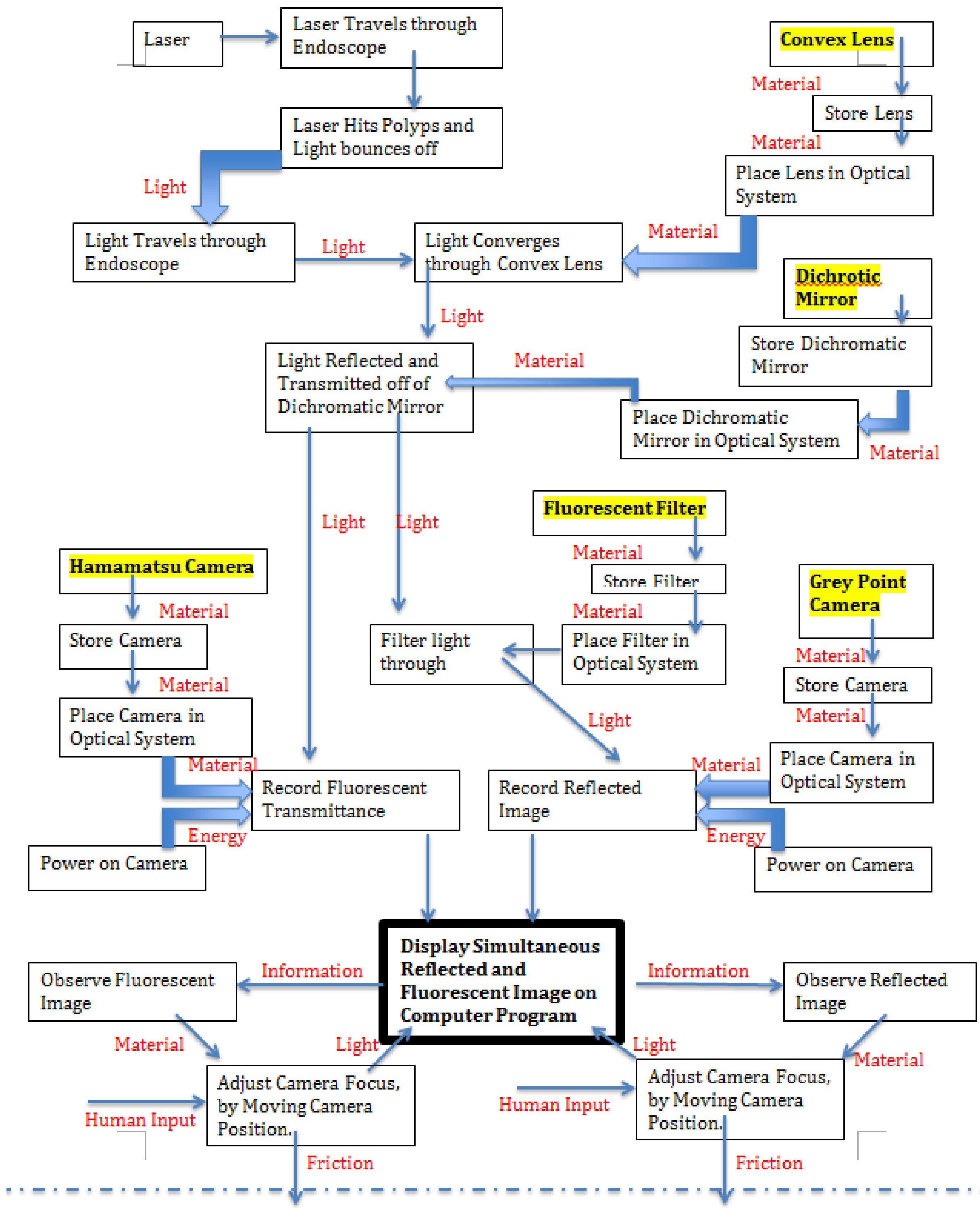

Design 1: Arm Rest Design

The Arm Rest design provides an alternate way of holding the system. The design features an armrest and a handle closer to the distal end of the system. The Hamamatsu camera sits directly on an armrest constructed to rest on the forearm shown below in Fig. 9. The rest has a flat top that allows the camera to sit rigidly, fixed onto grooved pathways. A simple focus adjustment system is integrated into the base. A tuning screw at the back of the camera allows for slight forward adjustments while the front of the camera pushes against springs for backwards adjustments when the screw is reversed. A cage-like frame, also fixed onto the base, securely wraps around the camera. The design also features enclosed optical tunnels with housings for the filter, mirror, and lens extend from the baseplate and frame. There is a small gap between the fluorescent camera lens and filter so that the frame and optical housing stays in place when the camera is adjusted. The Point Grey camera is fastened by a frame projecting from the optical housing. A simple slot and pin or setscrew system is integrated into the camera for adjustments. A second handle under the position of the dichroic mirror provides a point of control. The handle additionally functions as a second supporting point that averts deflection as the entire length of the housing and endoscope will no longer simulate a cantilevered beam.

Figure 9: Annotated sketch of Arm Rest design

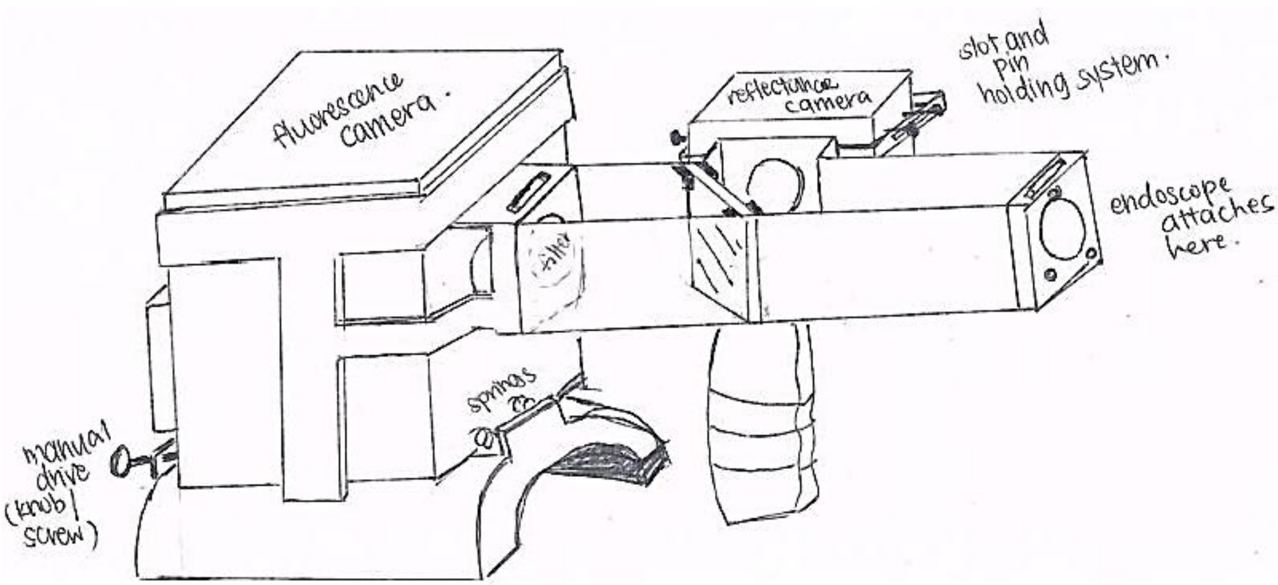

The above design incorporates tunnels that help prevent light scattering. The armrest helps distribute the weight of the larger camera by resting on the users forearm. However, from an ergonomic standpoint, resting 1.1kg on a users forearm could cause more strain and discomfort than holding the weight in ones hand. Maneuvering the endoscope with the users forearm forced to lie parallel and under the optical channel will be less flexible than doing so with a single grip. Additionally, the size of the camera requires the armrest to be much larger than a standard users forearm, which could make the system unbalanced and potentially tip over. Finally, the system in general is quite bulky. However, in our final design considerations the simple mechanical focus system shown here has potential to be included in our alpha design.

Design 2: Linear stage with light tunnels

The second design shown in Fig. 10 features a linear stage capable of making fine adjustments for the Hamamatsu camera's position. The filter will be placed in a holder and will be fixed on the stage as close as possible to the lens of the camera. The second design also includes closed optical channels between the optical components to prevent light scattering. The stage sits on a handle and base plate that extends to form the main optical tunnels. The tunnels are slightly smaller than the ends that project from the filter and the frame holding the smaller camera. The channels form a groove-sliding system for position adjustments of both cameras while keeping the main optical channel with lens and mirror fixed. A small foam or contoured rest under the base and close to the front end of the system gives a second support to increase stability and prevent deflection during the procedure.

While researching linear stages that had load capacities of 1kg, we found that the linear stages themselves have significant weight. Using this system could cause us to surpass our mass specifications. The linear stage offers an accurate but expensive focus adjustment system that is likely superfluous, as the Hamamatsu camera would probably be checked for focus once, fixed, and left unaltered for consecutive lab tests. The stage, which would require connecting plates from the camera and to the handle/base, will add significant height and consequently, volume to the design.

Figure 10: Labeled sketch of Design 2 that incorporates a linear stage

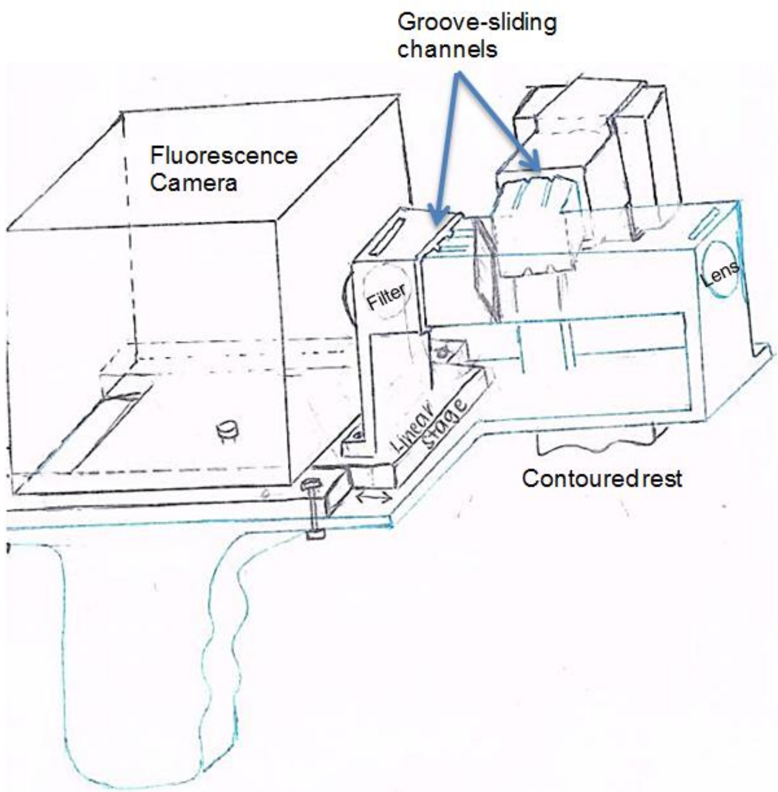

Design 3: Modified "Box" Model

The modified "box" model is a design modeled after the previous ME450 team's design. Besides the features discussed in the *Technical Benchmarks* section on Pg. 10, the modified "Box" design has the capability to hold the larger cameras and adjust the position of these cameras using slots and lead screws. Each camera also has two screws on either side of the container to secure the cameras after the final position has been achieved. The modified "box" additionally has a handle for comfort and a hand rest towards the distal end of the optical system for balance. Finally the modified "box" model uses lens holders for the fluorescent filter and convex lens, and a sturdy frame for the dichroic mirror, all of which the original "box" model did not feature. We used this model to evaluate all the newer and more advanced designs because this concept features all the basic needs of the device. The following labeled drawing indicates all the features specified.

Figure 11: Drawing for the modified "Box" design. Note in this drawing the cameras are not included in the model. Arrows are used to indicate the position of the cameras.

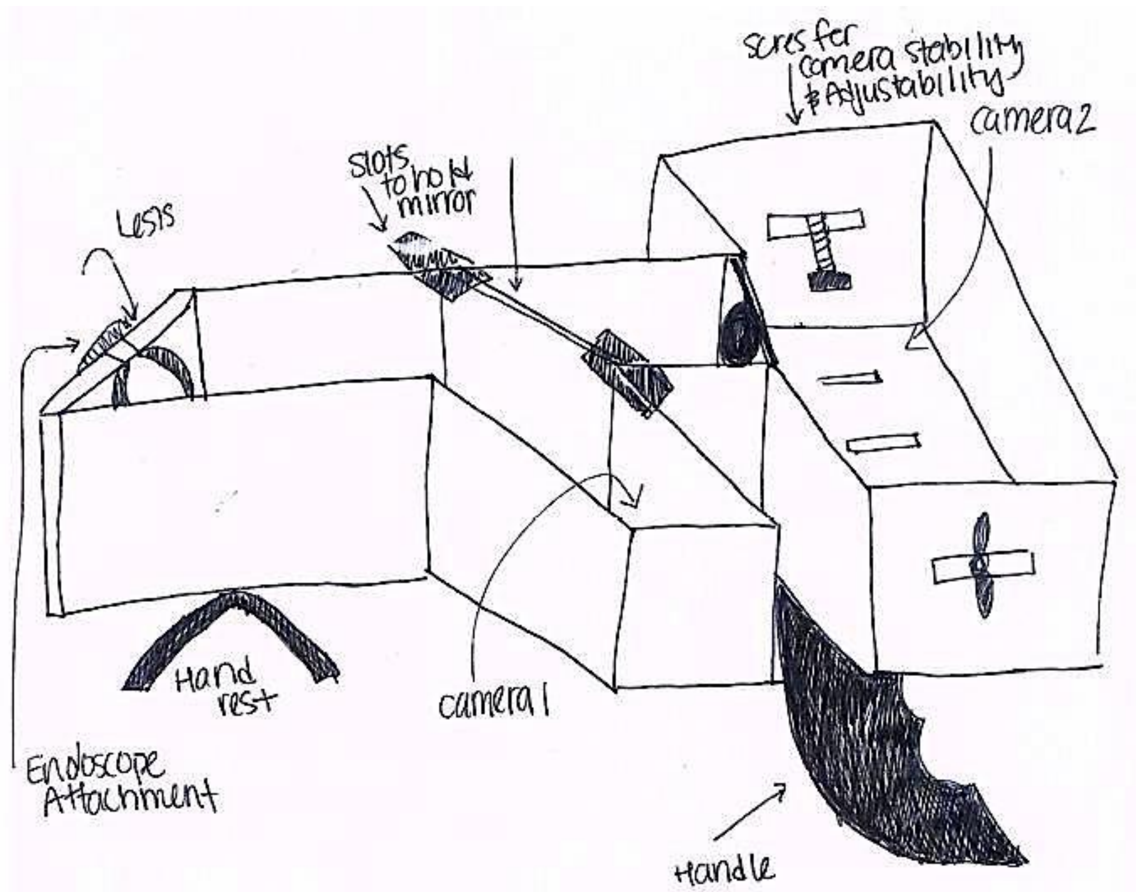

Design 4: Detachable Handle

This design features a detachable handle on Fig. 12. It will be attached to the housing by means of customized tracks that have been designed into the housing and the handle. The handle will also have three triangular extensions, with an additional small square extension, rising from the back end of the handle that will snap in to the housing. The housing will have three indents to receive the triangular snaps. When the handle is detached, the whole platform can then be attached to a tripod with a bolt connected to the tripod that screws through the base platform of the housing and directly into the Hamamatsu camera. Each camera will have slots beneath them. They will be accompanied by L-brackets placed behind the cameras. The L-brackets will have threaded holes that will allow a tuning screw to push the camera forwards to adjust focus. The cameras will then be tightened on the sides or from the slot area on the bottom.

The open circular platform will allow for easy access to the dichroic mirror and lens holder. The dichroic mirror will be placed in a padded holder with a tightening mechanism that can be put into a designed slot on the platform. The lens holder will be slotted in the shape of our lens so the lens will not move during the procedure. The housing has sloped walls in order to minimize the total mass. The downside to this design is that aligning the optical components would be difficult because of the geometry of the open platform and channeled areas for the cameras.

Figure 12: Labeled sketch of Detachable Handle with Tripod Adapter design

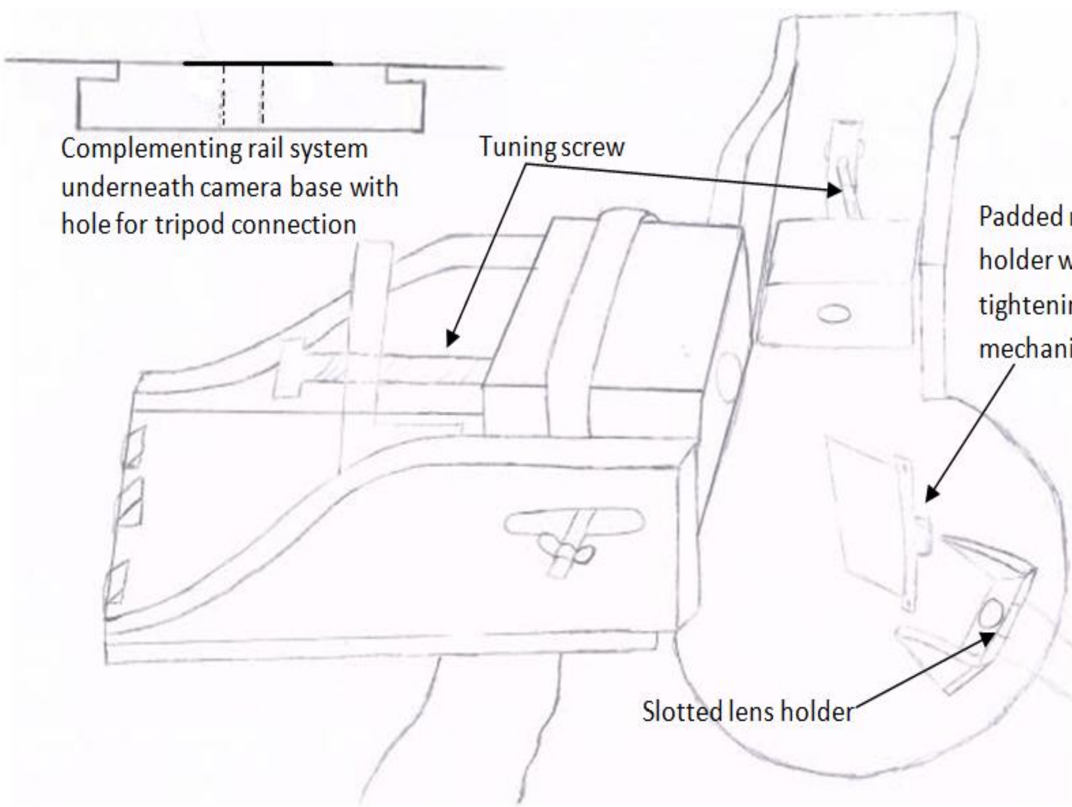

Figure 13: Additional sketch of detachable handle

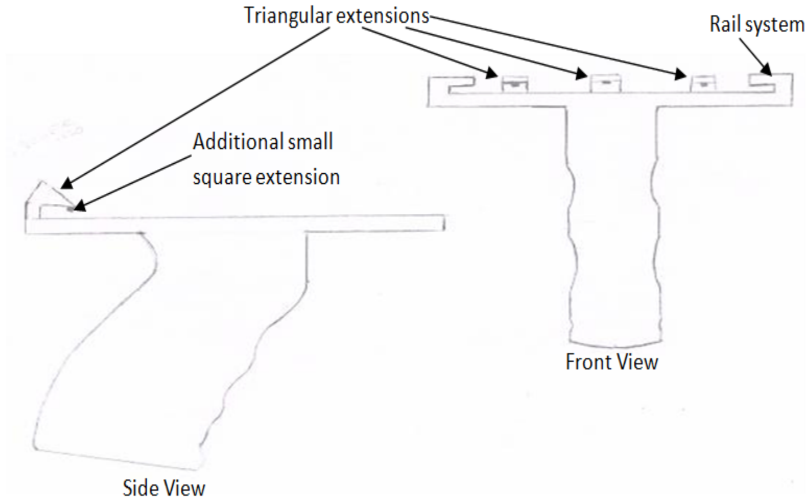

Design 5: Telescoping Lens

For one of the final designs in our concept generation process we revisited the simplistic use of slots for the adjustments needed for the Hamamatsu and Grey Point Research camera. This design features a lens cap that twists onto the Hamamatsu camera and positions the filter directly in front of the lens. Design 5 additionally features light channels, which can extend to the final position of the camera. The light channels connected to the lens and the dichroic mirror is rigid, but the end of the channels before reaching the camera can adjust to meet the adjusted position of the cameras. After the camera is adjusted, the tunnels can be latched into place by "bungee cord" connectors that are attached to the camera fixture. Finally, design 5 features a rigid handle attached to the base plate and underneath the Hamamatsu camera.

Figure 14: The following drawing is the mock up for the fifth final design for the quantitative endoscope project.

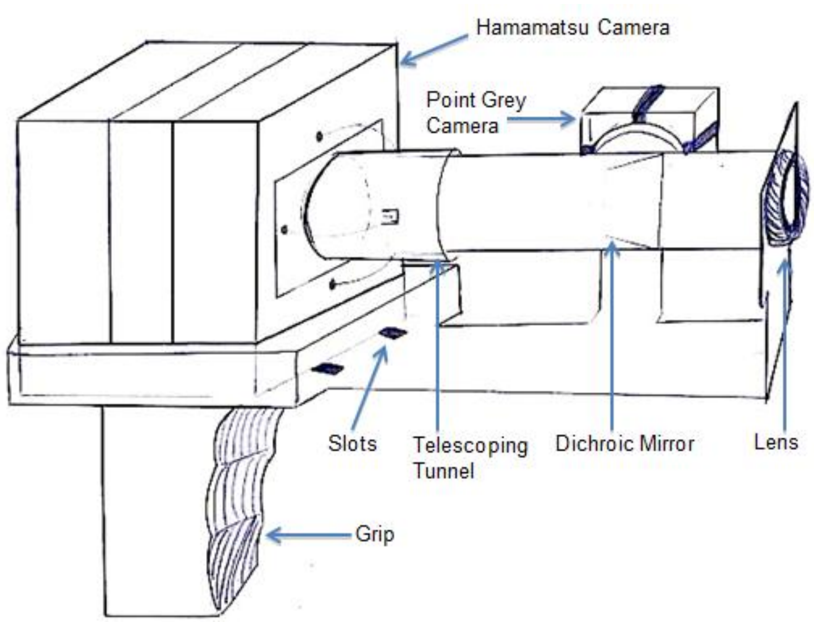

CONCEPT SELECTION

In order to properly evaluate our design, we used a Pugh chart. We came up with a list of criteria that each design would be judged on. We gave each criterion a weight ranging from 1-5, 1 being the least important and 5 being the most important factors to take into consideration for our Alpha design. For our datum, we used the previous ME 450 “box” design on Fig. 4, Pg. 10 with the added capability of holding the Hamamatsu and Point Grey Research camera.

We considered camera adjustability, ease of aligning optics, and the fastening of optical components as our most important factors. Even though we decided incremental movement isn't necessary for both cameras based on our sponsor’s feedback, we still need the cameras to be adjustable. If the system is not adjustable and the measurements are off even a small amount, than the focus of the cameras, and therefore the quality of the images, will not be acceptable when the two images are superimposed. The optics in our system must have the capability of being easily aligned. If they do not have this capability, we will spend an excessive amount of time determining exactly where these components have to be. If the system has a channel or tube that the components are being placed in, the alignment will be easier. In addition, the optical components must be tightly fastened to the device, as one small deviation from its expected position could throw off the mid-plane optical axis and therefore cut off some of the image gathered from the endoscope.

Our design must also have a stable grip that can be held and an overall mass and volume that have been minimized. Furthermore, the system should be easy to assemble when the researchers need to perform a test. Having the system be capable of attaching to a tripod is not essential to our Alpha design, but would be a beneficial accessory to include. Being able to store our design in a suitable manner and constructing our device so manufacturing and assembly are not difficult will also be considered. Based on these ideas we then evaluated our designs on the Pugh chart below.

Figure 15: Pugh Chart evaluating our 5 top concepts. All of our design concepts scored above the datum.

			1	2	3	4	5
Description		Modified 450 Design (Incorporating bigger cameras)	Arm rest system	Hamamatsu on linear stage with tunnel system between lenses	Modified "box" design with slot adjustments with tuning screw	Detachable handle with tripod adapter	Preventative light scattering tunnel
Sketch			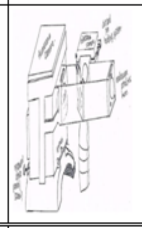	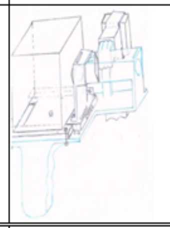	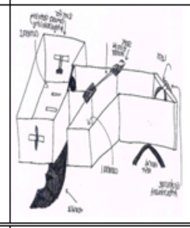	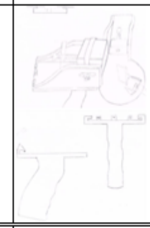	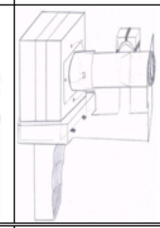
Criteria	Weight	Datum	Design 1	Design 2	Design 3	Design 4	Design 5
Camera adjustablilty	5	0	1	1	0	1	0
Stable grip	4	0	1	1	1	1	1
Overall mass	4	0	0	-1	0	1	1
Overall volume	3	0	1	1	0	1	1
Ease of manufacturing/assembly	2	0	-1	-1	0	-1	-1
Ease assembling required components	4	0	-1	1	0	0	0
Ease of aligning optics	5	0	1	1	0	-1	1
Storage	2	0	0	0	0	1	0
Adaptability for tripod	3	0	0	0	0	1	0
Fastening for optical component stability	5	0	1	1	0	-1	1
+		0	19	23	4	18	21
0		0	3	2	9	1	4
-		0	6	6	0	12	2
Net Score		0	13	17	4	6	19

All of our design concepts scored above the datum (Modified 450 Design). Although design 5 scored the highest value, we decided to incorporate ideas from other designs that we felt would make the best possible Alpha design while satisfying the customer specifications and engineering requirements.

THE ALPHA DESIGN

The Alpha design incorporates telescoping tunnels found in Design Concept 5 in Fig. 14 on Pg. 22, a dovetail mechanism for the adjustment of the Hamamatsu camera, slot adjustments for the Point Grey Research Camera, and a detachable handle utilizing the rail system from Design Concept 4 in Fig. 13 on Pg. 21.

Figure 16: Annotated sketch of the Alpha design

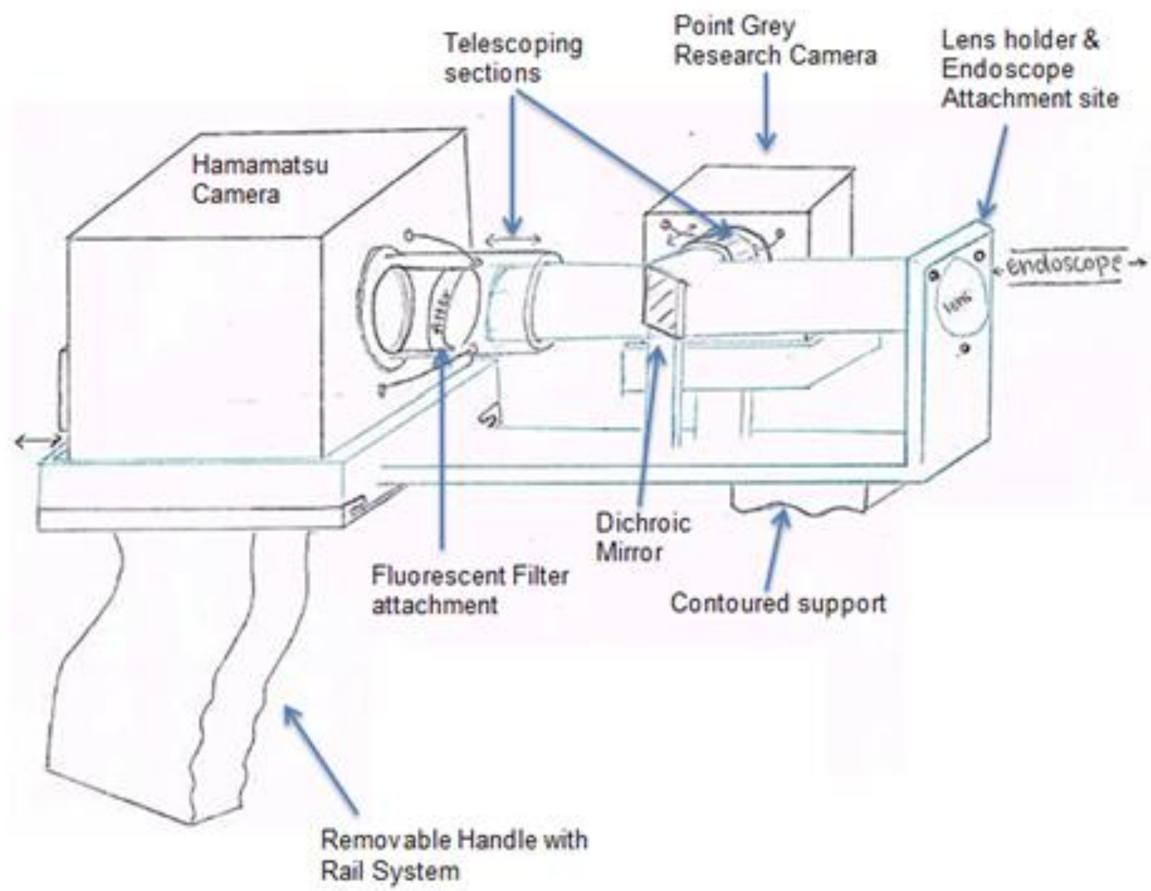

The Hamamatsu and Point Grey Research cameras, the lens, the endoscope attachment site, the dichroic mirror, and the optical channels are integrated into a single base plate. The dichroic mirror is positioned at a 45 angle and rigidly supported by the base plate. The light channels enclose the dichroic mirror from all directions. The Hamamatsu camera is positioned directly behind the lens and captures the fluorescent light transmitted through the dichroic mirror. The Point Grey camera is at a right angle, and captures the reflected light off of the dichroic mirror. Additionally, the Point Grey camera sits on an elevated platform connected to the base plate such that the lens of the smaller camera is on the same plane as the main lens, and second camera lens. As shown in the diagram above, the main lens is encased in a custom lens holder attached to the front wall. Taps for the endoscope connections will be made around the lens on the front wall. Finally, The midpoint of the lens, mirror, and both cameras lenses are all positioned on the same optical axis.

A slot and tuning screw system is used to adjust the focus of the Point Grey camera. On the platform where the camera sits there will be two slots through which the camera will be secured using the existing screws on the bottom of the camera. A lead screw through a threaded hole in the wall behind the camera adjusts position.

The Hamamatsu camera uses a more sophisticated dovetail sliding joint for adjustments which better accommodates the camera's much heavier mass and broader base. There is a ¼-20 UNC hole of 5 threads in the base of this camera. Utilizing this hole, the camera will be fixed onto a sliding plate. The plate then sits in the sliding hole with a complementary shape on the main base plate. The camera has one degree of freedom to slide backwards and forwards. Set screws reach the sliding plate and secure the camera in the final position. Like the railway system of Design Concept 4 shown in Fig. 13 on Pg. 22 the base plate will feature a complementary sliding joint that will accommodate the removable handle and adaptor for a tripod.

Figure 17: Dovetail sliding joint and removable handle

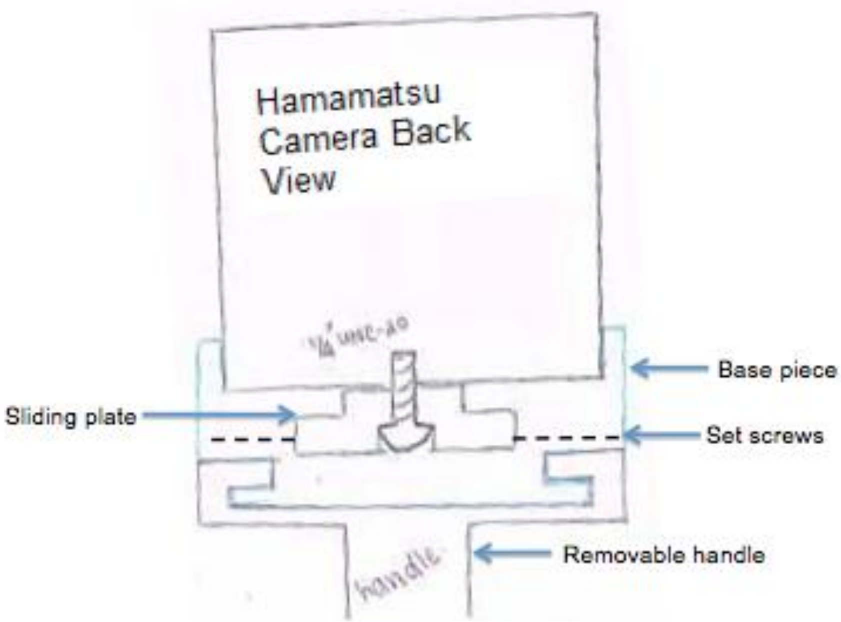

The single band pass filter for the fluorescent light will be fixed directly onto the Hamamatsu camera in this design. The Hamamatsu camera has a rim around the lens hole that is threaded. The filter's housing can be screwed right onto this threaded rim.

Figure 18: Filter housing and threaded rim of Hamamatsu camera

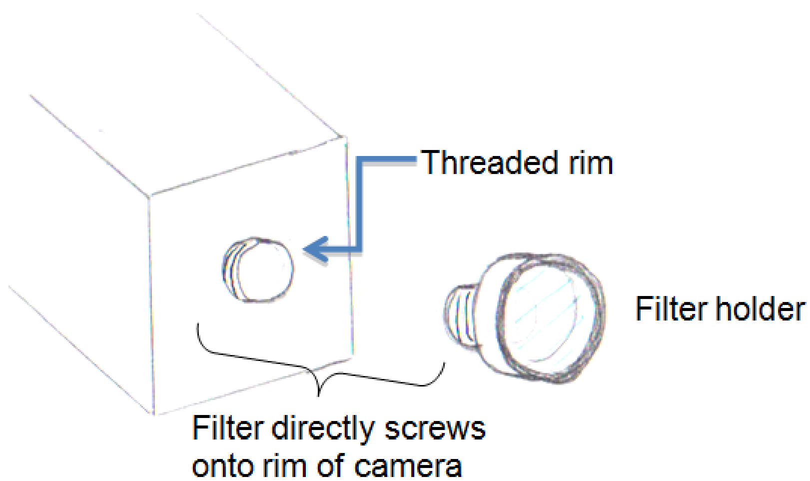

Light scattering is effectively prevented using the telescoping tunnels idea from Design Concept 5 shown in Fig. 14 on Pg. 22. These tunnels are found at both ends of the main optical channels and reach the two cameras. If either camera is adjusted, the corresponding telescoping tunnel will slid to meet the new camera position. Small fasteners from the camera face can be used to hold the channel in place against the camera after final focus positions are found.

Figure 19: Annotated sketch of telescoping tunnel to prevent light scatter

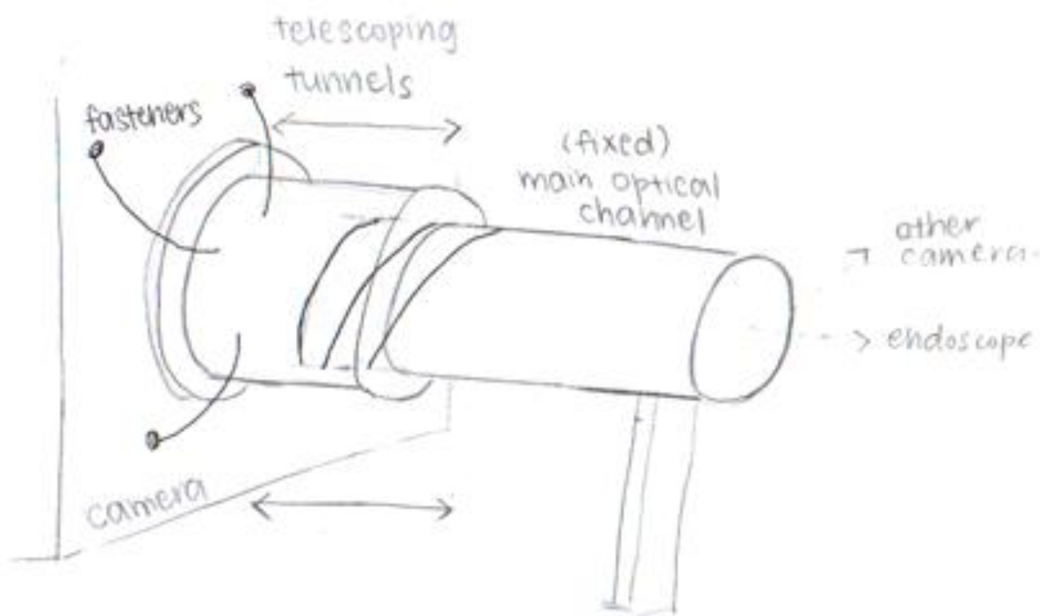

Figure 20: Top down view of cameras and telescoping tunnel adjustments

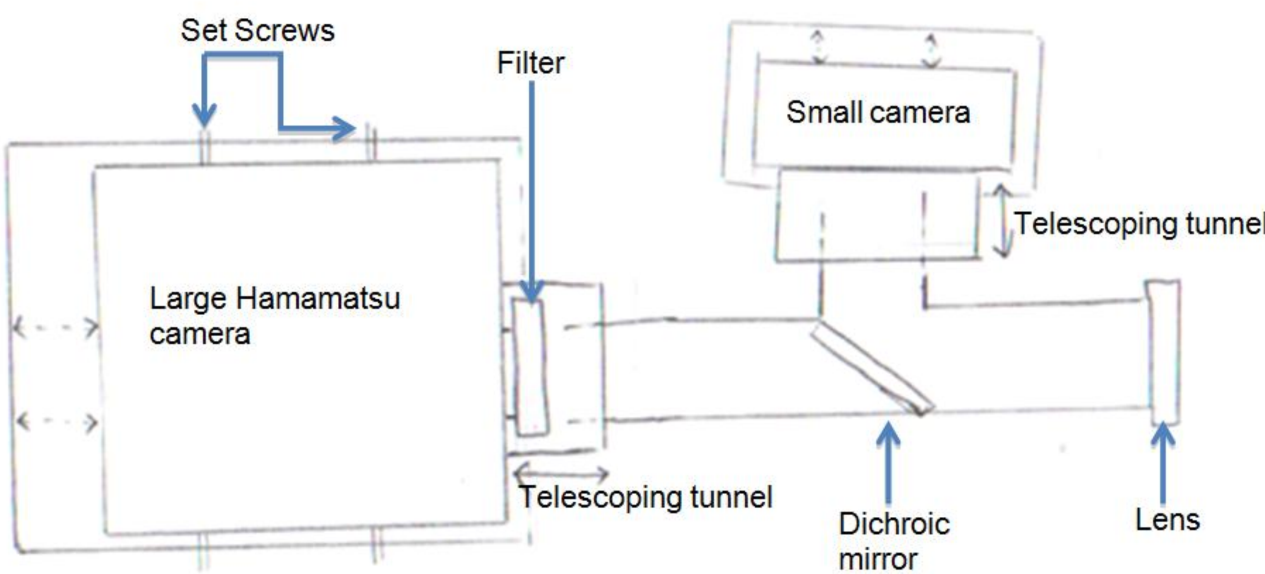

Alpha design Prototype

A physical model of the Alpha design was initially constructed out of cardboard and paper. The prototype helped us to see the potential of the dovetail and railway system and made our design more compact and adaptable than we had first envisioned. However, the modelling also illustrated that integrating a square mirror with vertical support from the base into cylindrical tunnels is going to be a challenge. A possible solution we discussed is making the section of the optical tunnels square where the mirror is situated. Options will be explored more thoroughly during the CAD process in the coming week.

Figure 21: Prototype of Alpha design

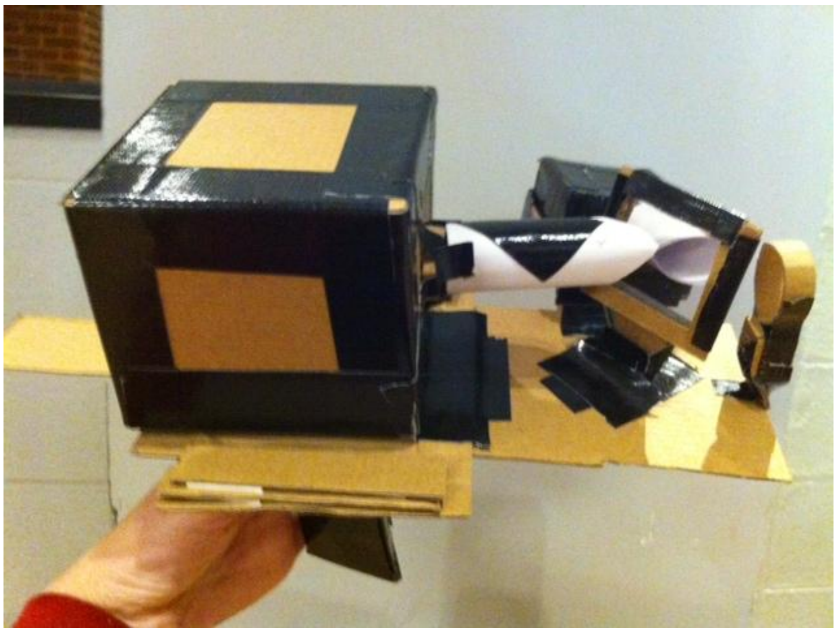

PARAMETER ANALYSIS

Optical Experimentation

After Design Review 2, we preformed optical experiments to determine focus points of the Hamamatsu and Point Grey Research cameras on October 22nd at our sponsor's laser laboratory in the Biomedical Science Research Center.

All optical components were mounted on ThorLabs optical holders available in the laser lab. The Hamamatsu camera was mounted on a linear stage to enable position adjustments. Then the filter was placed right up against the camera lens because it needs to be as close to the camera as possible. The height of all the optical components was adjusted so that the optical axis (their midpoints) is aligned. Forks held instruments in place on an optical breadboard.

First, the 35, 40 and 50mm lenses were tested. Laser light at 671nm was emitted from the tip of the endoscope at a plate with fluorescent beads. The lenses were leveled with respect to the endoscope in a ThorLabs lens holder. A white card was held behind the lens to gauge the focal point. The focal point occurred at a very short distance after the lens for the 35mm and 40mm lenses. This meant that the camera positions would be too close to the lens to be feasible. A

100mm lens was tested for reference. It resulted in a unfocused spot on the card at a far distance from the lens. The internal optics of the endoscope causes the exiting light to diverge, resulting in these ambiguous focal points. Ideally, the light exiting would be collinear light and the observed focal point would correspond to the product's listed focal lengths of 35, 40, 50 and 100 mm respectively. [11]

The best result was achieved with a 50mm lens. A distinct focal point was observed at about two inches from the lens, indicating feasible distances for the other optical components. Additionally, the 50mm lens satisfies our engineering specification for focal length to be between 20mm-50mm. Fig. 22 below shows the partial set-up used during the lens testing.

Figure 22: Partial set-up for optical experimentation excluding the Point Grey camera.

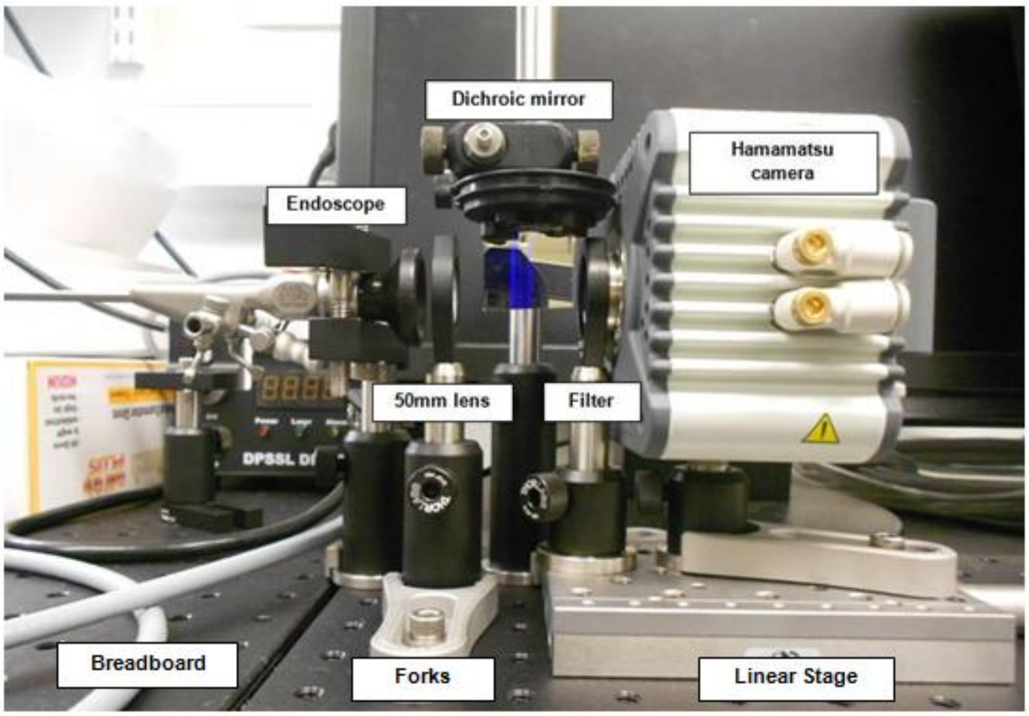

The Point Grey camera was placed perpendicular to the line between the Hamamatsu and the endoscope. This camera captures the light reflected off of the dichroic mirror which is placed at a 45° angle with respect to the light path between the lens and Hamamatsu camera. Fig. 23 on Pg. 30 shows the complete set up during the focus testing with the 50mm lens.

Figure 23: Complete set-up with both cameras during the focal point determination tests.

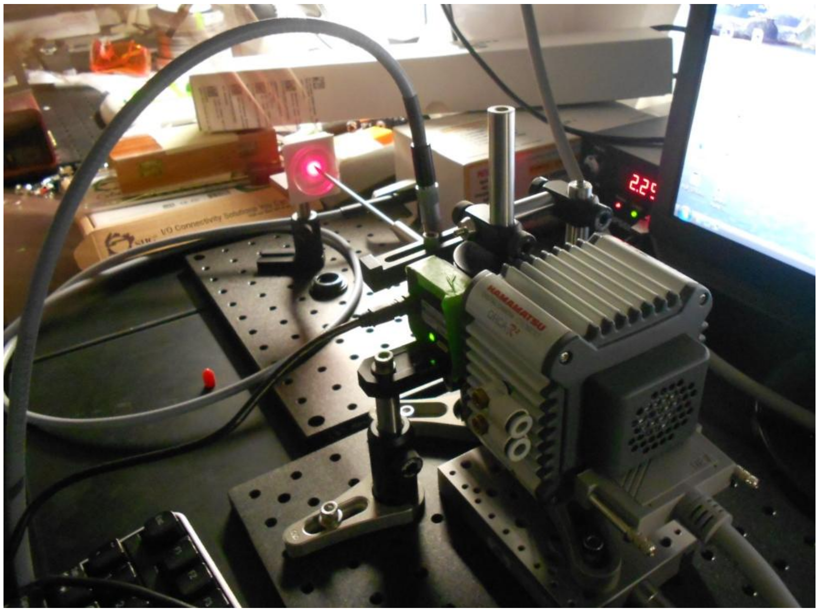

The Hamamatsu camera captured fluorescent images of the beads, while the Point Grey camera captured the reflectance. The image capturing was observed in real time on the computer using the software HCImage for the Hamamtsu camera and FlyCap2 for the Point Grey camera. Samples of images captured during testing are shown in Fig. 24 below.

Figure 24: Real-time images were used to determine camera positions, reflectance (left) and fluorescence (right).

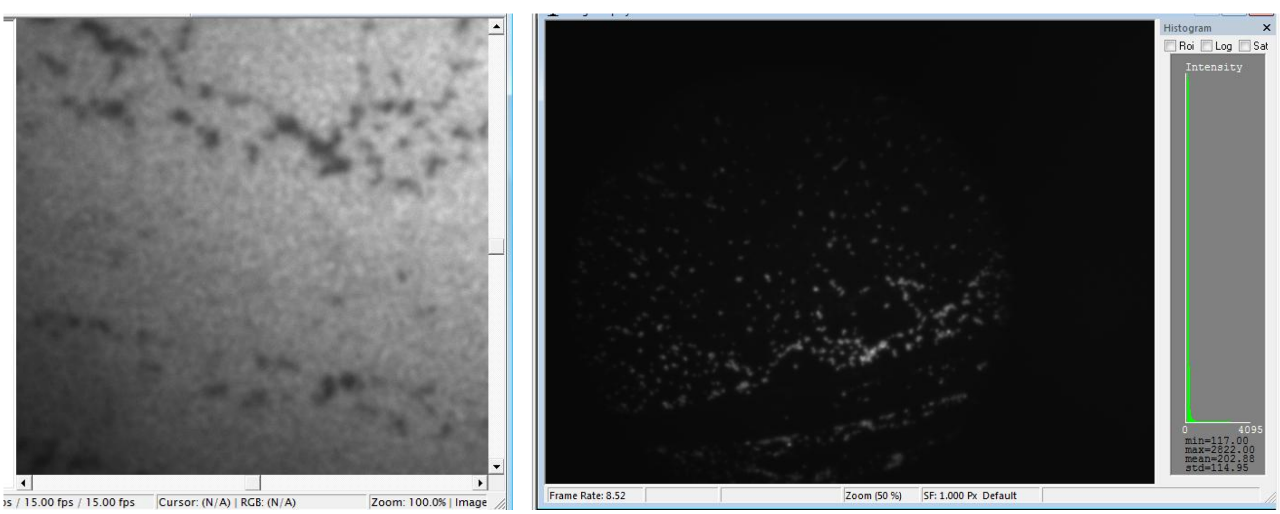

To determine the optimal position for the 50mm lens, the Hamamatsu camera was adjusted until a relatively focused image was captured. Then, the 50mm lens was repositioned until the clearest image was observed. The lens holder was clamped down in place with a fork. Again because of the diverging light exiting the endoscope, the optimal position for the lens was a few millimeters away from the endoscope. The distance between the lens and the endoscope needed to be accounted for in our final design.

The Hamamatsu camera was adjusted using the linear stage until the most focused fluorescence image was observed. The Point Grey camera was first adjusted along its horizontal axis until the image it captured was centered with respect to the dichroic mirror. This meant that it was along the central axis of the dichroic mirror. After the horizontal position was found, the camera was adjusted linearly forwards or backwards until the image on the screen was as focused as possible. The images were determined focused by our sponsor on a purely subjective basis. During the testing there is no way to calculate the clarity of the image, but we can observe to see whether the positioning of the optical components obstructs the image.

A Mitutoyo Series 500 caliper was used to measure all final positions. Three readings were taken for each distance and averages and uncertainties were determined. Results are summarized in Fig. 25 and Table 2 below.

Figure 25: Labeled final distances for all of the optical components

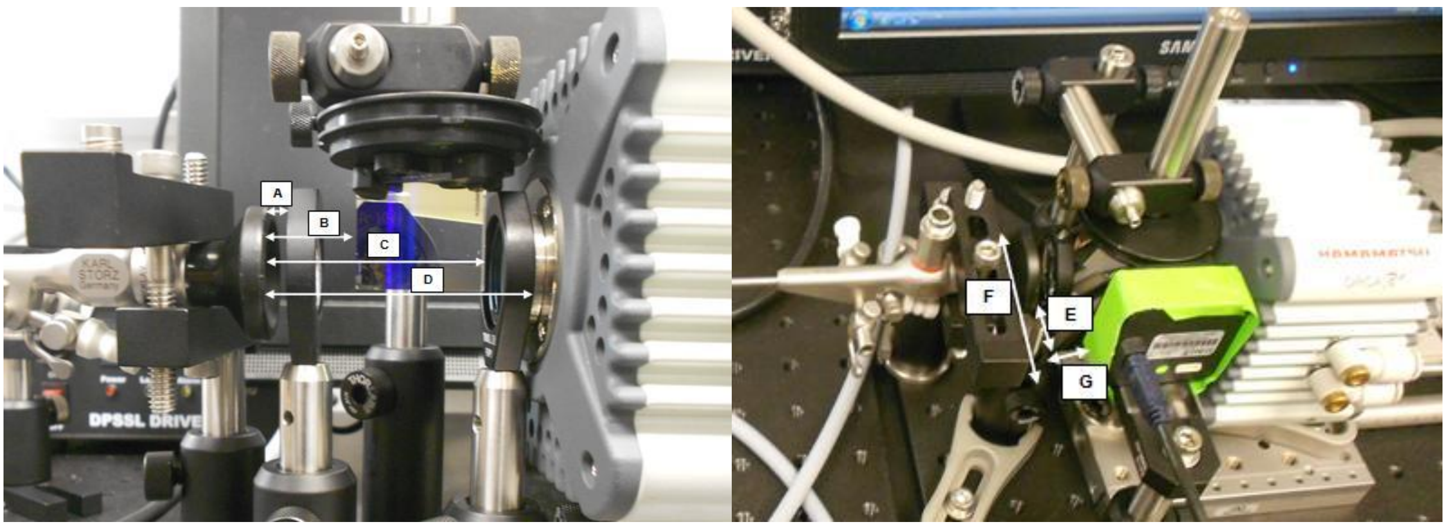

A: Front of endoscope to lens holder
B: Front of endoscope to nearer edge of mirror
C: Front of endoscope to farther edge of mirror
D: Front of endoscope to rim of Hamamatsu camera
E: Nearer side of endoscope to front of Point Grey camera
F: Farther side of endoscope to back of Point Grey camera
G: Front of endoscope to nearest side of Point Grey camera

Table 2: Measurements for all the optical positions with uncertainties measured in mm.

Position	A	B	C	D	E	F	G
Measurements	5.35 5.33 5.71	19.32 19.33 19.40	45.48 44.84 44.92	54.63 54.82 55.05	10.55 9.57 9.73	61.31 60.58 57.47	11.01 9.82 11.15
Average (mm)	5.5± 0.3	19.35 ±0.06	45.1±0.5	54.83±0.3	9.95±0.7	60 ± 3	11 ± 1

To validate results from the experiment, a dismantled set-up was reconstructed one week later on October 26th. Laser light was emitted through the optical components and images were captured. The validation of the measurements enabled us to verify all measurements used in our SolidWorks design.

Physical dimensions

Measurements of the endoscope pictured in Fig. 26 and labeled in Table 3, and features on the cameras shown in Fig.'s 27-28, and labeled in Table 4, were taken to aid in the SolidWorks modeling process.

Figure: 26: Image of the endoscope and the petri dish holding the fluorescent beads.

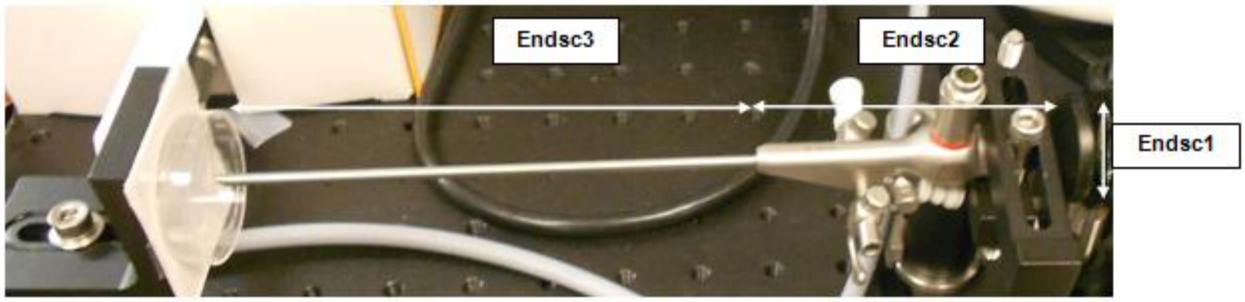

Table 3: Measurements of the endoscope for the SolidWorks design.

Endoscope	1 Diameter	2 Main Fixture	3 Probe Length
Measurements (mm)	31.74	92.12	137.68
	31.73	91.91	137.44
	31.65	91.99	137.39
Average (mm)	31.71 ± 0.07	92.01 ± 0.15	137.5 ± 0.2

Figure 27: Image of the various protrusions of the Hamamatsu camera required for our SolidWorks design.

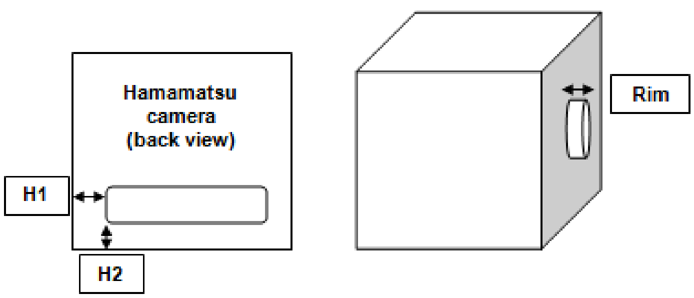

H1: Cord to side of camera
H2: Cord to base of camera

Table 4: Measurements of the various protrusions on the Hamamatsu camera.

	H1	H2	Rim
Measurements (mm)	11.79	12.77	2.43
	11.66	12.88	2.50
			2.52
Average (mm)	11.73 ± 0.09	12.83 ± 0.08	2.48 ± 0.07

Figure 28: Image of the various protrusions on the Point Grey Research (Chamelon) camera.

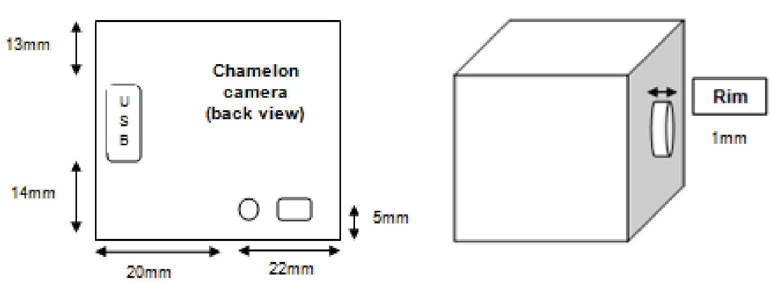

PROTOTYPE DESCRIPTION

As stated throughout the report, our final design and our prototype are the same for this project. The prototype we plan to create will be to scale and ready for immediate use by our sponsors for colorectal cancer research in mice. If the product registers a clear, focused, and usable image the Michigan Network for Translational Research (NTR) center has every intention of using the system for the current research done in the lab. Our main concerns for the prototype is that all our concepts are proven successful for the needs and design requirements based on response from our sponsor. The most important proof of concept with this design is the focus of the cameras and the ability to use the design to identify the cancerous polyps in the mouse colon. During our validation process thoroughly explained on Pg.'s 43-45, these requirements will dictate whether the design was successful and if we met the needs of our sponsor. The optical housing we designed is a "one off" item used as a laboratory instrument for the NTR and not a product for mainstream research. The product specifically meets the research needs of our sponsor and the testing done at the NTR.

In future developments of this project many adjustments can be designed. During the design process we brought up different ideas with our sponsor including making the system adjustable for different camera sizes for future cameras they may purchase. Although they decided that this idea was unnecessary, the idea is just a demonstration of future progressions possible for the design. Additionally, our sponsor did say they want to try to make a system that combines three images: reflectance, white-light, and fluorescence. However, for this to be possible, two laser probes need to be inserted into the endoscope with more complex image filtering integrated into the system. For our project they decided this was out of the scope of their current needs, but both of these ideas could be integrated into a future system.

Finally, current feedback from our sponsors about our design has been entirely positive.

FINAL DESIGN DESCRIPTION

After our Alpha Design concept was completed we needed to determine the dimensions of our final design. We empirically determined the focus points of the Hamamatsu and Point Grey cameras as described in the Optical Analysis section on Pg.'s 28-31. The measurements from the set-up of our optical system were used for the final design. Once the measurements were finalized, we were able to accurately design the housing and various fixtures we would be manufacturing. The housing components we are manufacturing in house and the fasteners and optical components we are purchasing are all described in the following section.

The Dovetail sliding mechanism

The dovetail sliding mechanism is a 20mm high piece that will slide on one of the surfaces of the base platform. The piece will fit into a grooved path on the base platform that constrains the mechanisms side to side motion and only gives the piece one degree of freedom. The through hole in the middle of the component is to attach the Hamamatsu camera firmly to the dovetail's top surface by a lock washer and bolt. The component also features an extension protruding from the back of the device. On this extension, there is a depressed area that will provide a comfortable grip for the user to adjust the position of the dovetail sliding mechanism while the Hamamatsu camera is in place. The dovetail mechanism can be seen in Fig. 29 on Pg. 34. For a more in depth dimensioning, see Appendix D from Pg. 67.

Figure 29: Isometric, side, and top views of the dovetail sliding mechanism with over all dimensions

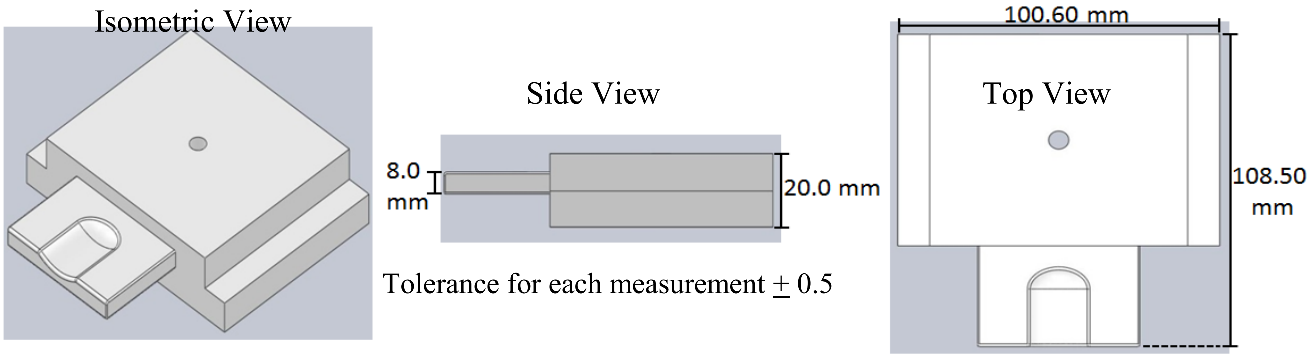

Detachable handle

The detachable handle features symmetrical contours on each side to comfortably fit the user's hand. The top of the handle features a railway system that will connect to the base platform. Both sides of the railways contain a hole that will be used to secure the handle to the base platform. Dimensioned images of the handle can be seen below in Fig. 30. For more in depth dimensioning, see Appendix D on Pg. 67.

Figure 30: Isometric, side, and front views of the handle

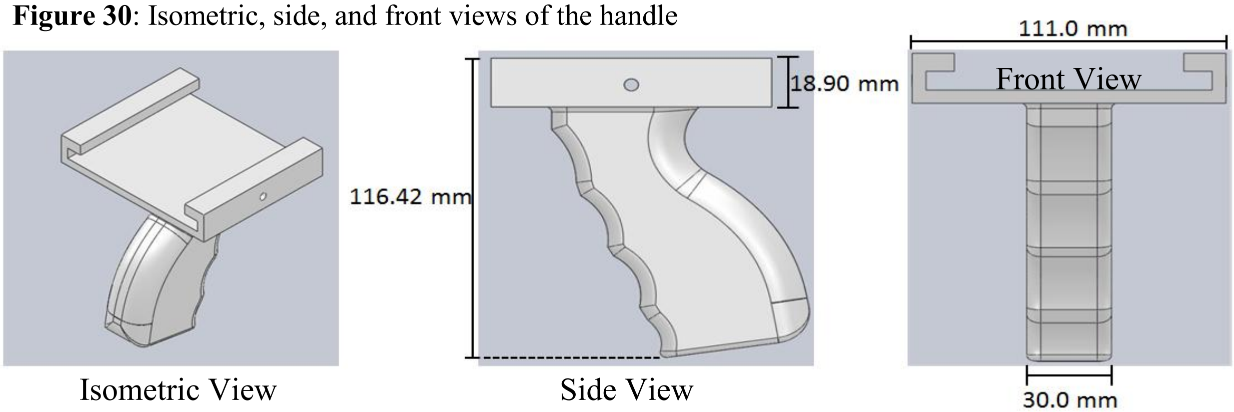

Tolerance for each measurement + 0.5

Base Platform

The base platform is the most involved piece that we will be manufacturing. The bottom of the base has a rail system that will complement the rail system built into the handle. Right above the rail system is the surface that the dovetail slide mechanism will be placed on. On both sides of this surface there are grooved pathways that will allow the dovetail to have only forwards and backwards motion. We have incorporated circular cutouts into the walls in front of both cameras to ensure that the walls do not interfere with the camera lenses and the light path. The Point Grey Research camera sits in front and to the left of the Hamamatsu camera. The base of the Point Grey Research camera's platform has slots for adjusting the camera's position and focus of the image. The Point Grey Research camera platform is directly attached to the Hamamatsu camera platform.

The mirror holder and main lens holder are attached to the base by a second smaller platform extending from the Hamamatsu camera wall. The main lens holder is shaped to hold a ThorLabs convex lens holder. The lens holder will fit into the compartment and be secured by a screw that goes through the base and screws into the threaded region of the lens holder. Also on the platform are two 2mm high ridges that have been positioned at a 45° angle to help align the mirror holder. With these ridges, the maximum angle deviation the mirror holder could have is 5°, which is comparable with our measurements found in the lab. In between the ridges there is a hole for the mirror holder to be screwed into the platform. Two holes, one on each side of the railway system are placed to secure the handle to the base platform. Four holes, two on each side of the base platform, will be used to hold the dovetail sliding mechanism in place. There is one threaded hole in the wall behind the Point Grey Research camera to provide controlled forward motion to focus the camera. Labeled and dimensioned images of the base platform can be seen below in Fig. 31. For more in depth dimensioning, see Appendix D on Pg. 67.

Figure 31: Isometric, side, and top views of the dovetail sliding mechanism.

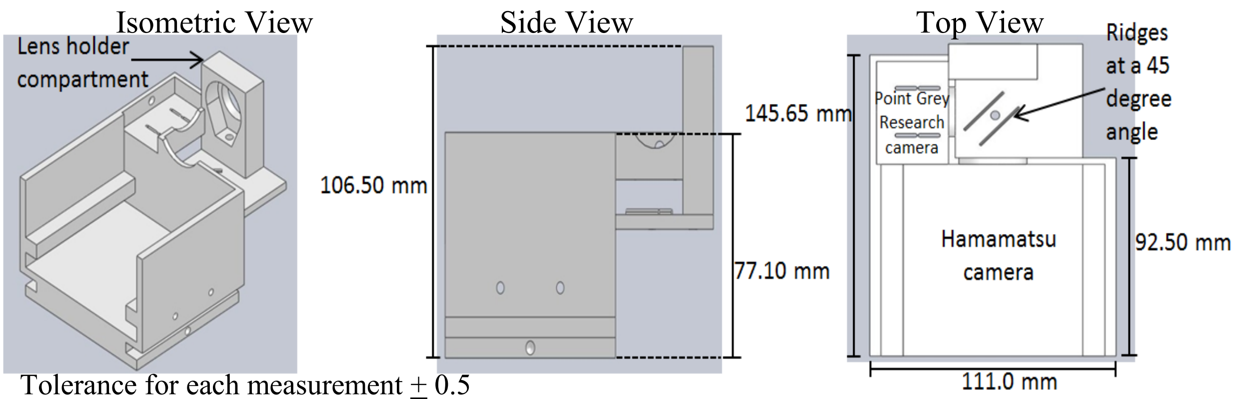

Tolerance for each measurement ± 0.5

Mirror holder

The mirror holder will be used to hold the dichroic mirror at a 45° degree angle. It has a 2mm deep slot on the top surface to cover as little of the mirror as possible so the maximum area of the image from the endoscope can be translated to both cameras. The mirror holder has two threaded holes on the far sides of the back face that will accommodate set screws that will secure the mirror. There is a threaded hole on the bottom of the mirror holder that will help to secure the component between the ridges on the base platform. Dimensioned images of the mirror holder can be seen below in Fig. 32. For more in depth dimensioning, see Appendix D on Pg. 67.

Figure 32: Isometric, back, and side views of the dovetail sliding mechanism.

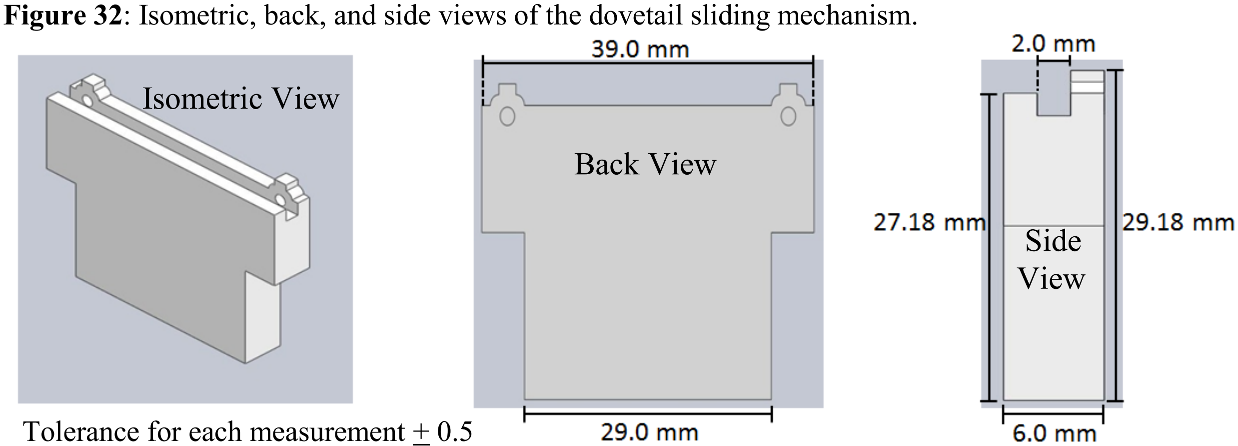

Tolerance for each measurement ± 0.5

Assembly Process

The handle slides onto the rail system of the base platform and lines up with the holes on each side of the base platform's rail system. The clearance between the handle and base platform is 0.1mm, which will allow the handle to move with added friction to help secure the handle in place and make sure there is very minimal movement during the procedure. The Hamamatsu camera has a threaded screw from its base, which will be used to secure the camera to the dovetail mechanism via a lock washer and bolt. The dovetail mechanism slides into the grooved pathways of the base platform and is allowed to move until focus for the Hamamatsu camera has been achieved. At this point the four thumb screws will be placed into the two holes on each side of the base platform securing the dovetail in place. The clearance between the dovetail and base platform is 0.2mm, which will allow the dovetail mechanism to freely move until it needs to be secured in place. The mirror is placed between the ridges and secured with a screw. Exploded views of the assembly can be seen below in Fig. 33.

Figure 33: Exploded views and assembly of base platform, dovetail mechanism, handle and mirror holder.

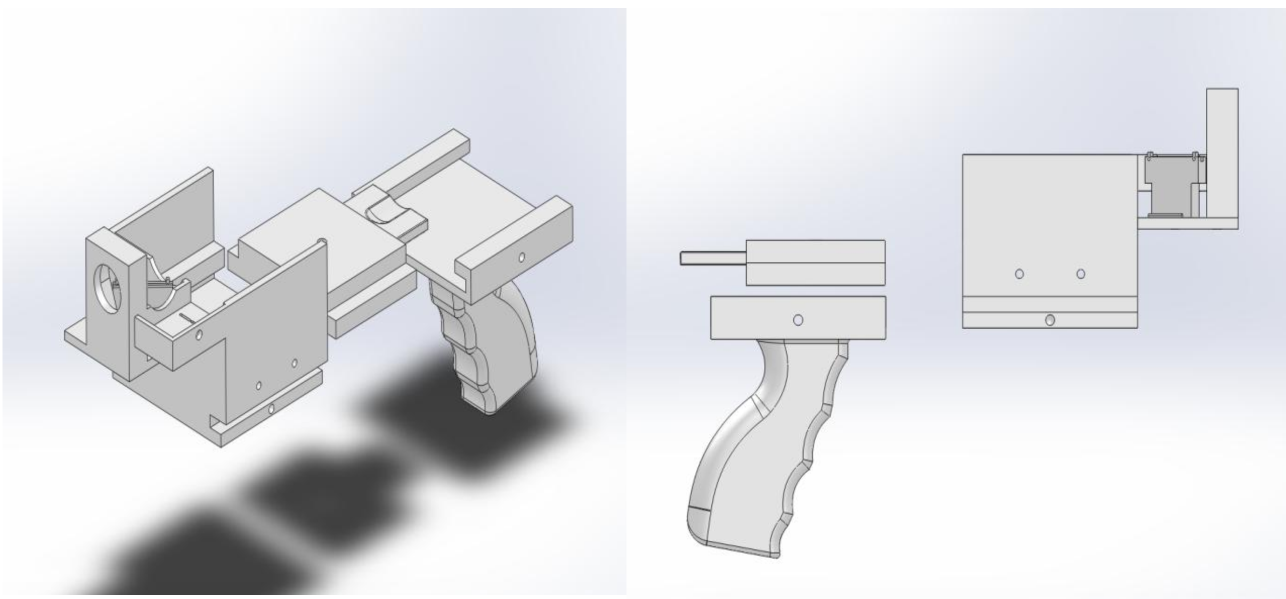

Fasteners

In order to secure the assembly together, we will be using various purchased fasteners identified in the bill of materials in Appendix A on Pg. 53. The handle will be held firmly in place by two quick release pins that pass through the handle and into an indentation in the base platform demonstrated in Fig. 34.

Figure 34: Handle being fastened to base platform by quick release pin.

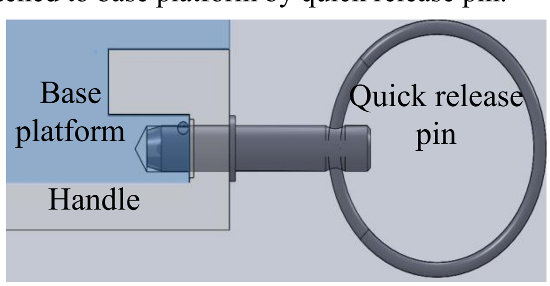

The dovetail slide mechanism will be secured in place by four thumb set screws, two on each side of the base platform, seen below in Figure 35.

Figure 35: Dovetail slide mechanism being secured by thumb set screws.

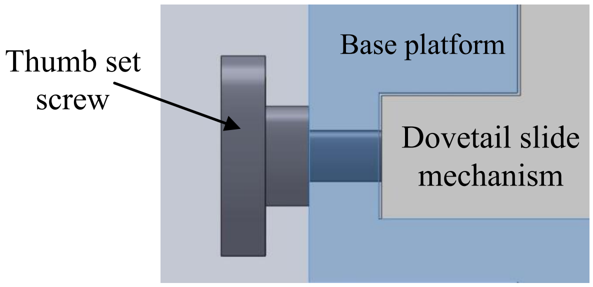

The lens holder has a threaded hole and will be secured through the lens holder compartment by a thumb screw. The mirror holder will also be secured by a thumb screw inserted into the threaded hole on its bottom face pictured in Fig. 36 below.

Figure 36: Mirror and lens holder fastened by thumb screws.

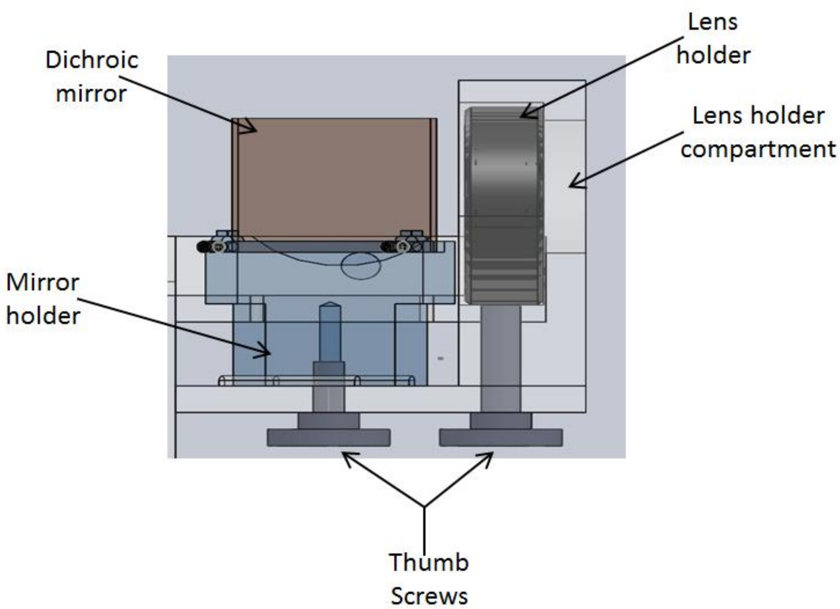

The full assembly with all optical components and fasteners included is provided in Fig. 37 on Pg. 38.

Figure 37: Isometric (top), Side (bottom left) and Top (bottom right) views of full assembly.

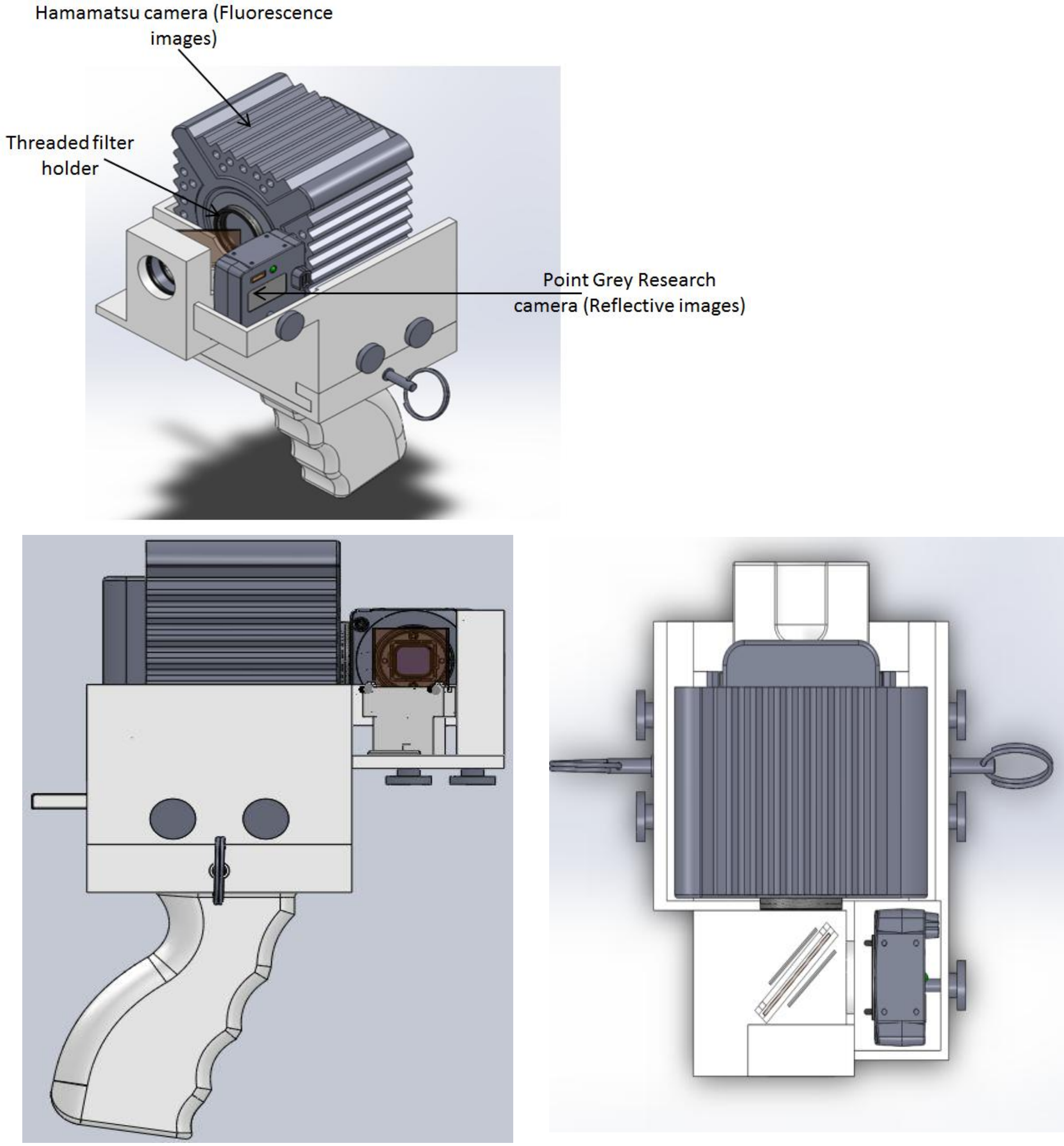

Exclusion of Telescoping Tunnels from Alpha design

In our original Alpha design that we presented in Design Review 2, we had included a telescoping tunnel that would extend from both camera lenses to the mirror and an additional tunnel from the mirror to the lens holder compartment. However, after determining the focus points of the cameras we realized we did not have enough room to include these tubes as they began to interfere with other optical components during our modeling phase.

MATERIAL SELECTION

Following the development of our preliminary SolidWorks model, CES analysis was used to guide the materials selection process. Our main material concerns for our design is the bending due to the weight of the endoscope 137mm long acting 55mm away from the main structure of the baseplate. Any deflection on the platform connecting the Hamamatsu camera to the main lens can affect the optical alignment of components and cause obstruction in the image.

Detailed CES analysis for the baseplate and handle components is found in Appendix C on Pg. 59. For all components the density of the material was plotted on the X-axis against Young's modulus on the Y-axis using the CES material selection program. ABS plastic was found to be the most suitable material choice. The material chosen for all the components needs to be able to carry the load from the optical components and cameras without deformation. Additionally, the housing needs to maintain a mass within our specifications. A broader analysis for the best suitable material for the entire housing system on a whole was also conducted to validate the apparent choice of ABS plastic for all components.

Limits for the material analysis were determined by the project requirements of our design. The system needs to be lightweight, which requires a restriction on the density of the material. The engineering specification for mass allows a maximum of 2kg for the entire system. Subtracting the masses of the cameras and other optical components the total mass of the housing cannot exceed 0.86kg. The total volume of the housing components is shown in Table 5.

Table 5: SolidWorks calculations for the volume of main system components

	Base plate	**Dovetail slide**	**Handle**	**TOTAL**
Volume (mm^3)	309102.09	138552.77	211090.54	0.00066 m^3

An approximate maximum density for the material was derived using the mass of 0.86 kg and the total volume of .00066m^3. The density was calculated as $\rho \approx 1300$ kg/m^3. This was the upper constraint of density. The Young's modulus helps quantify the stiffness of the material and impacts bending moment and deflection, which is a critical limiting factor. As a constraint to narrow results to the strongest materials, a minimum Young's modulus of 10^9 Pa was chosen. A price limit of $30/kg was also put to keep costs of the housing and handle reasonably low and within our price restrictions of $400 including the fasteners and optical components.

A gradient-line of 2 was then used on the resulting CES graph to further restrict the results to materials with the best density to shear strength ratio. Table 6 on Pg. 40 summarizes the limits used. Fig. 38 on Pg. 40 displays the final graph.

Table 6: Limits used for materials selection

Density	Max 1300 kg/m^3
Price	Max $30/kg
Young's Modulus	Min 10^9 Pa

Figure 38: CES Materials Analysis of Young's Modulus (Pa) versus Density (kg/m^3)

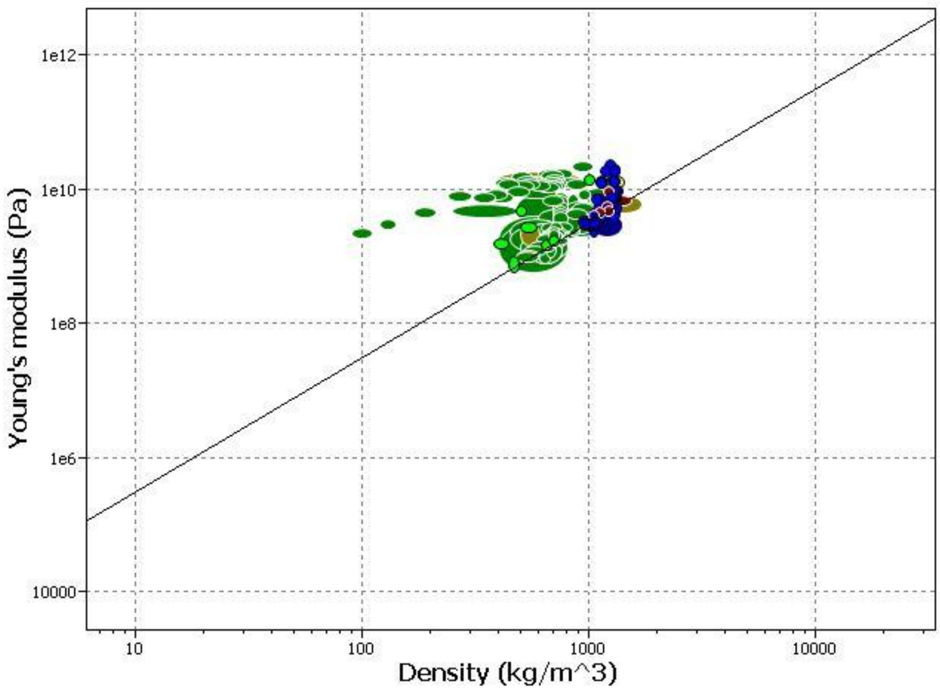

The results were very close to those for the individual components found in the Appendix C (Pg. 59). Top materials were ABS plastics, other plastics (PA, SMA, SPA), aluminum foams and woods. ABS plastic was selected, given both its properties and manufacturability (Fabrication Plan, Pg. 43).

Design analysis assignment

The complete design analysis assignment is found in Appendix C on Pg. 59. The CES software was used for the material and manufacturing process selection. The assignment highlighted the importance of understanding every component's purpose and constraints, while finding material indices for selection. SimaPro was used in the design analysis for environmental sustainability assignment in which ABS plastic and a light Aluminum alloy were compared in their impact on the environment. The sustainability assignment underscored the importance of considering the fundamentals of where a material comes from (how much resources did it take to be manufactured) and where it goes after use (impact of degradation, environmental damage) during the process of material selection. Solving just the design problem is not enough, environmental sustainability has to be considered as well. In addition to these assignments, a safety report was also written. It showed the importance of thoroughly understanding safety concerns for parameter analysis experimentation, validation testing procedure, and the method of assembly for the final product.

PROTOTYPE ENGINEERING ANALYSIS

Finite Element Analysis

A Finite-Element Analysis was conducted using Solidworks 2012's SimulationXpress to estimate the theoretical deflection and stress in the base plate. The Finite-Element analysis was used to validate our material selection against our engineering specifications of deflection less than 2mm along the base platform between the Hamamatsu from wall and the lens holder.

As shown in Fig. 39, the base enclosing the Hamamatsu camera was restricted as fixed during this analysis. We evaluated the deflection for an extreme case for when the endoscope is inserted in the mouse and there is additional pressure on the end of the system. We approximated the force to be up to 5N, and for a conservative analysis applied a downward force on the lens holder. A load of 0.4N was also assigned on the small Point Grey camera's platform to account for the mass. The results of the stress and deflection analysis are shown in Fig. 40 below, and Fig. 41 on Pg. 42.

Figure 39: Location and direction of loads prescribed for Finite-Element Analysis.

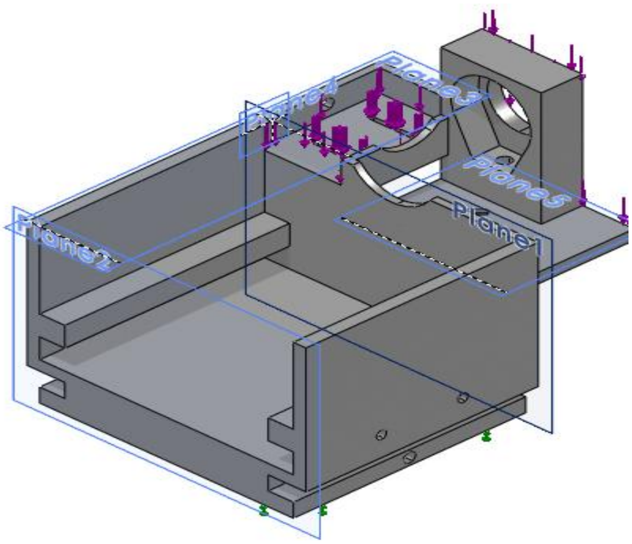

Figure 40: Results of the stress analysis with a maximum stress of 1MPa on Plane 1.

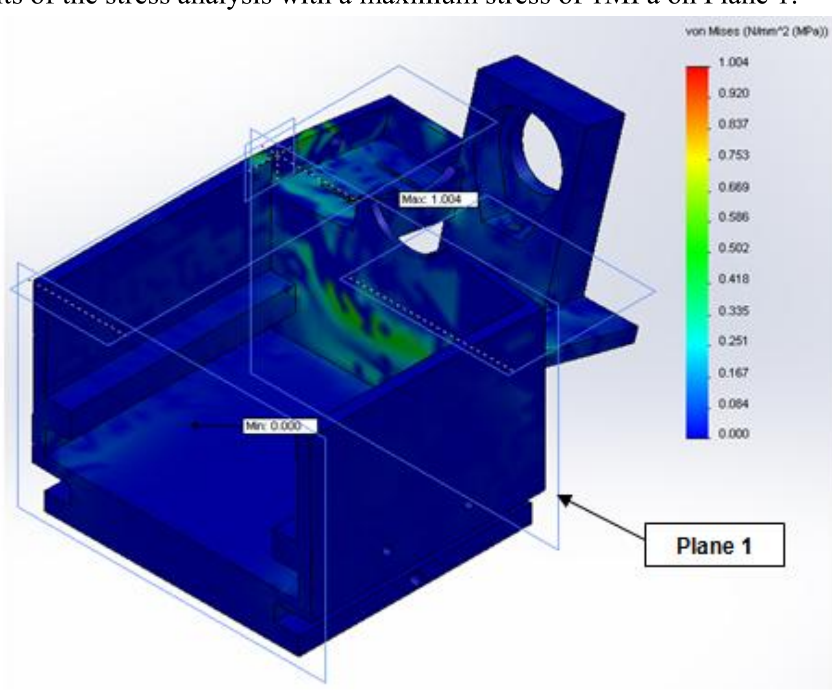

Figure 41: Results of the deflection analysis with a maximum deflection of 0.013 mm on face of lens housing indicated by the red and yellow coloring.

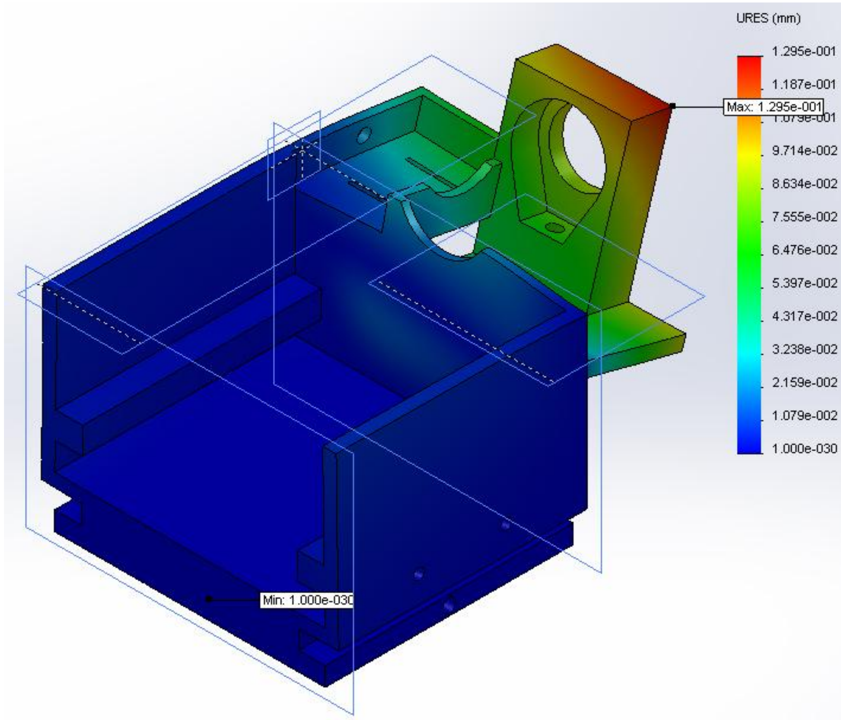

Maximum stress of 1MPa is an entire order less than the Yield strength of ABS plastic. The deflection of 0.13mm is also well below the engineering specification of 2mm maximum deflection. The results of the FEA validated our choice of ABS plastic and further validated our engineering specifications.

Friction analysis

In order to determine if friction would be a prominent issue when moving the dovetail sliding mechanism, we calculated the amount of force needed to overcome static friction. We researched the coefficient of static friction between two ABS plastic surfaces and found minimal information because ABS plastic is not usually used in applications involving wear. We were able to find the coefficient of friction (static) for ABS plastic on steel, which was 0.5, and used this value to provide a conservative estimate for the force needed to overcome static friction [12]. The calculations are shown below.

$$F = \mu N \qquad \text{Eq. 1}$$

Where μ is the coefficient of static friction (0.5), N is the normal force subjected on the base platforms surface by the dovetail sliding mechanism and Hamamatsu camera and F is force needed to overcome the force of static friction.

The mass of the camera is 1.1kg and the dovetail slide mechanism is .126 kg and the acceleration due to gravity is 9.81m/s^2.

$$F = 0.5 * (1.1 + .126) * 9.81$$
$$F = 6.01\ N$$

The average pull force that the index finger (bent at a 90 degree angle) exerts on an object is calculated by a source to be 60 N [13]. Compared to this value 6.01 N will easily be overcome by the user when maneuvering the Hamamatsu camera on the dovetail sliding mechanism.

FABRICATION PLAN

Our prototype will be rapid prototyped in ABS plastic at the University of Michigan 3D Lab in the Duderstadt center using the Dimension Elite Fused Deposition Modeling (FDM) machine. Four separate pieces will be printed – the handle, the dovetail slide, the base plate, and the mirror holder.

Material selection showed that plastics and epoxy resins were best suitable for our design. Considering manufacturing with plastics and the resources available in the university, 3D printing and laser cutting are the two most feasible options. Accurate optical alignment is the most crucial requirement for our prototype. The use of the laser cutter for multiple 2D pieces would require epoxy and multiple fasteners for assembly of the housing and would risk compromising the focus lengths calculated in the lab and additionally adding unnecessary weight. Compared to laser cutting, 3D printing will be more successful for our design because the lab can fabricate the entire baseplate in one piece. Therefore assembly will not be a factor that could compromise the position of the optical components.

The UM 3D lab has both a 3D printer that utilizes starch-silicon or plaster variants and an FDM machine that uses ABS plastic. Even though epoxy resins are suitable for our design as shown in the CES analysis, ZP150 3D only uses plaster with epoxy. The UM 3D lab recommends the use of ABS plastic for functional components because the ABS is more durable than brittle plaster. [14] Additionally, the current single camera system described in the Technical Benchmark section on Pg. 10 was also manufactured with ABS plastic from 3D printing.

The FDM machine works by melting and projecting plastic through a nozzle and building the prototype layer by layer. A support material to help shape the model is delivered simultaneously through another nozzle. At the end of the process, the support material is removed by physically prying it away or with a Sodium Hydroxide bath for harder to reach residue. Additionally, for our free moving parts within the design there needs to be a .1mm tolerance between moving components. The critical tolerances are for the sliding of the dovetail mechanism and the rail system for the attachment of the base to the handle. The surfaces between the handle and the base plate have a .1 mm tolerance to allow for some friction and security once the system is in use. The FDM machine is highly suitable for our design as it allows for a minimum wall thickness of 2mm, tolerance of 0.10mm, and 0.20mm for free moving parts.

The holes for the set screws holding the dovetail mechanism and the hole at the base of the mirror holder will be tapped. Once in the lab the optical components are first secured before the parts of the housing are assembled and secured. Once the rapid prototyping is complete the device can immediately be used for testing in the lab.

VALIDATION PLAN

The validation of our design requires four different studies. First an ergonomic study of the optical system will be conducted with different researchers using the device. The ergonomic study will help identify the “ease of use,” “light-weight,” and “comfortable” design requirements we specified. During the cancer screenings we can observe how the researcher handles the system, and if there seems to be discomfort or imbalance during the procedure. The repetition of certain hand, arm, and wrist motions can lead to injury; therefore we want our system to cause minimal stress and strain in the arm and hand muscles used.

Additionally, we plan on timing the set-up and adjustments procedure for the system before the mouse studies. Main concerns during this process are from the impact of friction from the material and the sliding adjustments for the cameras. However, as stated in the Fabrication Plan on Pg.43, the 3D lab specified if there is a 0.2 mm tolerance between components, the components should move freely. In the engineering specifications of the report we specified that friction is a possible mechanical challenge for our design. Even after we've calculated a theoretical frictional impact based on the material, we still need to consider the impact during assembly and use.

The second validation test is an analysis of the quality of the images produced by our device, which will be a subjective response from our sponsors. We need to identify if the optical alignment meets the expectation of the sponsor, and our set-up of the optical components registers a clear and focused image in their Matlab visualizing software. If the positions of the components were measured correctly there should be no side interference in the images from components in the way of the lenses or mirror.

The final test requires us to verify that our system meets the engineering specifications we stated in Design Review 2. Fortunately for our project we can test for all of our engineering specifications. Furthermore these specifications can be measured theoretically using SolidWorks. In the Prototype Engineering Analysis section on Pg.'s 41-43 we measured the theoretical mass, volume, and deflection using SolidWorks analyses.

Table 7: Outputs for the Theoretical Analysis of Volume, Mass, and Deflection

Engineering Specification	Current Limits	Analysis Results
Mass	1140-2000 g	676 g
Maximum Storage Volume	$6.3x10^{-3}m^3$.	$0.00066m^3$
Deflection acting 55mm from beginning of the platform.	< 2mm	0.13 mm

To validate these simulated measurements, we plan on evaluating the mass and volume of the system after fabrication. For the maximum storage volume we will create a box with the dimensions specified on Pg. 13. For the maximum mass we will use a scale that reads grams to measure the mass of the entire system including the optical components. Lastly, for the deflection of the material we will be able to identify a possible deflection during testing. If we identify this problem we will need to deduce whether the base plate is level with all the components intact.

Finally, we have already validated the focus length of the main lens. Within the design we chose a lens of 50mm, which is the outer bound of our engineering specification.

Fig. 42 on Pg. 45 is a chronological plan for validation of the factors specified above. Because our prototype is our final project, our sponsor can immediately indicate whether our design successfully met the needs of their department and whether the design can be used for experimentation and research in the lab.

Figure 42: Progression for Validation of Optical Housing Design.

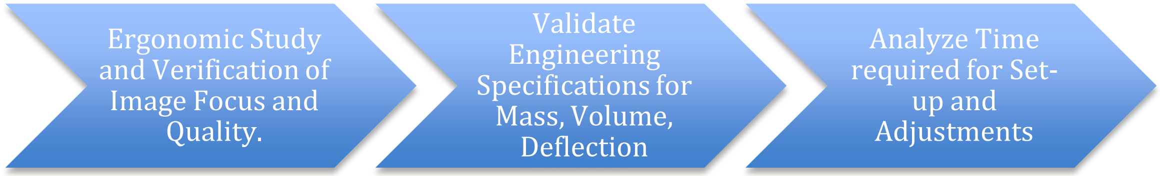

VALIDATION RESULTS

After the design was fabricated we validated our device for the engineering specifications we proposed and the image quality of the polyps during examination of the mouse colon. We concluded that our device met all of our engineering specifications we initially created for our design criteria. The following table sites the final storage volume and mass we measured after fabrication. Additionally, we validated the ergonomic specifications during the testing of our device in the laser laboratory of the Biomedical Science Research Building. The following image shows the validation process for the optical alignment of the device and the ergonomic factors we considered.

Table 8: The initial engineering specifications and final outcomes of our design.

Engineering Specification	Proposed	Final Outcomes
Total Mass	$1150g \leq m \leq 2000g$	1772 grams
Maximum Storage Volume	$.006375\ m^3$	$.004675\ m^3$
Maximum deflection at Endoscope	$\leq 2mm$	0.013 mm
Focal Length	$30mm \leq f \leq 50mm$	50mm

Figure 43: Supang using the device for inserting the endoscope into the mouse colon.

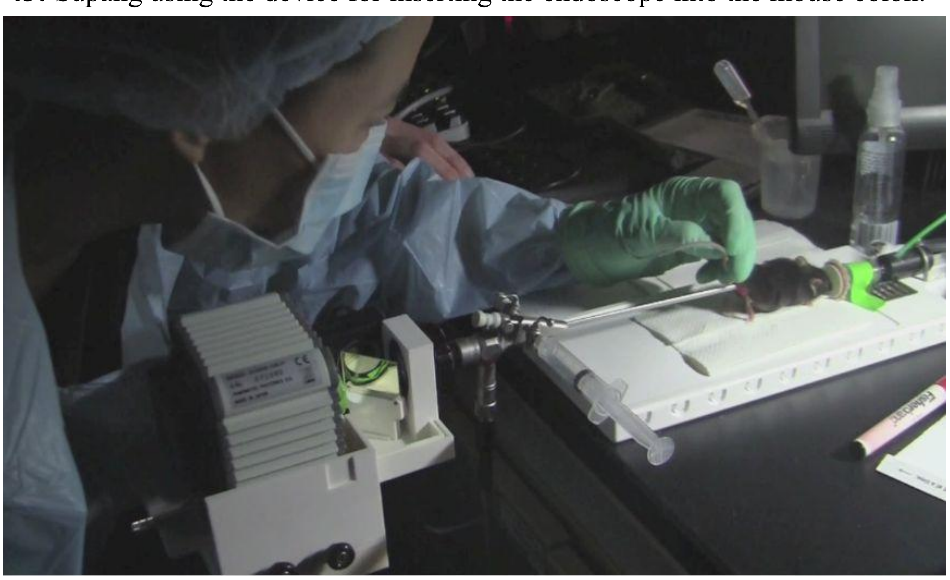

During the testing we were able to find focused images for both the fluorescent and reflectance cameras. Additionally, we found that the tripod made handling the system easier on the researcher. During the entire validation process there were not ergonomic concerns while using the device on the tripod adaptor.

We found during the validation process that preparing the device for the procedure and placing the optical components into the housing was a timely process. Some components are difficult to install and the screws required for mounting the Point Grey Research camera are small and difficult to use. However, once the components were installed they were secured for the entire procedure and did not introduce any unnecessary motion. Our sponsors plan to leave the components installed into the system once the final focus positions are found. So, the set-up time is not a concern.

DESIGN CRITIQUE

As previously stated, during the validation process we found that our device meets all the engineering specifications we proposed. Additionally, focused images were observed for both the Hamamatsu and Point Grey Research cameras. During the mouse studies we found that the most successful means of using the device is on a tripod rather than using the handle we designed. Even though we met our goal of creating a housing with a low mass, the weight of the Hamamatsu camera makes it difficult for the researcher to hold the system steady while scoping the mouse. The unsteadiness makes it difficult to discern whether the image is focused and when to capture images of the polyps. Although the tripod provides support for the system, the ability for the researcher to move the device in different directions to find the polyps is restricted. The ideal tripod adaptor would have a track so that the user can move the endoscope into and out of the mouse.

When the optical components are removed from the housing and then replaced the position of the optical axis may move, which could result in a cut-off image. Every time the optical components are repositioned there is a higher probability that a different circular image is displayed, some better than others. This variability could be corrected if the components are permanently placed in the device after a full circular image is observed.

During the focus testing for the cameras we used a petri dish with fluorescent beads to determine the focus points for the Point Grey Research camera and Hamamatsu camera. Throughout the procedure we observed that the position of the Hamamatsu camera within a 10mm range did not change the resolution and quality of the image. However, during the animal testing, it was difficult to find a position where the Hamamatsu camera was focused. Therefore, the testing with the beads was a bad representation compared to the actual testing environment.

The focus adjustment mechanism we designed for the Point Grey Research camera is difficult to use while the cover is on the device. Although, the cover is not necessary to preform the procedure, our sponsors expressed interest in providing additional prevention against light scattering. Moving forward, we would design a mechanism similar to the dovetail slide used for the Hamamatsu camera. Even though the Hamamatsu camera has a substantial mass, it was easy to change the position of the camera throughout the cancer studies on the mice. We concluded that the sliding mechanism was a successful strategy for adjusting the Hamamatsu camera.

During the design process we were relayed that once focus points were found, they would be marked and left unchanged. Therefore once we find the correct position for the focus and the optical axis, the issues with the focus adjustments and the visibility of the circular image will not be a future issue. Additionally, the design had many rigid specifications including the weight of the Hamamatsu camera, and the optical components that needed to be included into the design. Although the weight is still an issue for the use of the device, the extra weight results from the equipment they allotted for this project. From the fabricating method we choose, future changes to the design will be easy to manufacture.

RECOMMENDATIONS

Throughout the semester it was difficult to identify the exact needs of the NTR researchers. To have the project run smoother in the future, we suggest that our sponsors clarify their needs as early as possible. Although, we did create a hand held system for the research, it is evident that the Hamamatsu camera is too heavy to record focused and steady images while holding the device. At the end of this process we would recommend a tripod adaptor that incorporates a track allowing the researcher using the device to move the whole system in all three directions. This would allow the researcher to move the endoscope more fluidly while scoping the mouse colon. Additionally, the fluorescent beads were a bad representation for the focus of the Hamamatsu camera compared to the response from the camera in the mouse colon. We suggest, either finding a better representation of the mouse colon or using a mouse to determine the focus point of the Hamamatsu camera.

CONCLUSIONS

Our team worked in conjunction with the Michigan Network for Translational Research Center. Our goal was to develop an "integrated system that can take videos in both white-light and near-infrared formats simultaneously," that researchers can use to help better their ability when identifying cancerous lesions in mice colons.

The existing system has to scope the mouse twice to capture the reflectance and fluorescence images. The images are recorded at different points in time causing asynchronous landscapes when trying to overlay the two images. A previous group tried to solve this problem, but their resulting prototype was considered too bulky and poorly organized.

By creating this integrated system with two cameras, reflective and fluorescence images can now be captured simultaneously. This will allow the respective images to be superimposed and for the geometry and orientation of the images to be identical helping to pinpoint the location of the abnormal tissue growth. Superimposing the reflectance on the fluorescent images corrects the images for the intensity of the laser light and shows the cancerous polyps more clearly.

Our research and conversations we had with our sponsors led us to establish a list of requirements and specifications that we accomplished during this project. We focused on minimizing total volume, total mass, and focal length. After interviewing current users, we found they wanted the option of a hand-held device because of the movement associated with the procedure. This request meant we had to direct serious attention to the weight distribution of the design as the two cameras have significantly different weights. We also wanted to implement a fine-tuning device so the researcher can bring the image into focus with ease.

Our solution to the Quantitative Endoscope Project is a dual camera system for the Hamamatsu and Point Grey Research cameras. The Hamamatsu camera has a dovetail sliding mechanism for focus adjustments, and the Point Grey Research camera has slots and a tuning screw. Additionally, we accomplished designing an adjustable handle and tripod adaptor so that the users can choose between holding the device and anchoring the device to a tripod. We fabricated a cover at the request of our sponsors to diminish light scattering and dust particles interfering with the optical components in our system. We made our system compatible with a ThorLabs lens holder, so any lens holders the lab currently owns can be used to secure the main lens in our system. Finally, we fabricated a holder for the dichroic mirror that is guided to remain at a 45° angle.

During validation we were able to qualify the overall quality of our device and our solution. First, our design met all of our engineering specifications we proposed. The fabricated device is lightweight and the contoured handle is comfortable to hold. Additionally, during testing we were able to find focused images of the cancer polyps in a mouse model. However, as we found during testing, the weight of the Hamamatsu makes it difficult to use the device as a handheld system. The weight of the Hamamatsu camera is balanced throughout the device, but it is still difficult to remain steady while trying to observe a focused image of polyps in the mouse colon. Furthermore, the tripod adaptor proved to be a successful design. The device is secured and there are no ergonomic problems for the researcher. However, when the device is anchored to the tripod it is difficult to move the endoscope into and out of the mouse. Therefore, a tripod with a customized track to allow for motion is three directions would be more effective.

When the optical components including, the lens, cameras, dichroic mirror, and filter are secured they need to be adjusted so that the optical axis is aligned. Occasionally, once the components are installed the image shown through the software is cut-off due to the exact placement of the components. Finally, adjusting the Point Grey Research camera is more difficult than adjusting the Hamamatsu camera. Future designs should integrate a dovetail mechanism for both cameras. Overall, the device does succeed in its ability to capture focused images of the cancer polyps for the fluorescence and reflectance cameras. However, the design can be even more effective if a track, providing motion in the X-Y plane, was to be implemented into the tripod adapter and a better adjustment system for the Point Grey Research camera was to be installed.

ACKNOWLEDGEMENTS

We would like to thank Dr. Thomas Wang and his team at the Network for Transitional Research for the access to their labs and the optical instrumentation they allowed us to test for this project. Additionally we would like to give a special thanks to Chien-Hung Tseng for her dedication to the project and help throughout the semester. Thanks to Supang Khondee for her help during the testing process and final input towards the device. Finally, we would like to thank our section instructor Elijah-Kannatey Asibu for his input and support, as well as Gordon Krauss for the opportunity to work with the NTR center and their molecular endoscope project.

INFORMATION SOURCES

In defining project motivation and understanding relevant background on colorectal cancer (Pg. 7-9), research papers published by our sponsors in the Network for Translational Research and other academic and medical sources were extensively studied. Personal interviews with researchers who currently use the endoscope set-up were conducted to understand our technical benchmarks and the project requirements (Pg. 10-11). Following the concept generation phrase, sponsor feedback was sought again and advised the Pugh chart comparison. Research on optical instrumentation, particularly in the form of technical specifications, was also conducted for engineering analysis.

Sponsor Feedback

Personal interviews with team sponsor Chien-Hung Tseng and primary researcher Supang Khondee were conducted following both Design Review 1 and the selection of our five preliminary concepts. During our discussion of our concepts, we gathered their feedback on features we had brainstormed. Key examples include advice that a linear stage for camera adjustment might be excessive, a critique of the arm-rest solution from a user-perspective, and experience-based reasoning on keeping the lens and mirror side of the optics rigidly fixed [15, 16].

The advice helped us avoid designs that adjusted optical components instead of the cameras for our final selection. The feedback was used for ranking final concepts on our Pugh chart. Demonstration of the optical testing tools used in the lab shown in Fig. 22, on Pg. 29 helped us understand engineering analysis and optical testing requirements. Our sponsors also suggested researching lenses with coating that would reduce reflection of incoming light [15, 16].

Product Research

Product catalogues from Thor Labs on convex lenses and technical data from Semrock's online catalogue on filters and dichroic mirrors were consulted. Following this, the team ordered 3 biconvex spherical lenses of 35mm, 40mm and 50mm focal lengths with –A coating that is appropriate for the laser's wavelength [17]. These lenses will be tested with Semrock's 716/40nm Brightline single-band bandpass filter [18] and 700nm edge Brightline single-edge dichroic beamsplitter [19] during the optical analysis stage that follows Design Review 2. Technical specifications are found in Appendix F on Pg. 75. Data, analysis, and precautions explained in the technical data will be used when we development an experimental procedure for optics testing.

For our alpha design, we researched existing real-world solutions to our sub-functions. The camera plate and quickshoe apparatus used in many film and large photography cameras provided a good benchmark that we applied in the development of the dovetail sliding joint for the large camera's adjustments.

Figure 44: Dovetail joint (bottom) camera plate (top right) and quickshoe system (top left) [20]

Further research on optical lens holders and their design specifications was also conducted to help us understand possible mechanisms for fastening the lens, filter, and dichroic mirror. Engineering drawings of the cameras were also sourced from the specifications of the Hamamatsu and Point Grey Research camera.

TEAM BIOS

Elizabeth Eisenstein

Elizabeth is a 21-year-old transfer student from The Cooper Union in Advancement for Science and Art in New York City. She transferred to The University of Michigan in Fall 2011 and plans on staying for her masters in the Biomedical Engineering SGUS program at the university. Over the past summer, Elizabeth Interned for Stryker Instruments in Kalamazoo, Michigan in the Global, Quality, and Operations department for the accessories unit for surgical drills used in orthopedic and neurosurgery. Aside from school Elizabeth is a member of Alpha Phi Omega Professional Community Service Fraternity, Phi Sigma Rho Engineering Sorority, and Pi Tau Sigma Mechanical Engineering Honor's Society. Additionally, Elizabeth participates in getting out the vote for the November 2012 election for Barack Obama.

Daniel Fuchs

Danny Fuchs was born and raised in West Palm Beach, Florida. Growing up with warm weather year-round allowed him to develop an interest in playing and watching a wide variety of sports. He and his family currently reside in Rye Brook, New York, where he has come to realize it is difficult to be a South Florida sports fan surrounded by Jets, Knicks and Mets fans. At a young age, Danny was always interested in how things worked and recalls reading a book titled "The New Way Things Work." Surprisingly, he can still remember the titling on the book being constructed from gears and other various mechanical devices. Danny developed a stronger interest in mechanical engineering from one of his classes in high school. One of the projects he was assigned involved protecting a standard paintball from breaking with only pieces of foam. However, this foam was subjected to a 10-pound block that was dropped 15-20 feet above the paintball. He couldn't remember anyone designing a foam housing that was successful, but his journey into the world of engineering and design had just begun. The hands-on opportunity that mechanical engineering offers Danny, made it an easy career path for him to follow. He plans on finding work within the product development field once his illustrious undergraduate years conclude themselves.

Radhika Gurumurthy

Radhika Gurumurthy is a senior pursuing a dual degree in Mechanical Engineering and Screen Arts & Cultures with LS&A. She transferred to the University of Michigan in Fall 2010 after completing her freshman year at the National University of Singapore. Over the last 2 years as a wolverine, she has balanced her interests in both engineering and the arts. She was part of the 2010-2011 SWE team that came in second at the Team Tech competition sponsored by The Boeing Company at the 2011 national SWE conference in Chicago. As an Indian classical dancer, she performs extensively with both Michigan Sahana and the Maya dance team, on campus and off. Last summer, she took part in the Technical University of Berlin engineering summer program and worked on wind tunnel experiments for bluff body dynamics with TUB's Aeronautics department. She also interned at the global headquarters of Rolls-Royce Marine in her hometown of Singapore. After graduation in May 2013, she hopes to find full time employment in industry.

REFERENCES

1. ACS, American Cancer Society. Quick facts colorectal cancer: what you need to know--now. 2nd ed. Atlanta, GA (2008)
2. Z. Liu, S. J. Miller, B. P. Joshi, T. D. Wang, “Wide field near-infrared fluorescence endoscope for real-time in vivo imaging,” University of Michigan (2012)
3. S. F. Elahi, S. J. Miller, B. P. Joshi, T. D. Wang, “Targeted imaging of colorectal dysplasia in living mice with fluorescence microendoscopy,” Biomedical Optics Express: 981-986 (2011)
4. S. J. Miller, B. P. Joshi, Y. Feng, A. Gaustad, E. R. Fearon et al. “In Vivo Fluorescence-Based Endoscopic Detection of Colon Dysplasia in the Mouse Using a Novel Peptide Probe,” PLoS ONE 6(3): e17384. doi:10.1371/journal.pone.0017384 (2011)
5. R. M. Soetikno, T. Kaltenbach, R. V. Rouse, et al. “Prevalence of nonpolypoid (flat and depressed) colorectal neoplasms in asymptomatic and symptomatic adults,” JAMA;299(9):1027-1035. (2008)
6. T. D. Wang. Personal interview. (September 17, 2012)
7. S. Khondee. Email interview (September 13, 2012)
8. R. Upadhyay, R. A. Sheth, R. Weissleder, U. Mahmood, “Quantitative real-time catheter-based fluorescence molecular imaging in mice,” Radiology 245(2): 523-31 (2007)
9. B. P. Joshi. Personal interview (September 17, 2012)
10. C. Tseng. Personal interview (September 13, 2012)
11. C. Tseng. Personal interview (October 22, 2012)
12. Omniaplastica. Retrieved from: www.omniaplastica.it/english/datitecnici.html (October 31, 2012)
13. A. D. Astin, “Finger force capability: measurement and prediction using anthropometric and myoelectric measures,” Virginia Polytechnic Institute and State University (1999)
14. University of Michigan 3D Lab, Retrieved from: http://um3d.dc.umich.edu/ (October 31, 2012)
15. S. Khondee. Personal interview (October 1, 2012) (11)
16. C. Tseng. Personal interview (October 1, 2012) (12)
17. Thor Labs, America, Retrieved from www.thorlabs.com/newgrouppage9.cfm?objectgroup_id=4848 (October 1, 2012)
18. Semrock, America. Retrieved from: www.semrock.com/FilterDetails.aspx?id=FF01-716/40-25 (October 1, 2012)
19. Semrock America. Retrieved from: www.semrock.com/FilterDetails.aspx?id=FF700-Di01-25x36 (October 1, 2012)
20. Markins America. Retrieved from: www.markinsamerica.com/MA5/category.php?req=3 (October 6, 2012)
21. Ashby, M. F. "5: Material Selection - The Basics." *Materials Selection in Mechanical Design*. Oxford, OX: Butterworth-Heinemann. 65-84. Print. (1999)
22. CES Edupack software, Granta Design Limited, Cambridge, UK. (2009)

APPENDIX A: BILL OF MATERIALS

Table 9: The bill of materials for all components purchased for the quantitative endoscope project.

Item	Qty	Source	Catalog Number	Total Cost	Contact	Notes
M6 screw	1	Carpenter Brothers Hardware & Rental Center	1594-B	$0.75	(734) 663-2111	For Hamamatsu camera
Female Knob	1	Carpenter Brothers Hardware & Rental Center	55417-B	$3.00	(734) 663-2111	For tripod adapter
M2 screws	3	Jack's Hardware	4306-K	$1.35	(734) 995-0078	For bushing and endoscope attachment
Plastic-Head Thumb Screw With Socket Drive		McMaster-Carr	98704A520	$7.57 (pack of 10)		Dovetail set-screws
Shoulder-Style Quick-Release Pin	2	McMaster-Carr	98485A002	$1.78		For securing handle to base
Knurled Head Extended Point Thumb Screw		McMaster-Carr	90079A245	$4.63		PGR camera adjustment screw
Plastic-Head Thumb Screw 6-32 Thread, 5/8" Length	1	McMaster-Carr	91185A579	$9.99 (pack of 25)		Mirror holder screw
Plastic-Head Thumb Head, 8-32 Thread, 7/8" Length	1	McMaster-Carr	91185A582	$14.09 (pack of 25)		Lens holder screw
N-BK7 Bi-Convex Lens, Ø1", f = 50.0 mm, ARC: 350-700nm	1	ThorLabs	LB1471-A	$32.10		Main lens of system
M2 5mm bushings	3	Kozac Micro Adjustments	TB2-20-07	$3.97		For endoscope attachment screws
C-Mount	1	ThorLabs		$32.00		Mount for fluorescent filter
Mounting Pin	1	ThorLabs		$11.00		Mounting pin for Hamamatsu Camer
Silver Tip 18-8 SS Socket Set	1	McMaster-Carr	99934A140	$5.72 (pack of 5)		For securing dichroic mirror
ABS printing for main components (Dovetail, mirror holder, base, and handle).	1	UM3D Printing Lab	-	$250.00		All components for our device.

The following table lists the components made at the University of Michigan 3D lab and paid for within our $400 budget. The total cost for the printed items is $250.

Table 10: Device components fabricated by 3D printing

Part Name	Qty	Material	Color	Manuf. Process	Function
Dovetail slide mechanism	1	ABS plastic	Off-white	3D printing using FDM machine	Allow movement of Hamamatsu camera
Detachable handle	1	ABS plastic	Off-white	3D printing using FDM machine	Allow user to grip device; detach
Base platform	1	ABS plastic	Off-white	3D printing using FDM machine	Contain optical components and provide connections for handle and dovetail slide mechanism
Dichroic mirror holder	1	ABS plastic	Off-white	3D printing using FDM machine	Hold dichroic mirror in place

Table 11: The last two components printed at the 3D lab were paid for by the NTR for $96.

Part Name	Qty	Material	Color	Manuf. Process	Function
Tripod Adaptor	1	ABS plastic	Ivory	3D printing using FDM machine	Allow movement of Hamamatsu camera
Housing Cover	1	ABS plastic	Ivory	3D printing using FDM machine	Allow user to grip device; detach

Total cost for all items purchased through the Mechanical Engineering department: <u>$390.37</u>

APPENDIX B: Description of Engineering Changes since Design Review #3

CHANGES TO DOVETAIL MECHANISM

A new fastening procedure for the Hamamatsu camera was incorporated changing the design of the dovetail slide mechanism. We realized a screw connected to the Hamamatsu camera that we had previously thought could be removed, was actually fixed. The hole on the top face was enlarged. An extension piece on the bottom face was added with a smaller thru hole. Our team authorized this design change. Dimensions of the design changes are provided below. All other dimensions stayed the same.

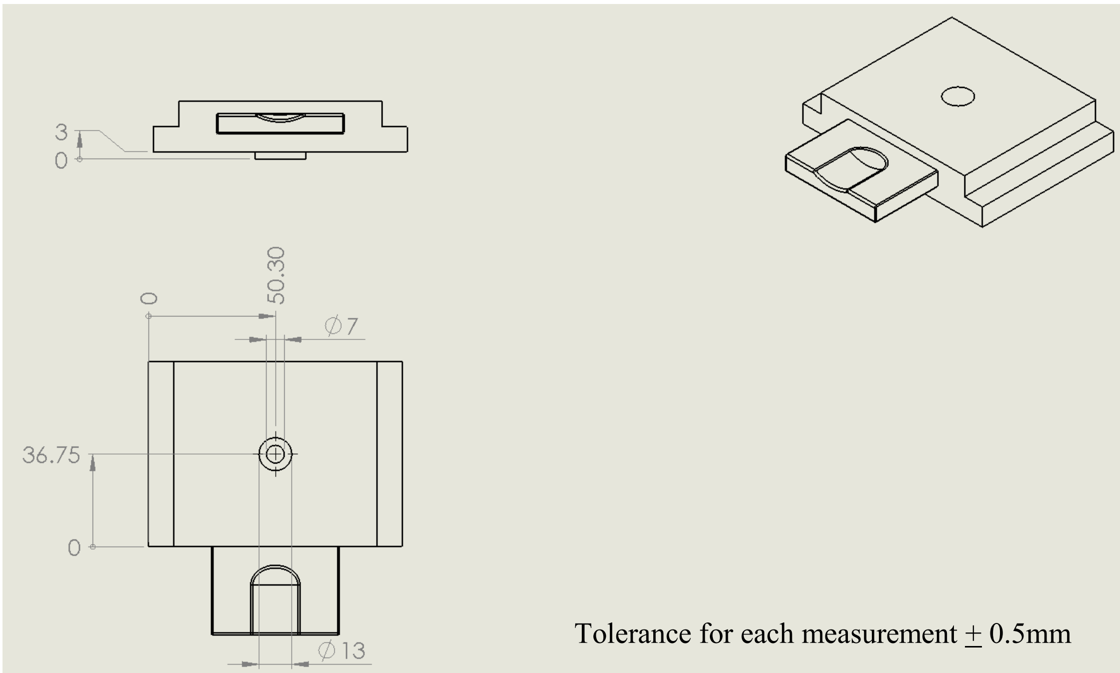

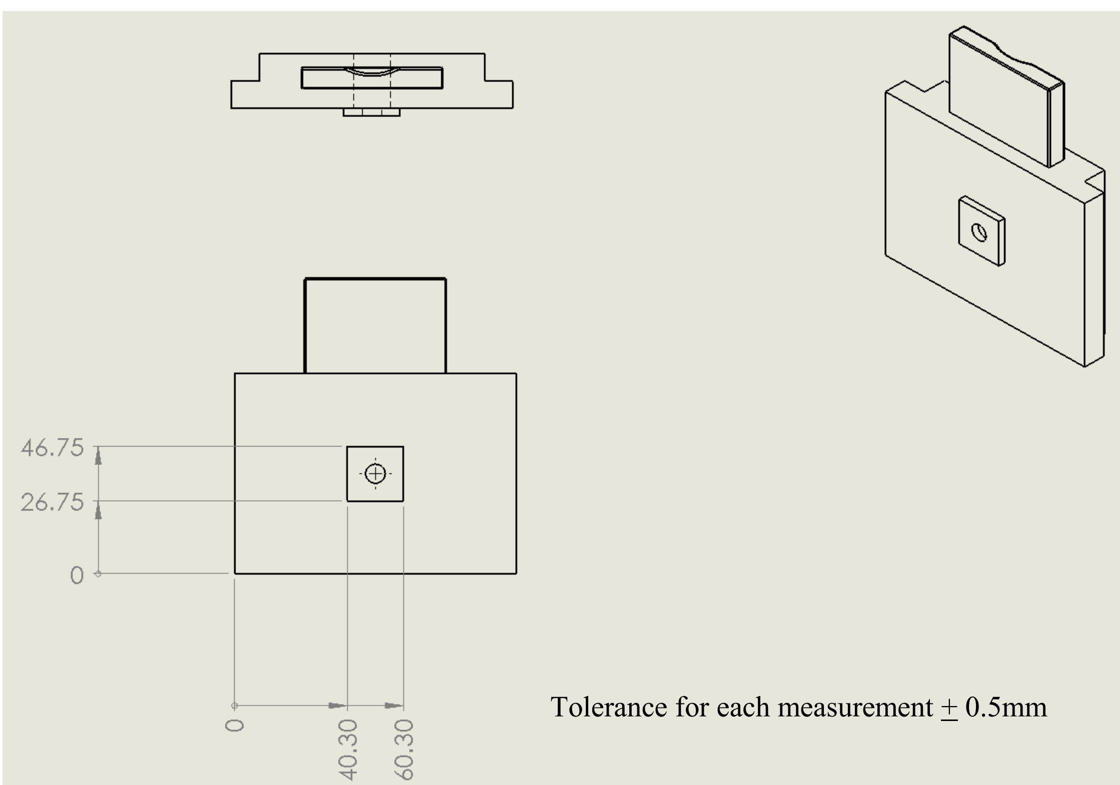

CHANGES TO THE BASE PLATFORM

In order to accommodate a cover for the housing we needed to add grooves into the siding of the platform so the cover can be secured. A rectangular section of the base platform, where the dovetail slide mechanism sits, was removed to allow the small extension from the dovetail and an M6 cap screw to slide without contacting the base platform. As a safety precaution, we added holes for a safety guard rod if the set screws holding the dovetail and Hamamatsu camera ever failed. Holes for threaded bushing inserts were added to the front face of the lens compartment holder to allow the endoscope attachment device to be secured to the base platform. The larger viewing hole on the front face of the lens compartment holder was reduced in size to allow for the threaded bushing inserts. The four slots on the Point Grey Research's platform camera were changed to two slots so the 3D printer could properly manufacture the design. A small area was removed above the hole on the railway system to allow the ball on the quick release pins to snap in. Dimensions of the design changes are provided below. All other dimensions stayed the same.

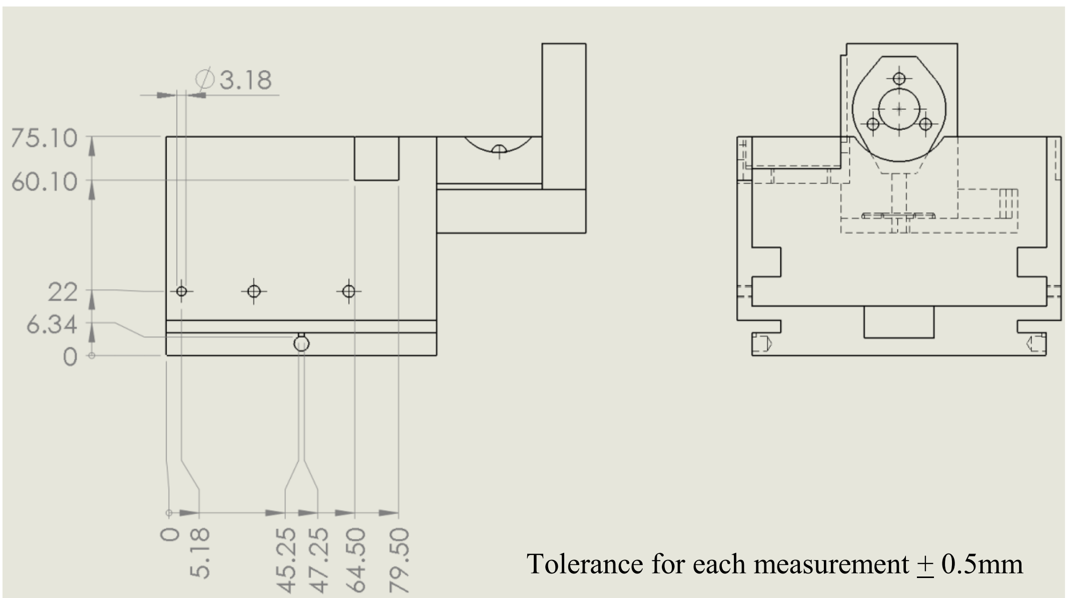

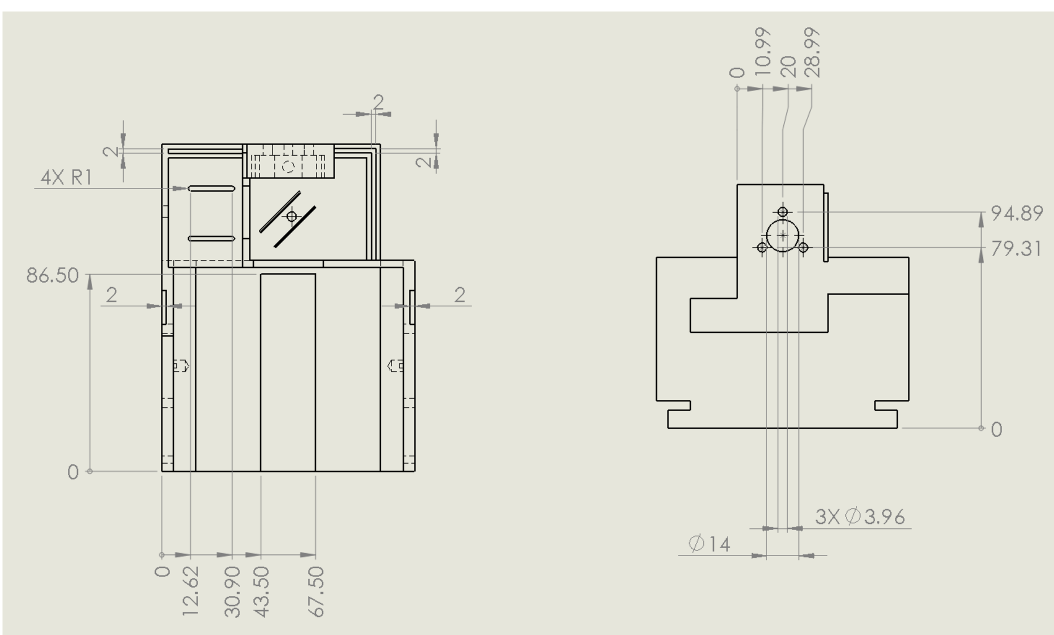

DEVICE COVER

As an accessory, our sponsor requested a cover to go along with the housing to aid in preventing light scattering during the procedure. In our original design we did not account for the camera wire extending from the Point Grey Research camera. We decided to cut a small area out of the side, after the cover had been manufactured, so the cover could still be flush with the base platform and not interfere with the camera wire. The design for the cover is pictured below.

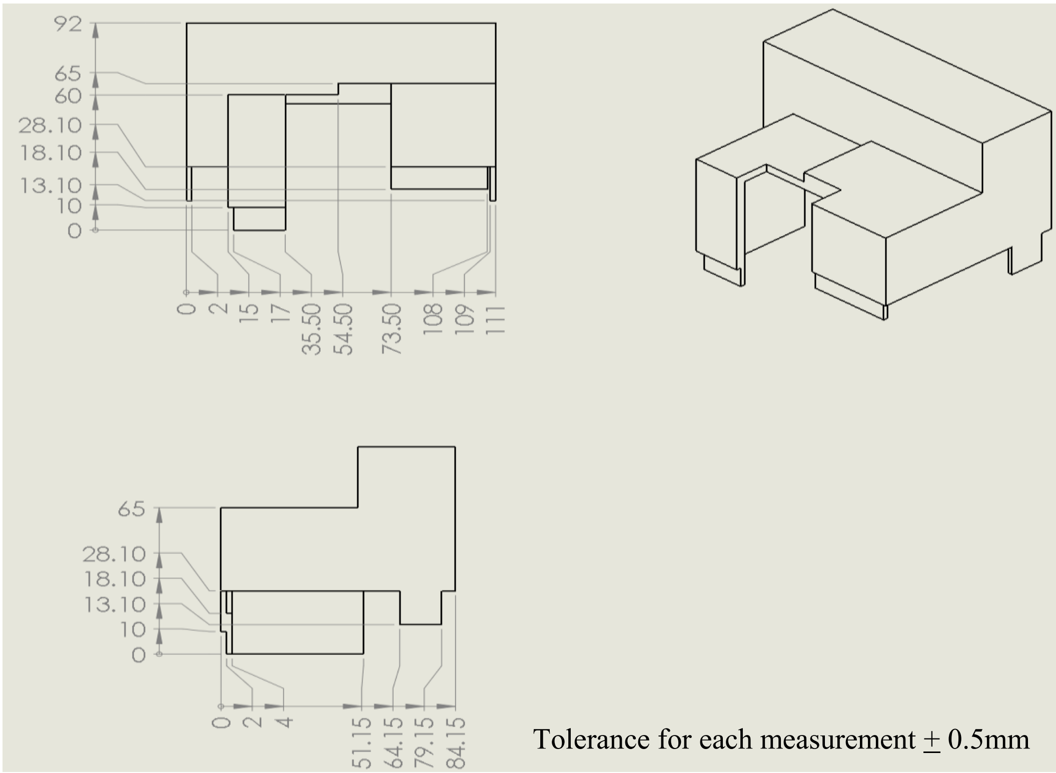

Tolerance for each measurement ± 0.5mm

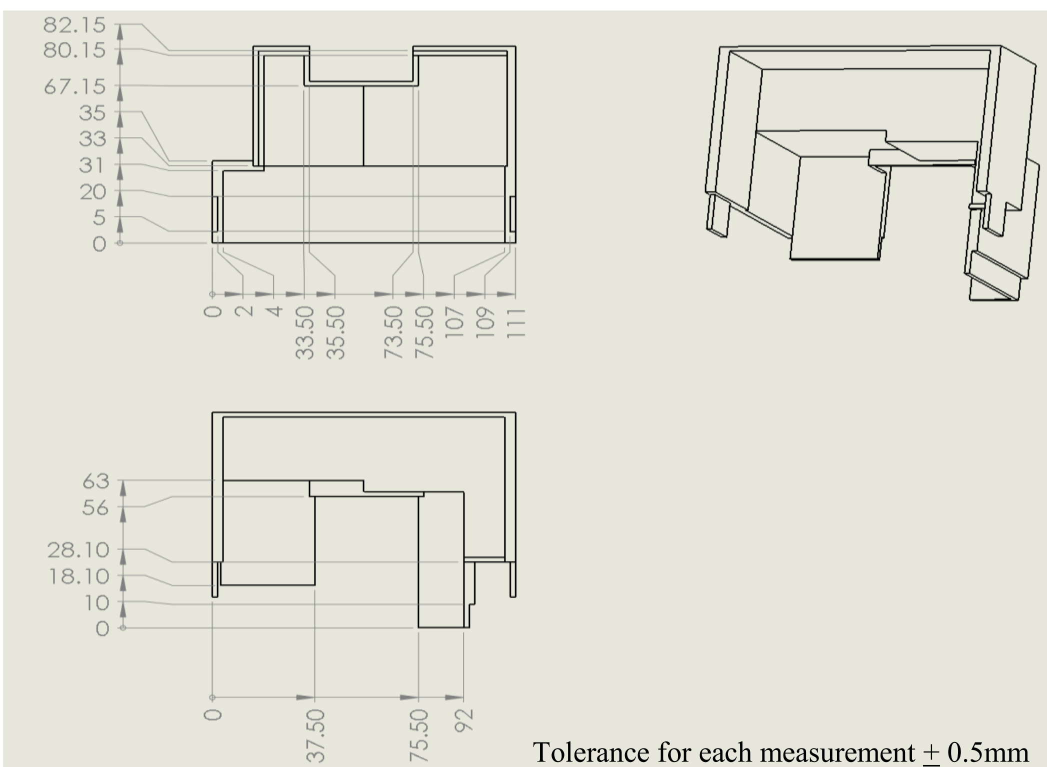

Tolerance for each measurement ± 0.5mm

TRIPOD ADAPTOR

Our sponsor requested to be able to attach our device to a tripod to have controlled movements during the procedure. The design for the tripod adapter is pictured below.

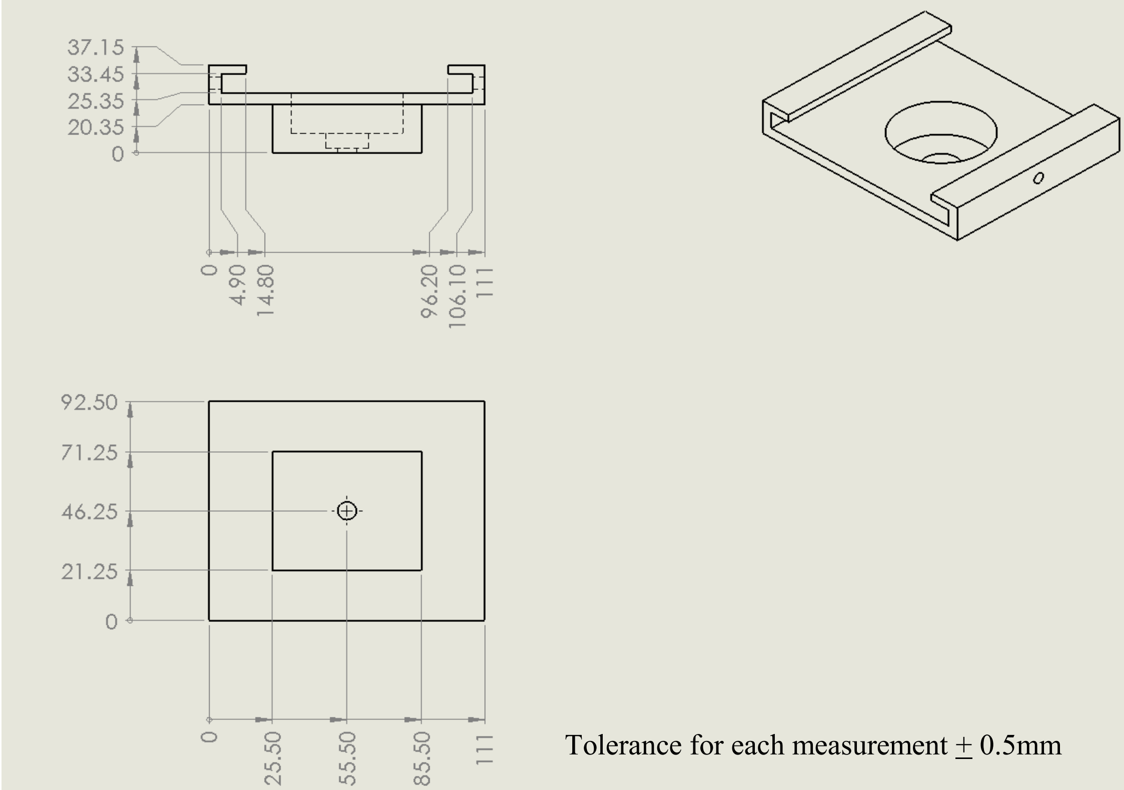

Tolerance for each measurement ± 0.5mm

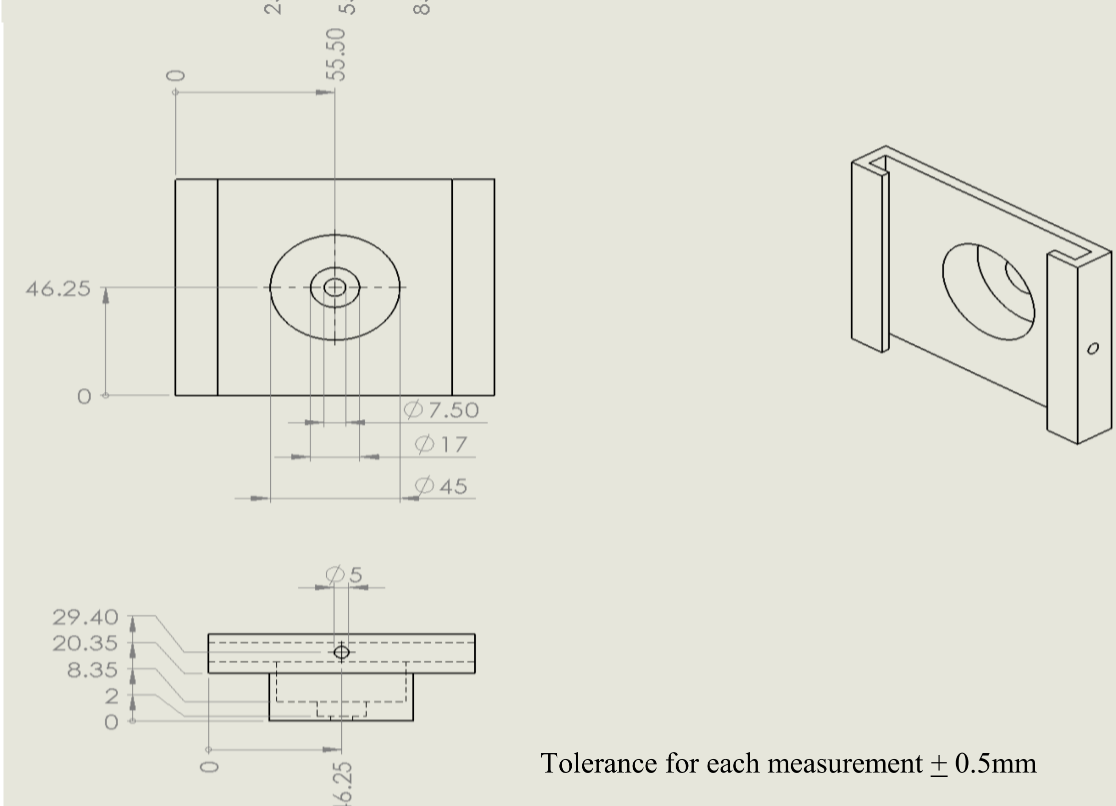

Tolerance for each measurement ± 0.5mm

APPENDIX C: DESIGN ANALYSIS

Material selection assignment on functional performance

Component 1: Base plate

The base plate supports the load of the two cameras and all optical components. It also carries the additional weight of the cover. While the portion of the base plate under the large camera sits on top of the handle, the front half of the base plate with the Point Grey camera, lens holder, mirror, and cover extends forward. It also carries the weight of the endoscope.

Our main material concern for the base plate is bending due to the weight of the endoscope 137mm long acting 55mm away from the main structure of the baseplate. Any deflection in the base plate, especially the front half, which connects the Hamamatsu camera to the main lens, can affect the optical alignment of components and cause obstruction in the image.

The base plate is treated like a beam undergoing bending. The weight of the base plate needs to be minimized, while the stiffness needs to be maximized. From the design, the volume of the base plate is fixed at 309102.09 mm^3. As per our engineering specification on stiffness for the housing in general, any deflection in the plate has to be less than 2 mm.

Since there is a constraint on bending, the material index for a light stiff beam is

$$M = \frac{E^{1/2}}{\rho} \qquad \text{Eq. 2}$$

where E is the Young's modulus and ρ is density [21]. Therefore, a line of slope 2 was applied on the logarithmic CES materials selection graph of E versus ρ.

As a soft constraint, a price limit of $30/kg was also put to keep the cost of the component reasonably low and the entire system including the fasteners and optical components within our price restriction of $400.

Material strength can also be maximized. So, a minimum limit of 10^9 Pa was used to narrow results down to the strongest materials. Also, an opaque material will help prevent light scatter. A limit was also set on the maximum density allowed. This was derived from a consideration of the entire optical housing.

The engineering specification for mass allows a maximum of 2kg for the entire system. Subtracting the masses of the cameras and other optical components the total mass of the housing cannot exceed 0.86kg. The total volume of the housing components is shown in Table 2 on Pg 60.

Table 12: SolidWorks calculations for the volume of main system components

	Base plate	Dovetail slide	Handle	TOTAL
Volume (mm^3)	309102.09	138552.77	211090.54	0.00066 m^3

An approximate maximum density for the material was derived using the mass of 0.86 kg and the total volume of .00066m^3. The maximum density for the base plate material was calculated as $\rho \approx 1300$ kg/m^3. The following quantities were used to restrict the material selection.

Density	Max 1300 kg/m^3
Price	Max $30/kg
Young's Modulus	Min 10^9 Pa
Transparency	Opaque

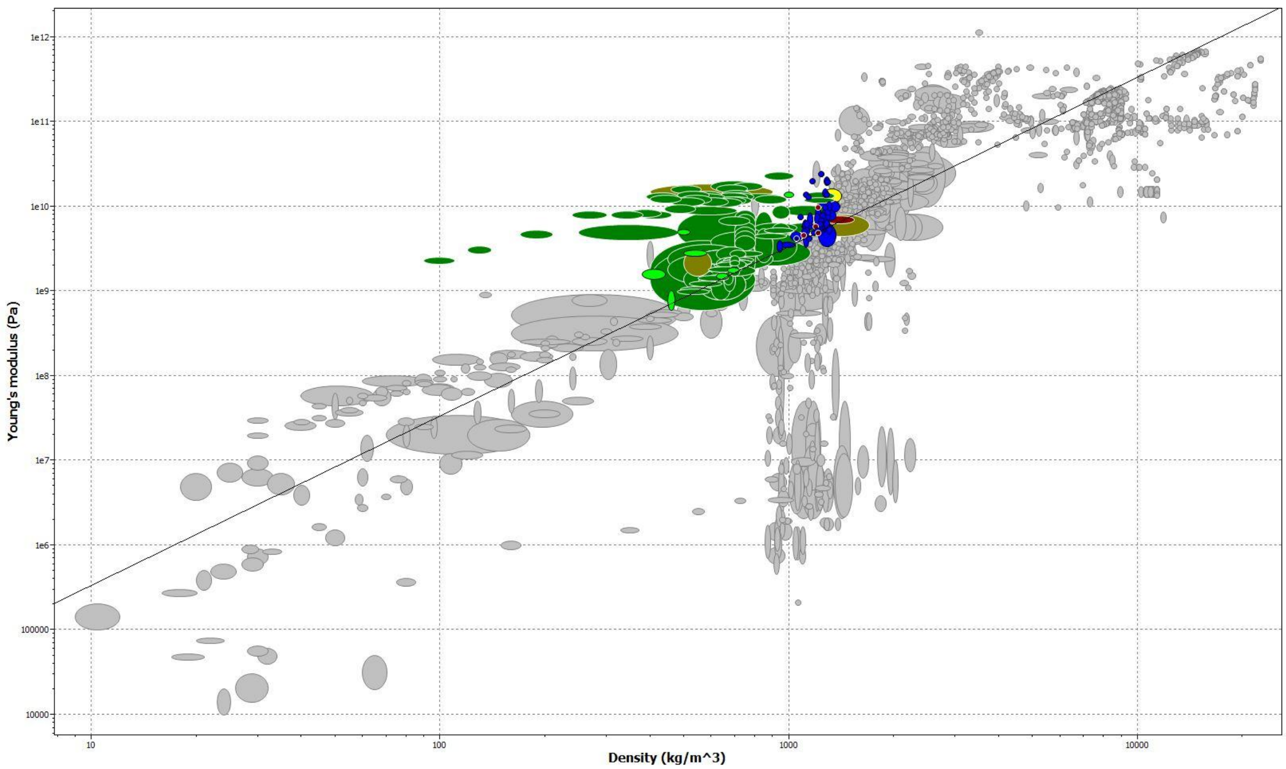

The top five materials suitable for the base plate as determined by the application of CES are ABS plastics, Aluminum foam, Woods: Balsa, Beach, Oak, Plywood, PA plastics, and SMA plastics.

Component 2: The handle

The handle supports the load of the dovetail slide mechanism, the base plate with all optical components and cameras, and the cover. The user holds it to carry the weight of the entire system. The handle is treated as a column in compression loading. For the derivation of a material index, a simple cylinder is assumed, so that

$$I = \frac{A^2}{4\pi} \qquad \text{Eq. 3}$$

where I is the moment of inertia, and A is the cross sectional area. Given that

$$m = \rho A l \qquad \text{Eq. 4}$$

where m is mass, ρ is density and l is the length of the column, substitution results in

$$I = \frac{m^2}{4\pi\rho^2 l^2} \qquad \text{Eq. 5}$$

The column will be design safe and avoid buckling elastically when

$$F < F_{crit} = \frac{n\pi^2 EI}{l^2} \qquad \text{Eq. 6}$$

Where F is the load, n is a constant on end constraints, E is the Young's modulus [21]. Substituting Eq. 6 into Eq. 7,

$$m > \left(\frac{4F}{n\pi}\right)^{1/2} (l^2) \left(\frac{\rho}{E^{1/2}}\right) \qquad \text{Eq. 7}$$

where brackets are ordered from left to right as functional requirement, geometry and material. The material index for a light, stiff column is

$$M = \frac{E^{1/2}}{\rho} \qquad \text{Eq. 8}$$

Therefore, a line of slope 2 was applied on the logarithmic CES materials selection graph of E versus ρ. Similar to the base plate, the primary soft constraint is to reduce cost of material by keeping it below $30/kg. Maximum density of the entire housing permitted was applied as an upper limit. Young's modulus also had a minimum cap like the case for the base plate, to limit results to the strongest materials. For the handle, transparency of the material did not matter.

Limits used:

Density	Max 1300 kg/m^3
Price	Max $30/kg
Young's Modulus	Min 10^9 Pa

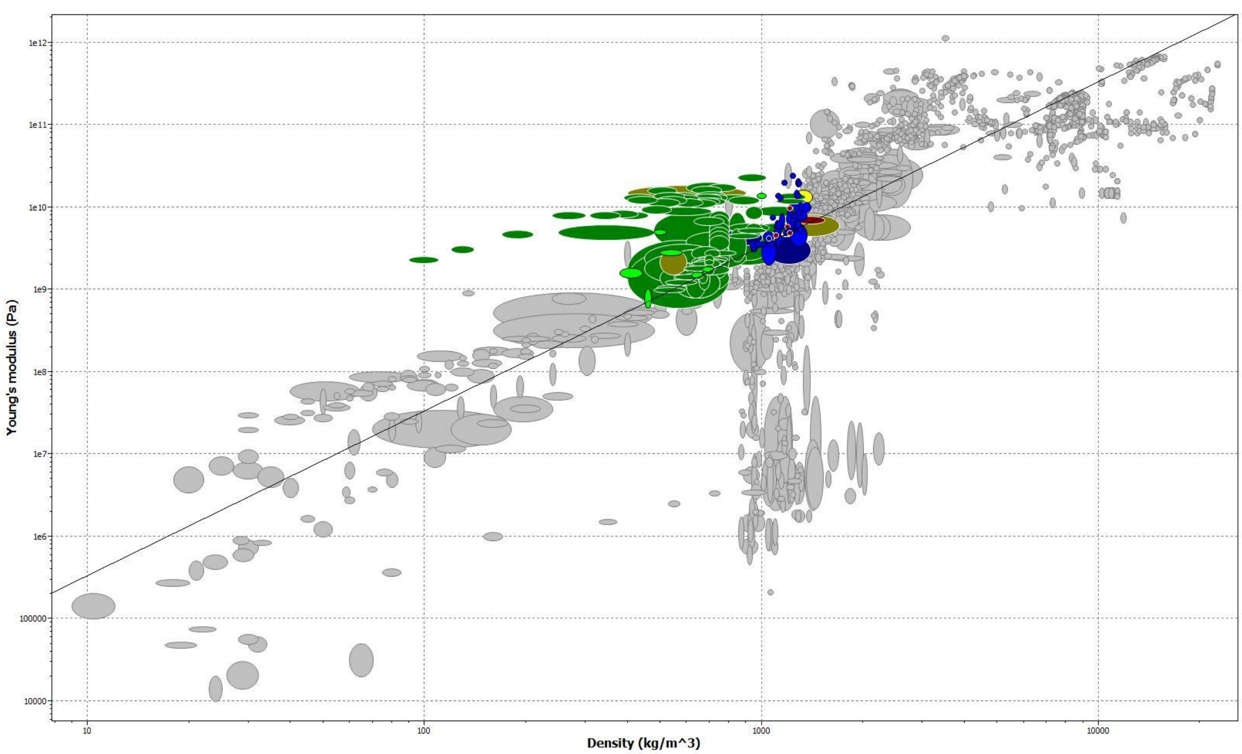

The top five materials selected by the application of CES overlapped with those for the base plateform: ABS plastics, Aluminum foam, Woods: Balsa, Beach, Oak, Plywood, PA plastics, SMA plastics.

Selection of ABS plastic

ABS plastic was selected from both its properties and manufacturability (Fabrication Plan on Pg. 43). First material properties were compared. All materials had comparable strength (Young's Modulus and yield strength), density, and price. Plywood and Aluminum foam however were an entire order lower in Hardness (Table 13). Considering the complex 3D geometry of the housing and the requirement for accurate optical positioning, fewer manufactured parts are preferred for assembly. Therefore, plastics, which are highly suitable for additive manufacturing processes, are preferred to woods. Both SMA, which is clear plastic used for optical fibers and PA, best known as nylon, are not suitable for the solid component manufacturing necessary for the design. Therefore, ABS was the best fit.

Table 13: Key properties of top 5 chosen materials from CES database [22]

	ABS (molding)	PA (general purpose)	SMA (molding)	Plywood	Al Foam
Young's Modulus (GPa)	1.1-2.41	18.9-1.11	2.34-3.24	6-9	13.2-14.8
Yield Strength (MPa)	18.5-40.7	48.1-60	35.9-55.8	34.4-42.1	25-30
Hardness (MPa)	54.9-120	151-167	106-164	36.6-44.7	24.5-29.4
Density (kg/m^3)	1010-1050	1190-1210	1050-1080	700-800	970-1030
Price (USD/kg)	3.17-3.49	6.5-7.15	2.62-2.88	0.33-1.01	8.29-10.4

Environmental Performance

The top two material choices that we identified using the CES software, were Acrylonitrile-butadiene-styrene (ABS) copolymer and an aluminum alloy ($AlMg_3$). We calculated that we would need approximately 0.6kg of ABS plastic or 0.72kg of $AlMg_3$ in order to construct our device. Using the SimaPro software, we evaluated the total mass of air and water emissions, raw materials, and solid waste shown below in Fig 45.

Figure 45: Bar graph comparing the Raw, Air, Water, and Solid Wastes of ABS plastic and Aluminum Alloy ($AlMg_3$).

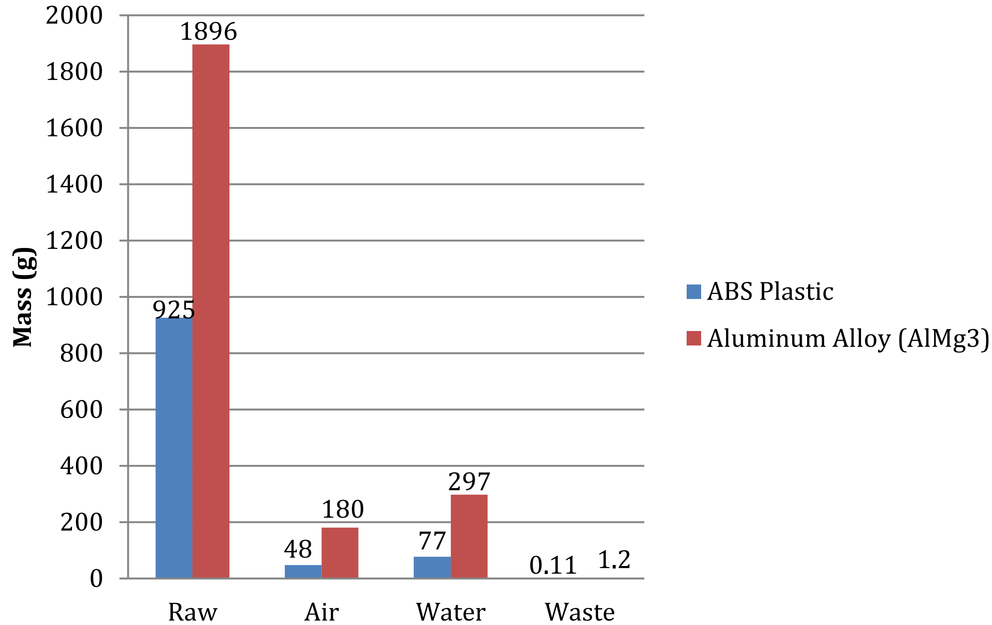

The total mass of solid waste was very small and therefore cannot be seen on the graph. $AlMg_3$ created more waste in each category and had a total of 2374.2g of waste, while ABS plastic had a total of 1050.11g of waste. We also evaluated which material would have a bigger impact on the environment within each of the EcoIndicator 99 damage categories. The results are shown below in Fig 46.

Figure 46: Bar graph comparing ABS plastic and Aluminum Alloy ($AlMg_3$) material performance in the EcoIndicator 99 damage classifications.

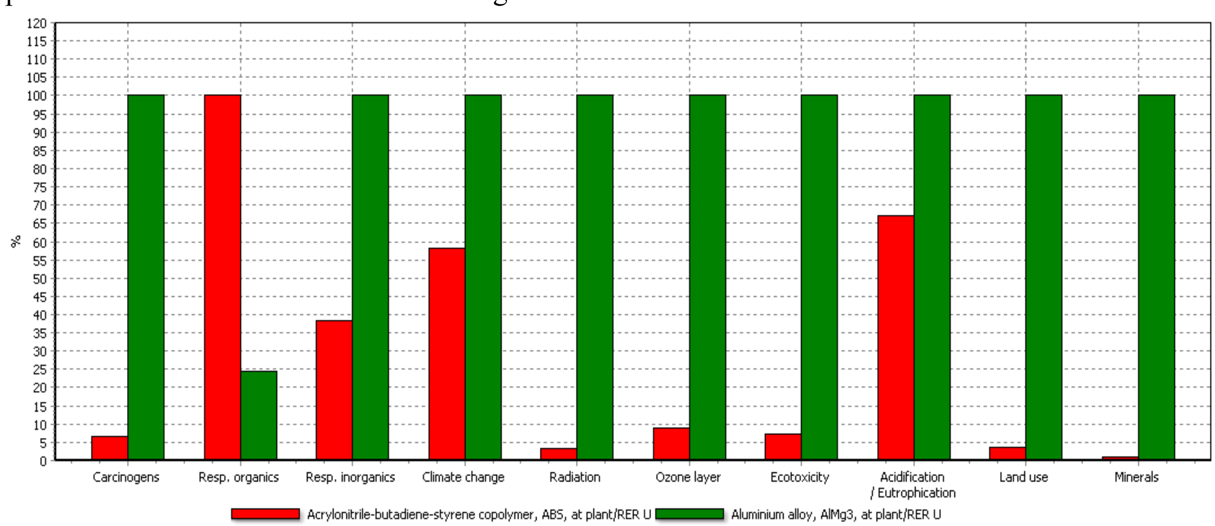

$AlMg_3$ had higher emissions in every category except for the Resp. organics category. In addition, ABS plastic had emissions under 50% for seven out of the ten classifications, when compared to the emissions of $AlMg_3$. Using SimaPro we were also able to predict which damage meta-categories are going to important based on the EcoIndicator 99 point values. The results can be seen in Fig. 47.

Figure 47: Bar graph comparing material performance in normalized damage meta categories.

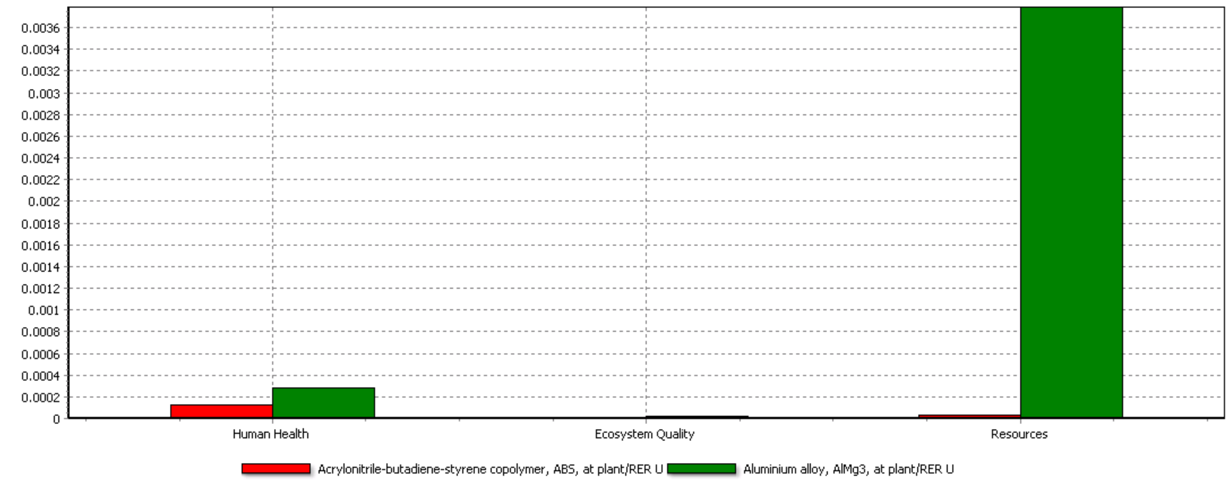

From the bar graph, it shows that the resources category will have the highest impact in the future as it has the highest value. SimaPro also normalized certain categories as well as assigned different weights to these categories that corresponded to different point values seen in Fig 48.

Figure 48: Comparison of ABS plastic and Aluminum Alloy ($AlMg_3$) performance in EcoIndicator 99 points.

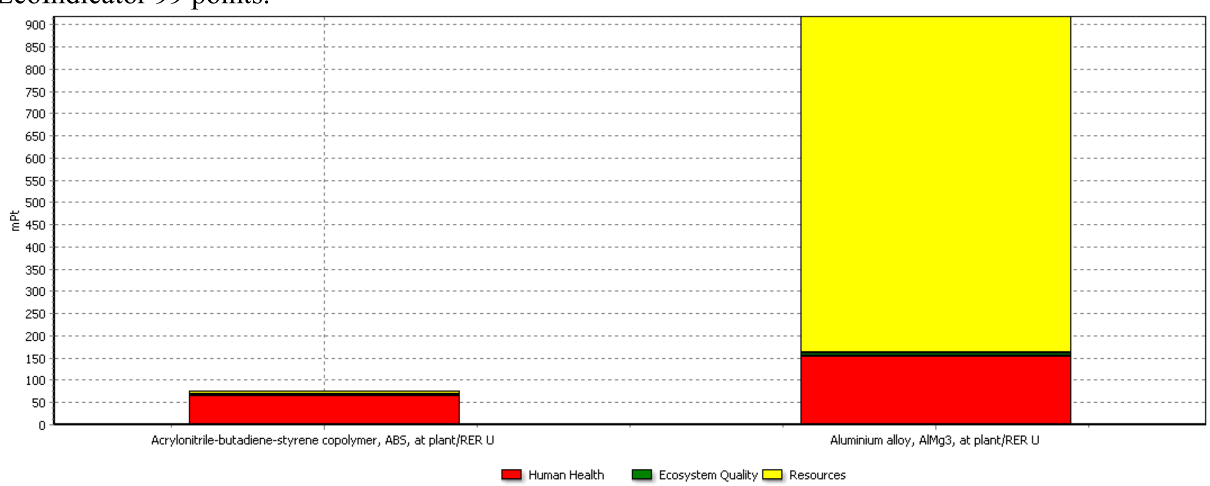

ABS plastic has a lower amount of points and therefore will be less harmful to the environment during production and use of our device. ABS has a less amount of adverse effects on the environment than $AlMg_3$ and consequently, is a better material to manufacture with when the life cycle of the whole product is considered.

Manufacturing process selection

The endoscope optical housing is highly specific to the requirements of our sponsor's NTR center research team. It is to be used for endoscopic research on mice models. The design cannot simply be scaled up for other forms of testing. In the event that this research expands to human testing, the entire optical and endoscopic system will change.
Given the design's specificity, only research teams conducting identical experiments with the same brand of endoscope, cameras and optical instruments will have a need for it. The real-world production volume will be in the 10s to a hundred at most.

A single material, ABS plastic was selected as the top choice for both the base plate and the handle. The CES manufacturing process selector was used to determine the best manufacturing process for the components. The materials bank was limited to just ABS plastic and the process was defined as shaping processes.

Our design provided the geometrical constraints. The components are 3D, hollow in the case of the handle and solid in the case of the base plate. The minimum thickness of walls is 2mm and the widest walls are 5mm thick. With these constraints prescribed, the relative cost of a single component was compared to the total batch size manufactured in the software.
Limits:

Shape	Solid and Hollow 3D
Part thickness	0.002 - 0.005 m

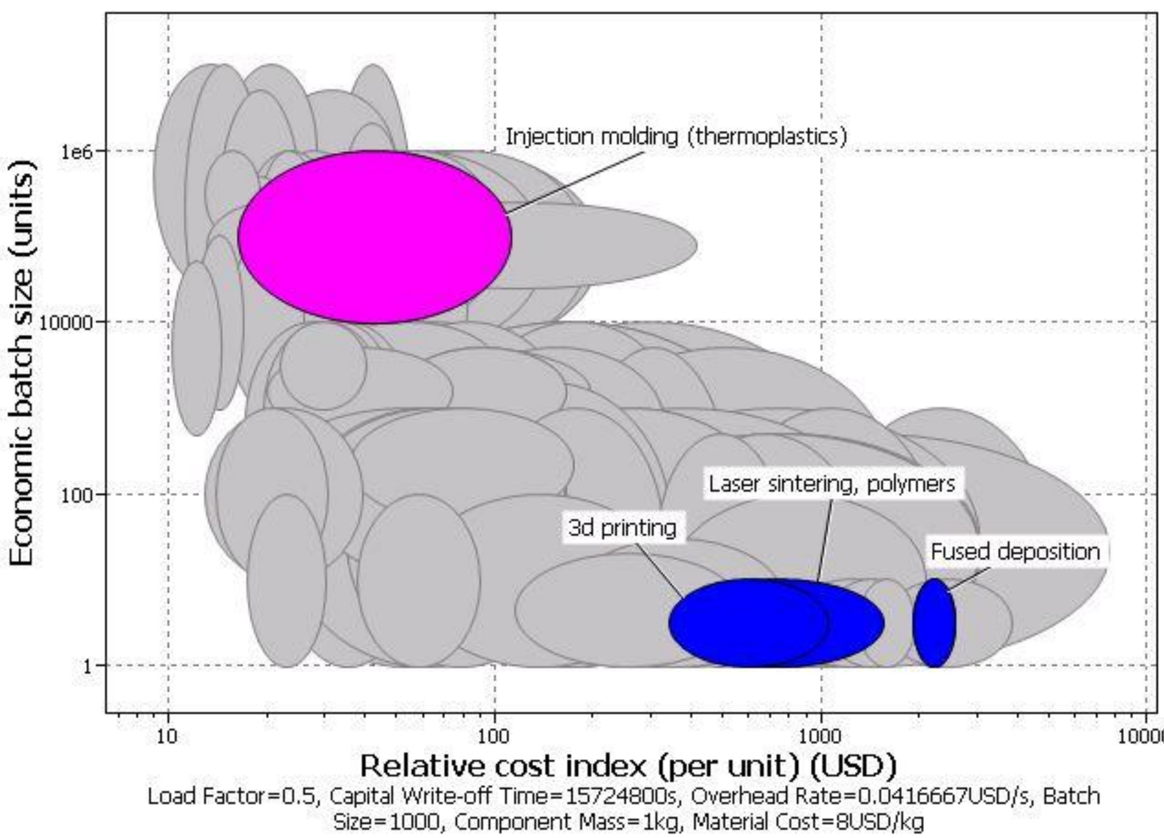

For a batch size smaller than one hundred, rapid prototyping processes like 3D printing and fused deposition are ideal. Injection molding is cheap per unit as shown in the CES analysis when the economic batch is over 10 000. Injection molding requires extremely expensive metal molds of the components to be first manufactured. Unless components are manufactured many tens of thousands of times, it is not more cost effective than additive processes like 3D printing or Fused Deposition.

While the additive manufacturing processes are quoted as close to $1000/kg, the cost incurred for a single complete prototype manufactured in the UM 3D lab on the dimension elite Fused Deposition Machine, was about half of that quoted by the CES analysis. Costs can be cheaper than the reference in the CES database. While $500-$700 per kg is still expensive, the experience with our sponsor shows that research groups are capable of affording such costs for precise and unique parts necessary for their experiments.

Both components carry loads and have similar requirements of being light and stiff. They are also closely assembled into the complete optical housing system. Given the same material choice, the same manufacturing process can be applied to them. Additive manufacturing then allows for different components to be arranged next to each other and be built in the same machine, simplifying the manufacturing process significantly. While the entire housing can take a total of over 20 hours to be built layer by layer, multiple components can be retrieved at the same time.

Customized design

It is more likely that different research teams will require slightly modified versions of the optical housing, tailored to their particular endoscope, cameras and lens focal length. Rapid prototyping processes simply require modified CAD drawing inputs to print or fuse the custom part. Injection molding on the other hand cannot accommodate changes as completely new molds will first need to be manufactured. Injection molding is a tool for mass production. In the case of equipment for highly specific research, custom production is necessary instead.

APPENDIX D: DIMENSIONED DRAWINGS

Dimensional Drawing of Dovetail Slide Mechanism (Dimensions are in millimeters)

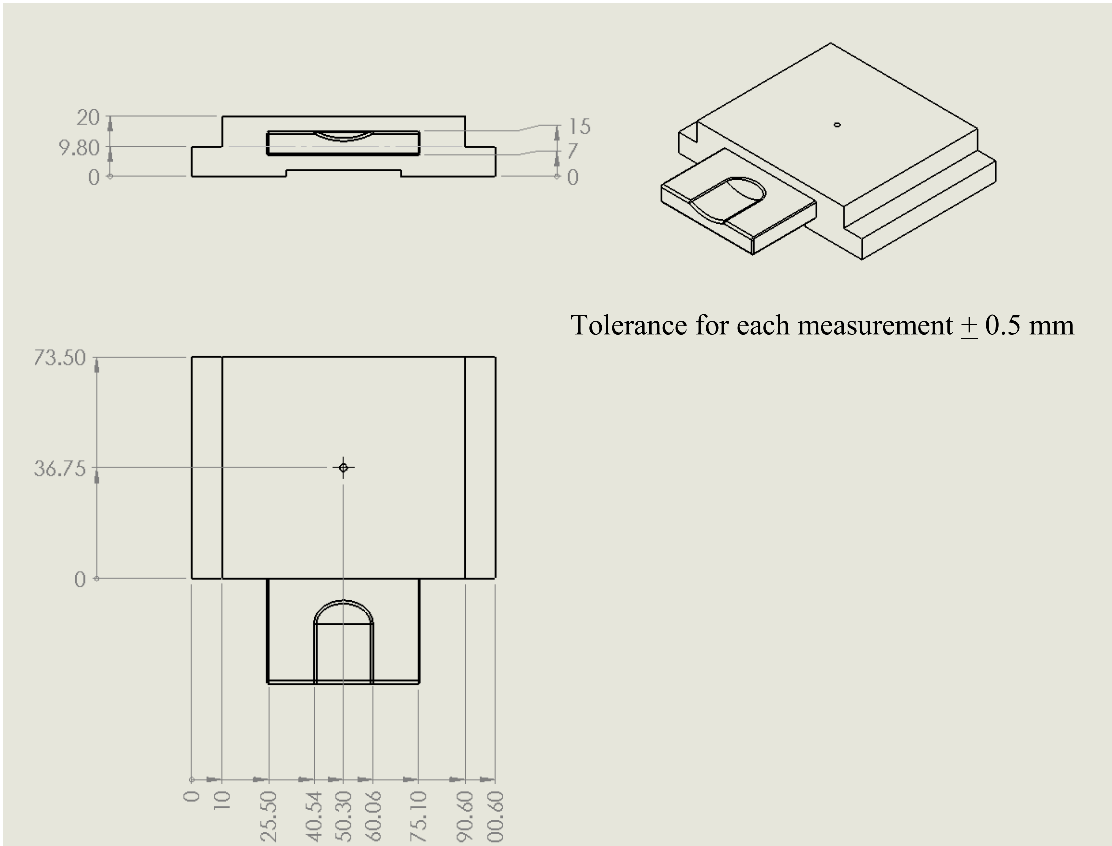

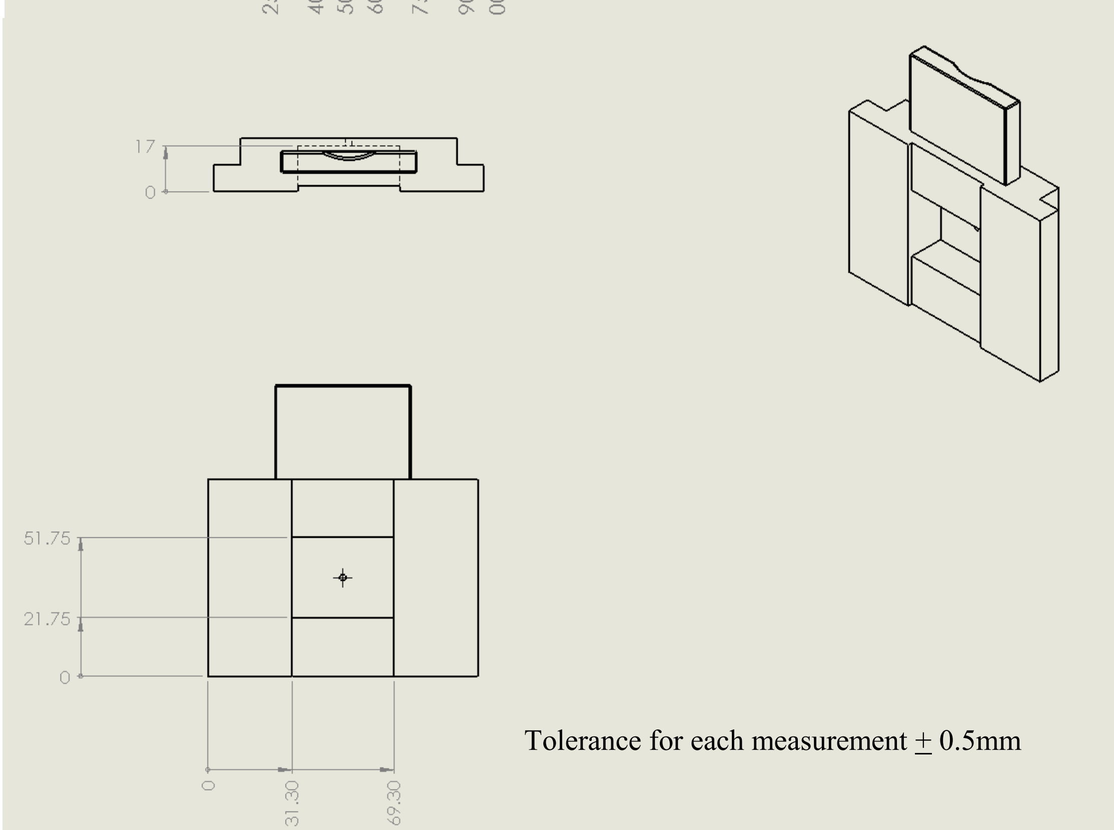

Dimensional Drawing of Handle (Dimension are in millimeters)

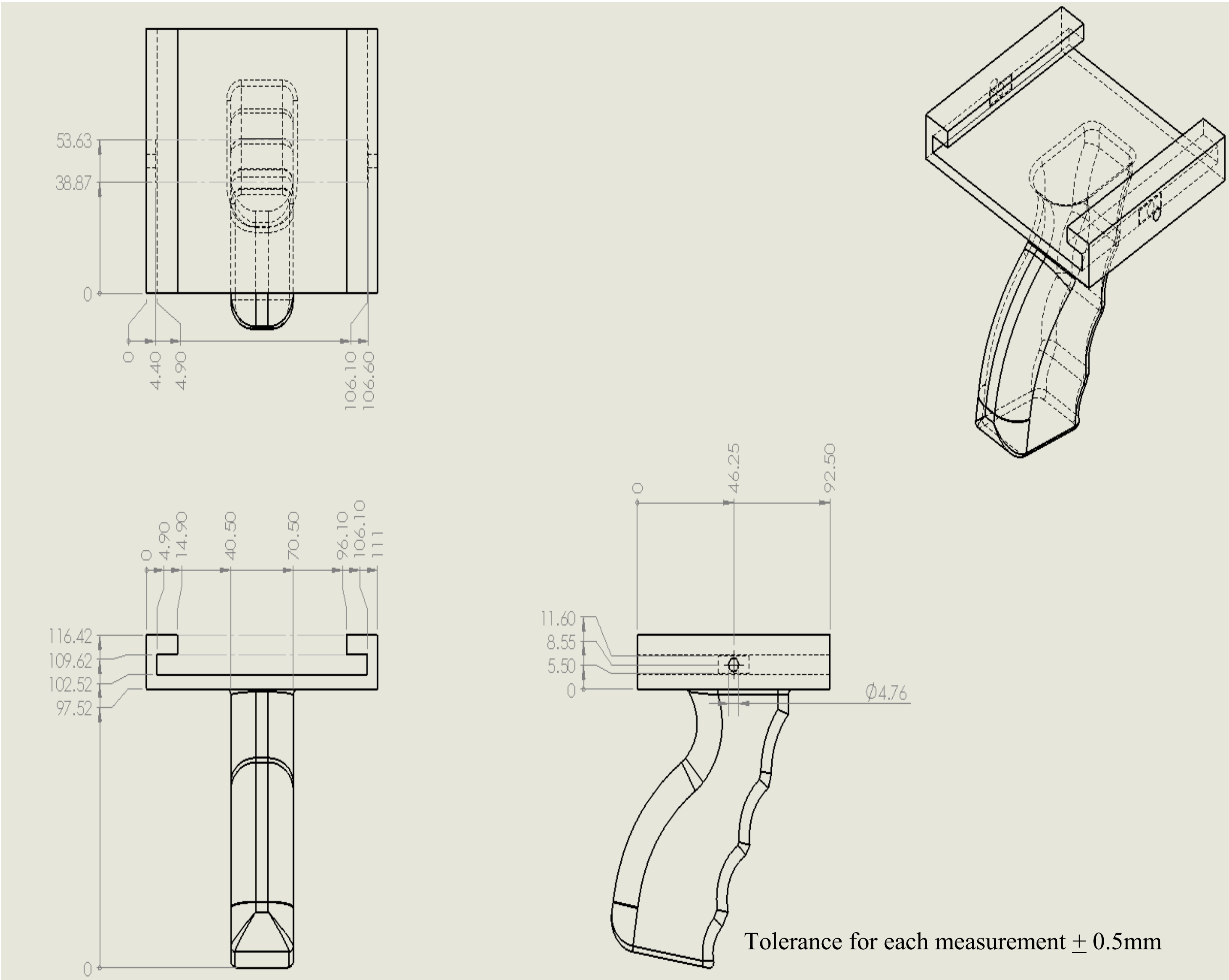

Dimensional Drawing of Base Platform (Dimension are in millimeters)

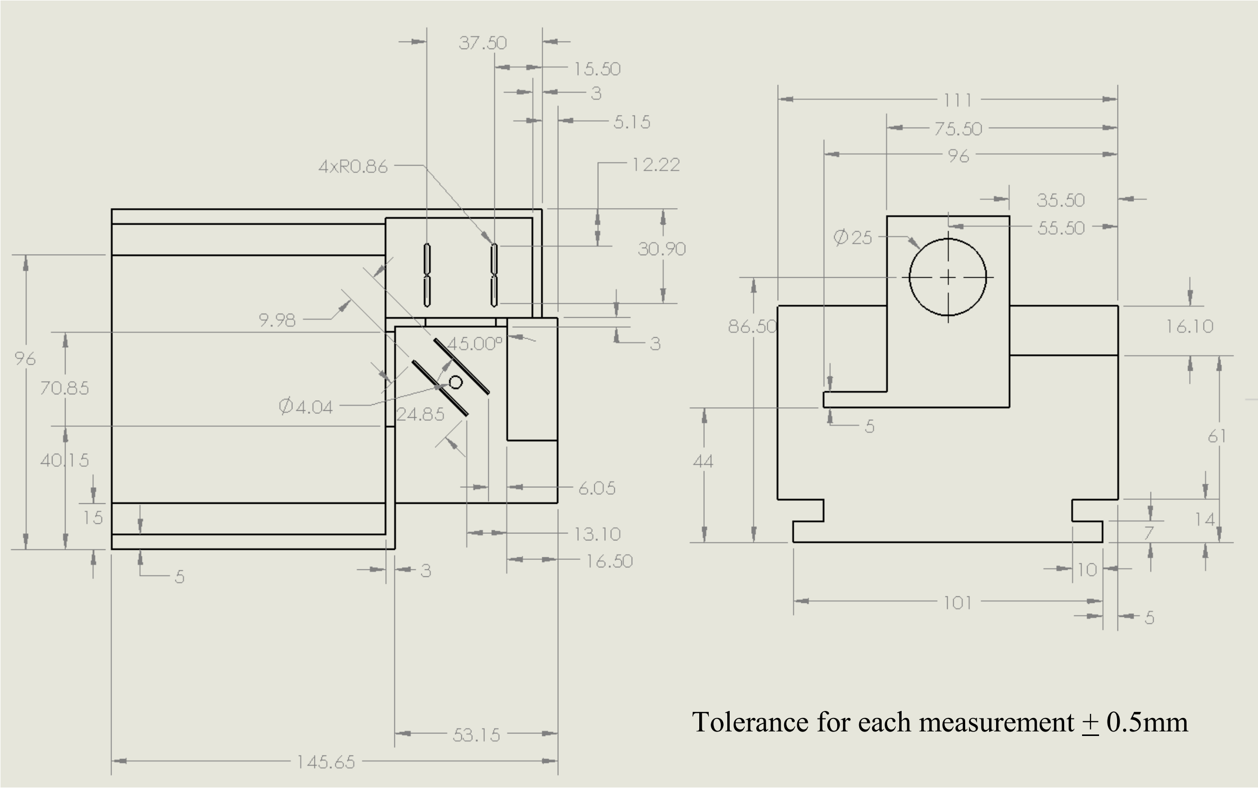

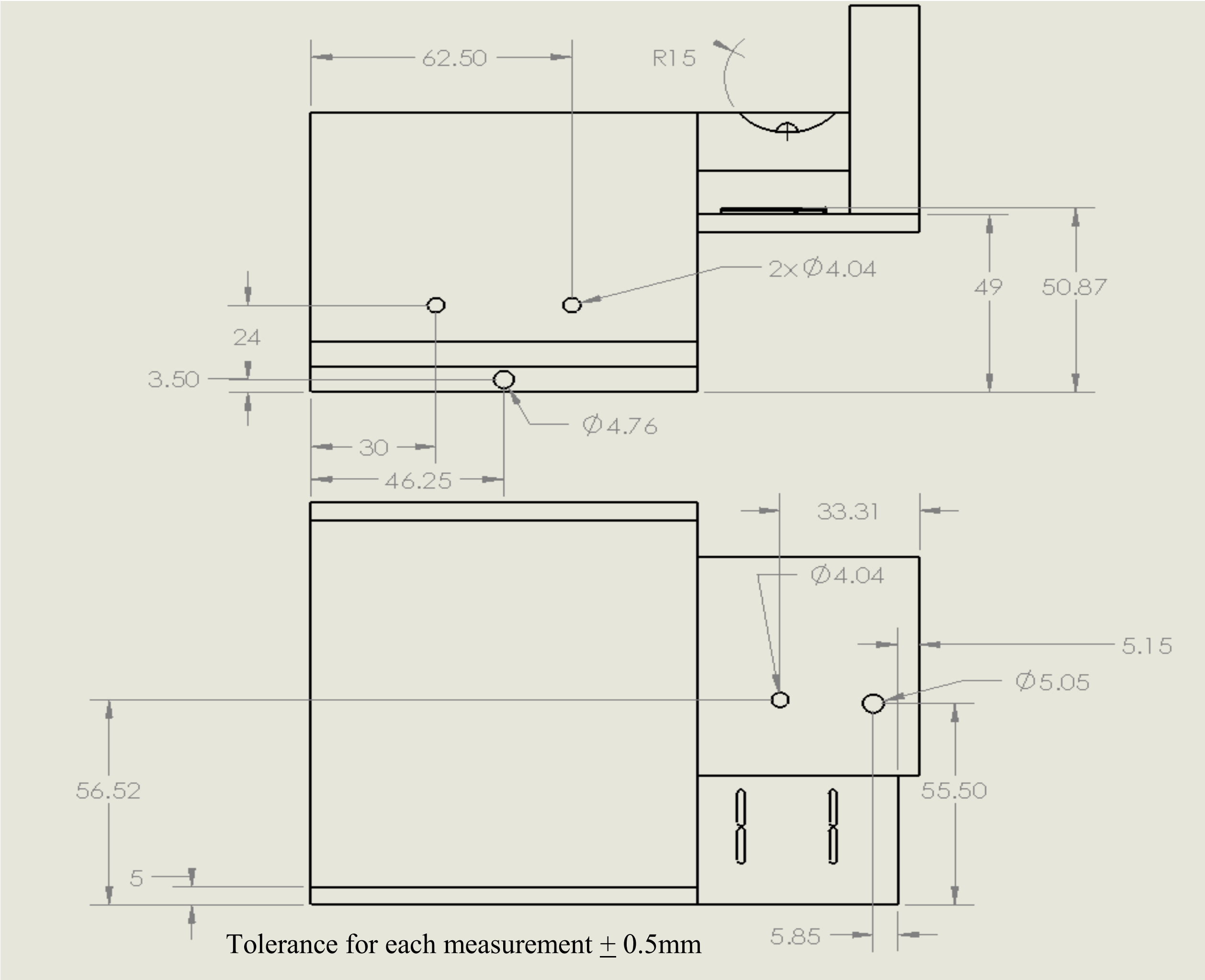

Dimensional Drawing of Mirror Holder (Dimension are in millimeters)

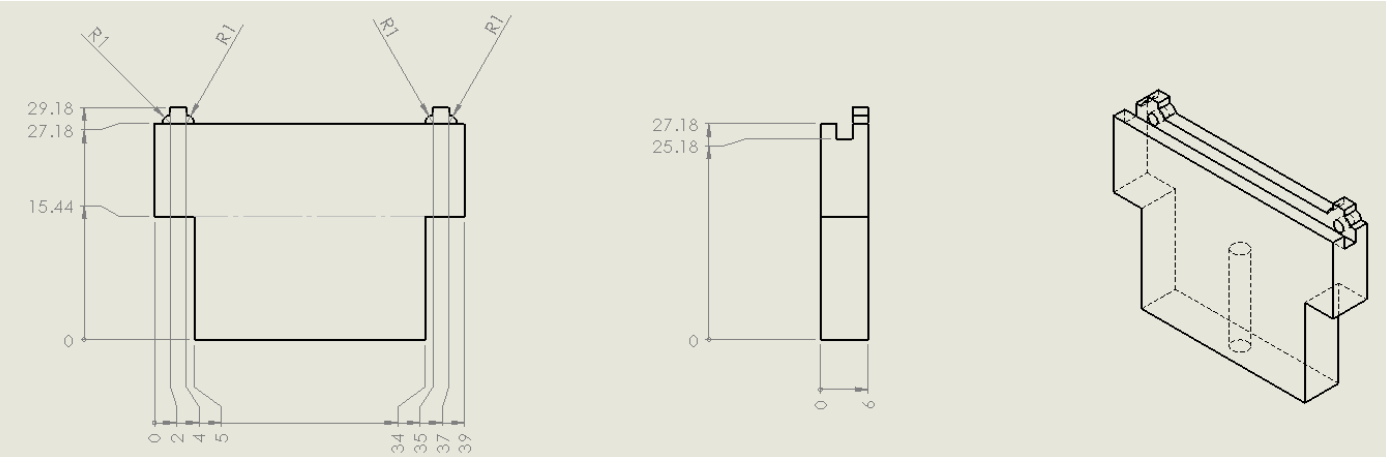

Tolerance for each measurement ± 0.5mm

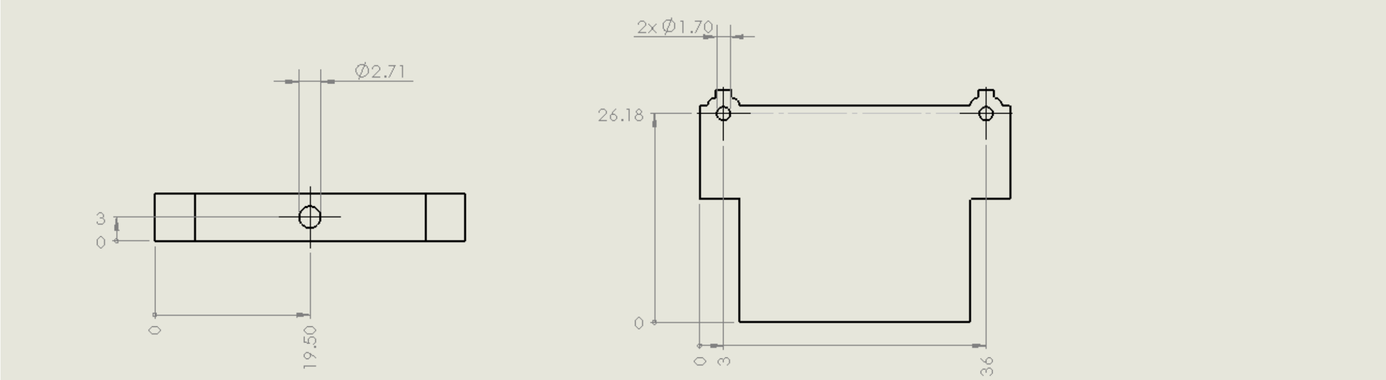

APPENDIX E: ADDITIONAL DESIGNS

Open-slotted platform idea

This design moves away from the channel layout of the previous ME 450 design. It incorporates a large platform that would be supported by pistol grip handle that has the capability of being detached from the platform. There would be slots on the top of the platform with additional pieces extending from the bottom of the platform beneath the slots so accessories can be added and secured via nuts and bolts. This design also places the Hamamatsu camera on a linear stage to allow the camera to move forwards and backwards to accurately adjust focus. The filter for the Hamamatsu can also be placed on the linear stage. The lens will be placed into a square piece that has been manufactured to allow the lens to sit securely. The square piece will have an extension at the bottom to be placed into the slot and bolted. The dichromatic mirror will be placed in a padded holder with a tightening mechanism that can be put into a slot on the platform. The endoscope will be attached to another square piece that will be built right into platform design. The Point Grey Research camera will be screwed into the platform and have slots

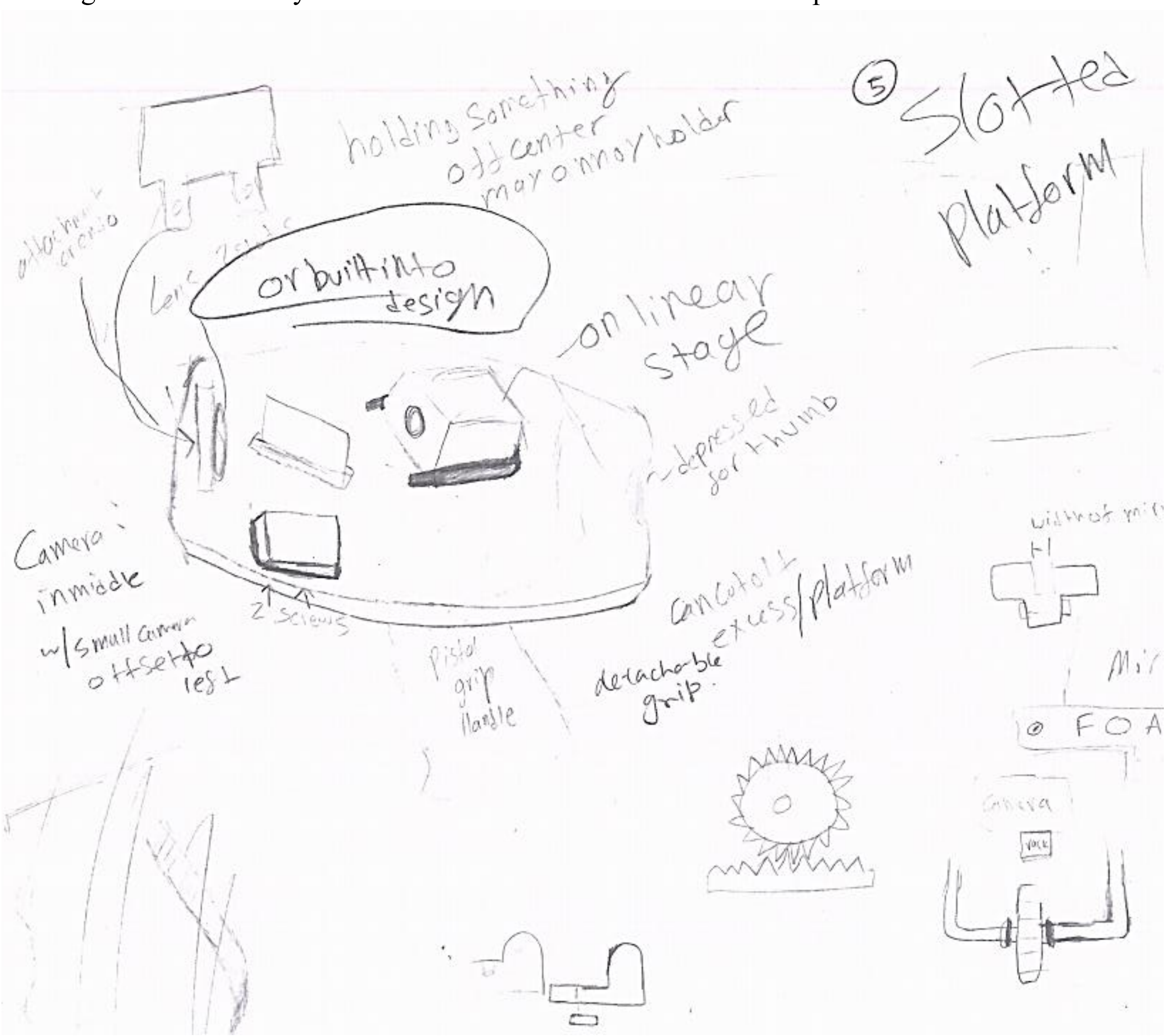

underneath to allow for movement. The back of the platform will have a depressed section for the user to comfortably place his/her thumb.

Camera in handle idea

The main aspect of this design is that the Point Grey Research camera will be placed into the handle of the device. A tuning screw will be used to move the camera up and down to adjust focus. Screws on each side will be able to tighten the camera to ensure it does not move around during the procedure. The dichromatic mirror will be placed in a padded holder with a tightening mechanism and will be attached to a standalone wall. The lens will be able to push fit into a rectangular piece from one side. To ensure it is stable during the procedure, a thin piece will be dropped behind it into a track manufactured on the sides of the rectangular piece. The Hamamatsu will be placed on an extending low friction platform with a curved support beneath it. The Hamamatsu will have a wall half the size of the camera surround the back and two sides. In front of the camera will be two springs and tuning screw that will come through the back wall. This spring system will allow the camera to move forward via the screw and backwards via the force exerted from the compression springs.

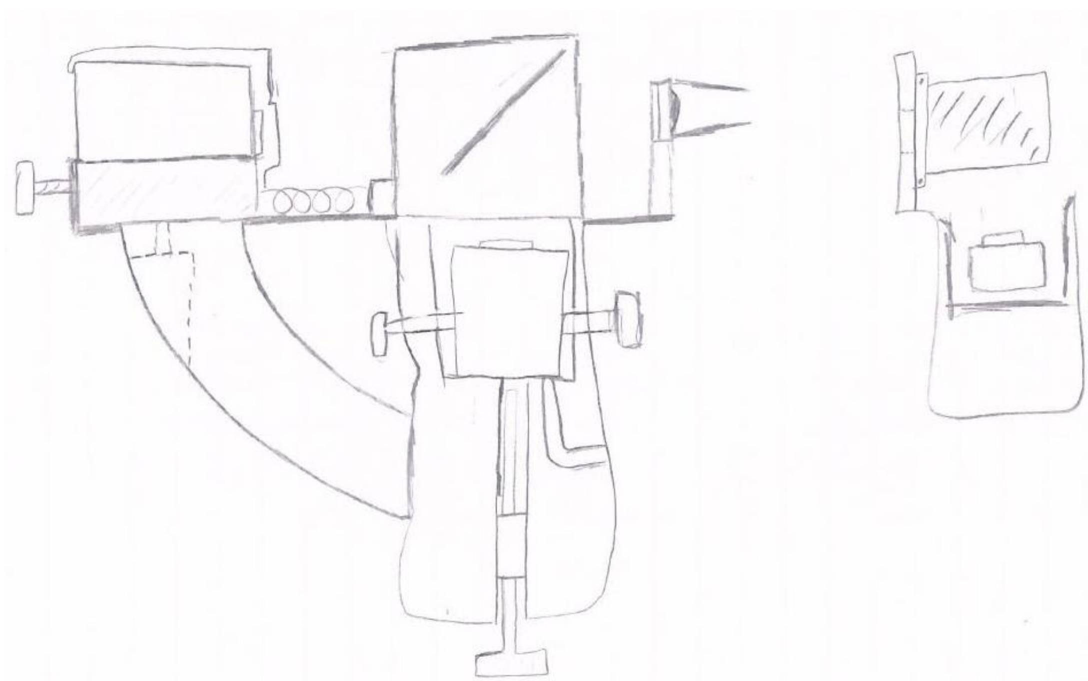

Individual Platform idea

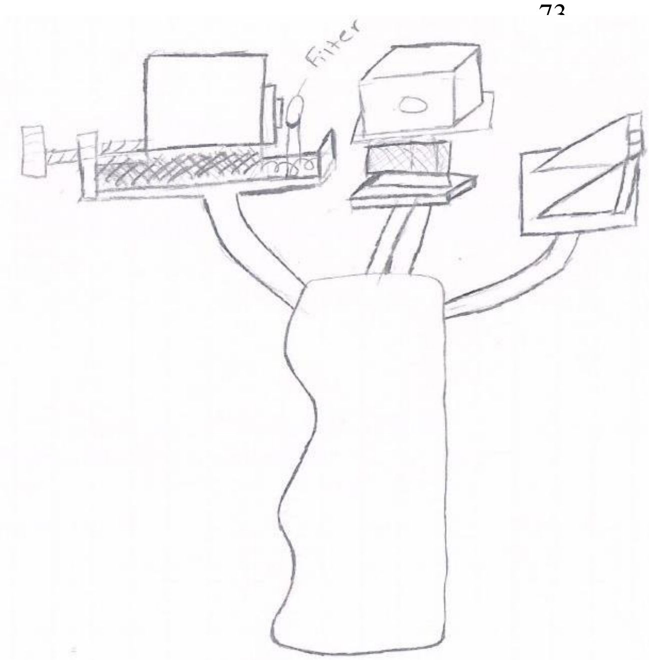

The handle would become the base and would have four pillars extending from the handle. On each of the pillars would be individual platforms. Each platform would hold a specific piece. One platform would hold the dichromatic mirror. Two other platforms would hold the two cameras. The Hamamatsu would have a 3-walled platform with the back open for a tuning screw to push the camera forward and a slot on the bottom to secure the camera to the platform. The filter for the Hamamatsu will be rigidly attached to the platform.

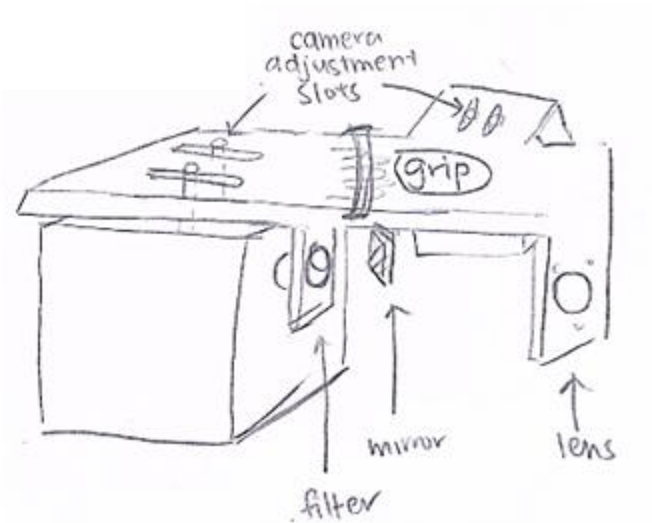

'Lantern' design

Grip and base plate are above the cameras/optics. Novel way of gripping and carrying system. Might be easier for repeated lifting and placing back down when compared to a handle. But cameras might not be that securely held. Maneuvering might be difficult too.

Sliding optics channels

The larger camera which might be problematic to secure can be held down permanently on a grip. The lighter optics and smaller camera section moves for focus adjustment instead.

Sponsor feedback:
Preference is to keep optics channel unmoving.

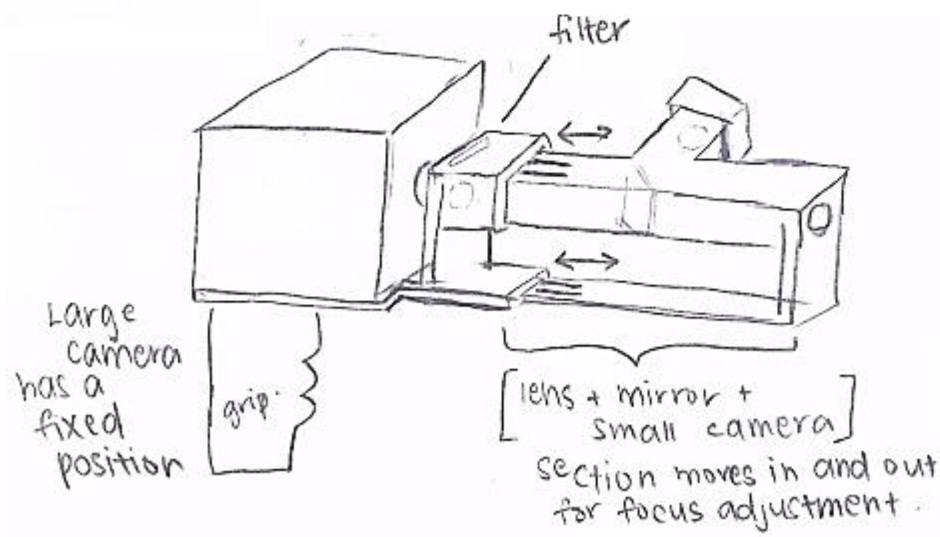

Ideas for Subsystems

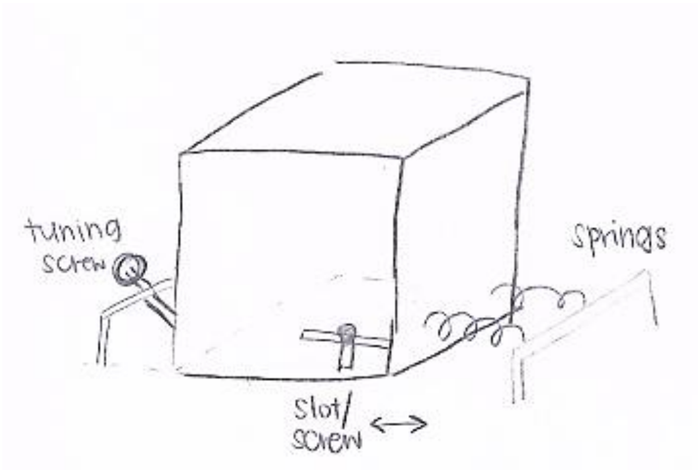

Drawing 4: A slot and tuning screw system for camera position adjustment: Camera screwed directly through a base with 1 or 2 slots. Tuning screw behind a bracket or backing can inch camera forward. Spring in the front will push camera back if screw is pulled back. Small camera can have a similar system.

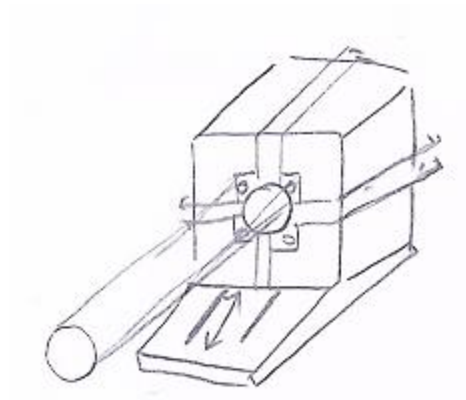

Drawing 5: A wrap around “cage”-like frame for cameras: To provide security and hold the cameras down onto base plate, but without the large volume of an enclosing ‘box’ design. Optical channel can be directly fixed onto the frame and project out from the camera.

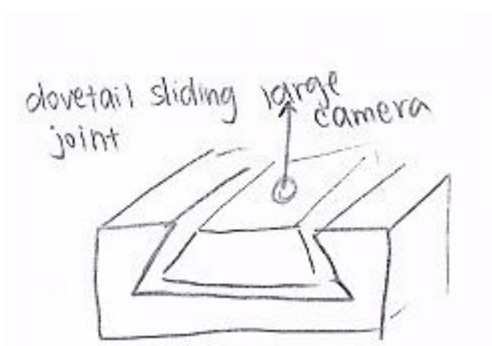

Dovetail sliding joint for camera position adjustment: Dovetail slide provides a much broader base on which the large camera can sit. It can slide back and forth in the base. Lock and key shape for slide and base.

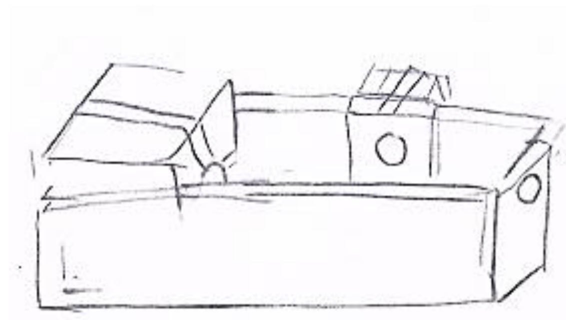

A half frame to house the cameras: Reduces total volume in comparison to a ‘box’ design. Also allows for the easy adjustment and removal of cameras. The lens can be rigidly held in a holder that is part of the frame. The mirror can be held by supports extending from the walls and base.

APPENDIX F: Specifications for Optical Components [18, 19]

716/40 nm BrightLine® single-band bandpass filter
Part Number: FF01-716/40-25

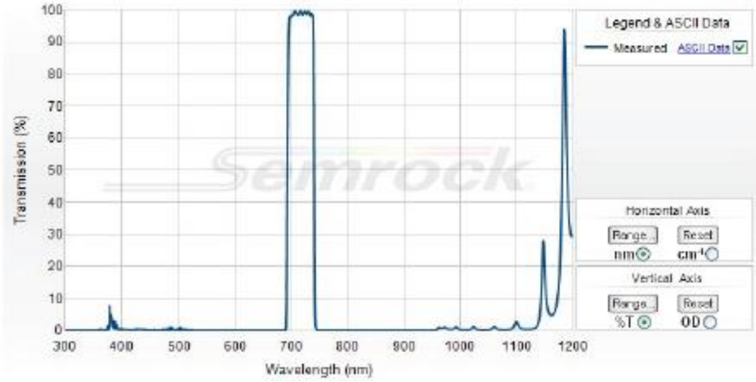

Semrock
A Unit of IDEX Corporation

Semrock, Inc
3625 Buffalo Road, Suite 6
Rochester, New York 14624

Main Phone: +1 585.594.7050 (worldwide)
Toll Free Phone: 866.736.7625 (866-SEMROCK)
(within US and Canada)

Your filter spectrum may differ slightly from the typical spectrum above, but is certified to meet the optical specifications noted below.

716/40 nm BrightLine® single-band bandpass filter

Individual fluorescence bandpass filters that have been optimized for use in a variety of fluorescence instruments. All thin-film, hard-coated construction for unsurpassed performance and reliability.

Part Number	Size	Price1	Stock Status
FF01-716/40-25	25 mm x 3.5 mm	$295	In Stock
FF01-716/40-32	32 mm x 3.5 mm	$483	Contact Us
FF01-716/40-20-D	20.0 mm x 2.0 mm (unmounted)	$395	Contact Us
FF01-716/40-23.3-D	23.3 mm x 2.0 mm (unmounted)	$295	In Stock

Don't see a size you need? Contact us for custom sizing – available in less than a week (sizing fee applies).

1) US domestic pricing only. If you are ordering from outside the US, please contact your nearest regional distributor for the correct list price.

Optical Specifications

Specification	Value
Transmission Band 1	T_{avg} > 93% 696 – 736 nm
Center Wavelength 1	716 nm
Guaranteed Minimum Bandwidth 1	40 nm
FWHM Bandwidth 1 (nominal)	47.2 nm
Blocking Band 1	OD_{avg} > 1 200 – 400 nm
Blocking Band 2	OD_{avg} > 2 400 – 545 nm
Blocking Band 3	OD_{avg} > 5 545 – 635 nm
Blocking Band 4	OD_{avg} > 10 635 – 675 nm (Design specification - measurement limited to OD 6.5)
Blocking Band 5	OD > 3.5 685.5 nm
Blocking Band 6	OD_{avg} > 5 754.6 – 925 nm
Blocking Band 7	OD_{avg} > 2 925 – 1050 nm
Blocking Band 8	OD_{avg} > 1 1050 – 1100 nm

General Filter Specifications

Specification	Value
Angle of Incidence	0 ± 5 degrees
Cone Half-angle	7 degrees
Optical Damage Rating	Testing has proven to show no signs of degradation when exposed to at least 6.0 W of power from an unfiltered xenon arc lamp over a 25 mm diameter (corresponding to 1.2 W/cm2) for over 500 hrs.
Effective Index	1.76

Physical Filter Specifications (applies to standard sized parts; contact us regarding other sizes)

Specification	Value
Transverse Dimensions (Diameter)	25 mm
Transverse Tolerance (mounted)	+ 0.0 / – 0.1 mm
Filter Thickness (Mounted)	3.5 mm
Filter Thickness Tolerance (Mounted)	± 0.1 mm
Clear Aperture	≥ 22 mm
Scratch-Dig	60-40
Substrate Thickness (unmounted)	2.0 mm
Substrate Thickness Tolerance (unmounted)	± 0.1 mm
Orientation	Arrow on ring indicates preferred direction of propagation of light

700 nm edge BrightLine® single-edge dichroic beamsplitter
Part Number: FF700-Di01-25x36

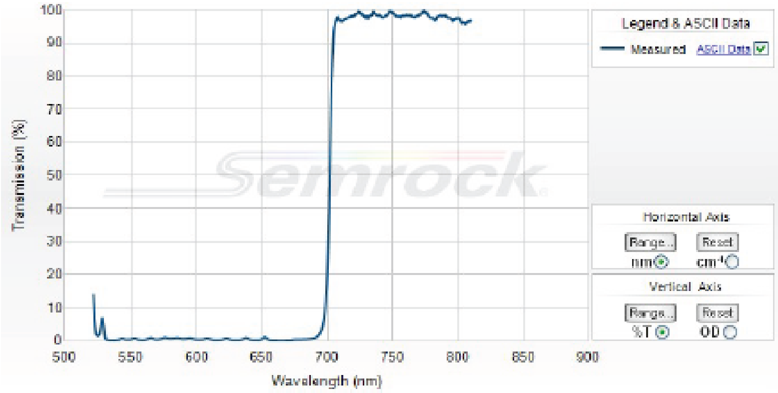

Semrock
A Unit of IDEX Corporation

Semrock, Inc
3625 Buffalo Road, Suite 6
Rochester, New York 14624

Main Phone: +1 585.594.7050 (worldwide)
Toll Free Phone: 866.736.7625 (866-SEMROCK)
(within US and Canada)

Your filter spectrum may differ slightly from the typical spectrum above, but is certified to meet the optical specifications noted below.

700 nm edge BrightLine® single-edge dichroic beamsplitter

Semrock offers a wide range of polarization-insensitive dichroic beamsplitters that exhibit steep edges with very high and flat reflection and transmission bands. Filters are available in versions optimized for wideband light sources, laser sources, multiphoton systems, Raman spectroscopy, image splitting, and laser beam combining and separating.

Part Number	Size	Price[1]	Stock Status
FF700-Di01-25x36	25.2 mm x 35.6 mm x 1.1 mm (unmounted)	$245	In Stock

Don't see a size you need? Contact us for custom sizing – available in less than a week (sizing fee applies).

1) US domestic pricing only. If you are ordering from outside the US, please contact your nearest regional distributor for the correct list price.

Optical Specifications

Specification	Value
Reflection Band 1	R_{avg} > 97% 532 – 690 nm
Edge Wavelength 1	700 nm
Transmission Band 1	T_{avg} > 93% 705 – 800 nm

General Filter Specifications

Specification	Value
Angle of Incidence	45 ± 1.5 degrees
Cone Half-angle	2 degrees
Optical Damage Rating	Testing has proven to show no signs of degradation when exposed to at least 6.0 W of power from an unfiltered xenon arc lamp over a 25 mm diameter (corresponding to 1.2 W/cm2) for over 500 hrs.
Flatness	Standard
Steepness	Standard
Effective Index	1.77

Physical Filter Specifications (applies to standard sized parts; contact us regarding other sizes)

Specification	Value
Transverse Dimensions (L x W)	25.2 mm x 35.6 mm
Transverse Tolerance	± 0.1 mm
Filter Thickness (unmounted)	1.05 mm
Filter Thickness Tolerance (unmounted)	± 0.05 mm
Clear Aperture	≥ 80% (elliptical)
Scratch-Dig	60-40
Substrate Thickness (unmounted)	1.05 mm
Substrate Thickness Tolerance (unmounted)	± 0.05 mm
Orientation	Reflective surface marked with part number - Orient in direction of incoming light